

Spatial and seasonal distribution of methane and its microbial oxidation in the water column of the central Baltic Sea

Dissertation

zur

Erlangung des akademischen Grades
doctor rerum naturalium (Dr. rer. nat.)
der Mathematisch-Naturwissenschaftlichen Fakultät
der Universität Rostock

vorgelegt von

M.Sc. Gunnar Jakobs
geb. am 15.07.1982 in Güstrow
Rostock, den 26.09.2014

Doctoral Committee:

1. Referee

Prof. Dr. Gregor Rehder
Leibniz Institute for Baltic Sea Research Warnemünde
Department: Marine Chemistry

2. Referee

Prof. Dr. Volker Thiel
Georg-August University Göttingen
Department: Geobiology

Day of submission: 26.09.2014

Day of defense: 18.12.2014

Contents

Preface.....	V
Abstract	VI
Zusammenfassung	IX
Motivation and Objective	XII
1 General Introduction.....	1
1.1 Generation and emission of methane.....	1
1.2 Aerobic methane oxidation.....	2
1.3 Anaerobic methane oxidation.....	4
1.4 Study area: central Baltic Sea.....	7
1.5 Methane production in the Baltic Sea sediments.....	8
1.6 Water column distribution and oxidation of methane in the Baltic Sea	9
1.6.1 Central Baltic Sea.....	10
2 Materials and Methods	12
2.1 Material and methods used in connection with the field studies	12
2.1.1 Analysis of methane, oxygen and hydrogen sulfide concentrations	12
2.1.2 Stable carbon isotope ratio of methane	13
2.1.3 Methane oxidation rates	13
2.1.3.1 Sampling and ^{14}C CH_4 tracer preparation	14
2.1.3.2 Sample processing.....	15
2.1.4 Vertical turbulent diffusivities	17
2.1.5 <i>pmoA</i> gene and transcript analysis	18
2.1.6 Biomarker analysis.....	18
2.2 Materials and methods used for the enrichment experiment	19
2.2.1 DAPI staining.....	19
2.2.2 Cell counting.....	20
2.2.3 Nitrate and nitrite concentrations	20
2.2.4 Denitrification rates.....	20
2.2.5 Analysis of methane and oxygen concentration.....	21

2.2.6	Methane oxidation rates	22
2.2.7	Stable isotope probing and NanoSIMS analysis	22
2.2.7.1	^{13}C CH_4 and ^{15}N NO_2^- incubations	22
2.2.7.2	Stable isotope probing	23
2.2.8	NanoSIMS analysis	24
2.2.9	<i>pmoA</i> gene analysis	25
2.2.10	Biomarker	25
3	Comparative studies of pelagic microbial methane oxidation within the redox zones of the Gotland Deep and Landsort Deep (central Baltic Sea)	27
3.1	Introduction	27
3.2	Methods	28
3.3	Study area	28
3.4	Sampling strategy	30
3.5	Results	30
3.5.1	Gotland Deep	30
3.5.2	Landsort Deep	32
3.6	Discussion	34
3.6.1	Microbial methane consumption in the Gotland Deep and Landsort Deep	35
3.6.1.1	Concentration and stable isotope pattern	35
3.6.1.2	Methane oxidation rates	35
3.6.1.3	Aerobic methanotrophs in the redox zone	38
3.6.2	Hydrodynamic controls on the fate of methane in the Gotland Deep and Landsort Deep	40
3.6.2.1	Vertical mixing	40
3.6.2.2	Lateral intrusions	41
3.7	Conclusions	43
4	Seasonal and spatial methane dynamics in the water column of the central Baltic Sea (Gotland Sea)	44
4.1	Introduction	44
4.2	Methods	44
4.3	Study area	45
4.4	Sampling	46
4.5	Results	47

4.5.1	Salinity and temperature distribution and temporal variations in the central Baltic Sea	48
4.5.2	Oxygen and hydrogen sulfide distributions and temporal variations in the central Baltic Sea	49
4.5.3	Mid- and deep water methane distributions, isotopic compositions and microbial turnover	50
4.5.3.1	Eastern Gotland Basin	50
4.5.3.2	Western Gotland Basin	54
4.6	Discussion	57
4.6.1	Influence of vertical mixing on the deep water methane distribution	57
4.6.2	Intrusions of saline water	61
4.6.3	Microbial response on varying substrate availability in the redox zone	62
4.6.4	Methane production in the oxic water layer	64
4.7	Conclusion	66
5	Bioreactor studies to investigate the methane-dependent denitrification under suboxic conditions within the redox zone of the central Baltic Sea	67
5.1	Introduction	67
5.2	Methods	67
5.3	Sampling strategy at the Gotland Deep redox zone	68
5.4	Cultivation procedure	69
5.5	Results	72
5.5.1	Microscopy inspection and cell counting	72
5.5.2	Oxygen concentration	72
5.5.3	Nitrate and nitrite concentrations	73
5.5.4	Denitrification rates	75
5.5.5	Methane oxidation rates	75
5.5.6	SSCP analysis	75
5.5.7	<i>pmoA</i> detection and DGGE analysis	77
5.5.8	Stable isotope probing	77
5.5.9	NanoSIMS analysis	78
5.5.10	Biomarker	78
5.6	Discussion	80
5.6.1	Development of microbial biomass	80
5.6.2	Methane oxidation coupled to denitrification	81
5.6.3	Phylogenetic and activity analysis	82
5.7	Conclusion	84

General conclusions and future perspectives	86
References	89
List of Figures	102
List of Abbreviations	104
Contributions to the manuscripts.....	106
Danksagung	108
Eidesstattliche Erklärung.....	109

Preface

The present thesis consists of a general introduction (Chapter 1), a description of the applied material and methods (Chapter 2), and three main chapters regarding the investigations of the spatial and seasonal distribution of methane and its microbial oxidation in the water column of the central Baltic Sea (Chapter 3, 4, and 5). The results of chapter 3 and 4 have been published in the peer-reviewed journals *Biogeosciences* and *Continental Shelf Research*. The results of chapter 5 are in preparation for publishing. The titles and authors of the papers and manuscript are listed below.

Chapter 3	Comparative studies of pelagic microbial methane oxidation within the redox zones of the Gotland Deep and Landsort Deep (central Baltic Sea)
Authors	Jakobs ¹ , G., Rehder ¹ , G., Jost ¹ , G., Kießlich ¹ , K., Labrenz ¹ , M., Schmale ¹ , O.
Status	published in <i>Biogeosciences</i> (2013)
Chapter 4	Seasonal and spatial methane dynamics in the water column of the central Baltic Sea (Gotland Sea)
Authors	Jakobs ¹ , G., Holtermann ¹ , P., Berndmeyer ² , C., Rehder ¹ , G., Blumenberg ² , M., Jost ¹ , G., Nausch ¹ , G., Schmale ¹ , O.
Status	accepted manuscript in press (online published) by <i>Continental Shelf Research</i> (2014)
Chapter 5	Bioreactor studies to investigate the methane-dependent denitrification under suboxic conditions within the redox zone of the central Baltic Sea
Authors	Jakobs ¹ , G., Schmale ¹ , O., Kießlich ¹ , K., Vogts ¹ , A., Blumenberg ² , M., Rehder ¹ , G., Nausch ¹ , G., Labrenz ¹ , M.
Status	manuscript in preparation

¹Leibniz Institute for Baltic Sea Research Warnemünde (IOW), Rostock, Germany

²Geobiology Group, Geoscience Centre, Georg-August-University Göttingen, Göttingen, Germany

Abstract

This thesis focuses on the determination of the spatial and seasonal methane distribution and the pelagic methane oxidation within the central Baltic Sea. A multidisciplinary approach was carried out that combines gas chemistry, methane oxidation rate measurements, and molecular biological analysis to investigate the pelagic methane oxidation within the redox zone in dependence on differing oceanographic conditions. For this reason, two representative sampling sites were chosen in the central Baltic Sea, the Gotland Deep (GD) and Landsort Deep (LD), which are characterized by a permanent stratified water column with a deep anoxic water body, separated by a redox zone, from the upper oxygenated water body. These sampling sites differ considerably in the disturbance of the redox zone and the vertical transport of reduced compounds (vertical mixing) towards the redox zones (chapter 3). In addition to this location-dependent investigation, the distribution and the microbial turnover of methane was examined over a two-year period (August 2011 – August 2013) along a transect from the eastern (EGB) to the western Gotland Basin (WGB), central Baltic Sea, in order to identify influencing factors and their impacts on the seasonal and spatial distribution of methane and to track changes in the associated microbial methane consumption (chapter 4). A further goal of this thesis was the investigation of the methane-dependent denitrification under suboxic conditions in the marine environment. For this purpose, a bioreactor experiment was carried out over several months to enrich process-involved microorganisms under specific conditions (chapter 5).

The comparative studies of pelagic microbial methane consumption within the GD and LD (chapter 3) show that the redox zones of both deeps are characterized by pronounced methane concentration gradients between the deep water and the surface water. This gradient together with a ^{13}C CH_4 enrichment, clearly indicates microbial methane consumption within the redox zones. Expression analysis of the methane monooxygenase identified only one phylotype of aerobic type I methanotrophic bacteria in both redox zones. The turnover of methane within the redox zones showed strong differences between both deeps, with a nearly four times lower turnover time of methane in the LD. Vertical turbulent diffusivities for both deeps were calculated on the base of the methane concentration profiles and the data on the methane consumption within the redox zone. The vertical transport of methane from the deep water

body towards the redox zone as well as differing hydrographic conditions (lateral intrusions) within the redox zone were identified as major factors that determine the pelagic methane oxidation.

The two-years study across the transect from the EGB to the WGB (chapter 4) demonstrates that enhanced vertical turbulent diffusivities in fall (November 2011) and winter (February 2012) lead to an enhanced flux of methane from the deep anoxic water towards the redox zone. In both basins, the increased vertical transport of methane in fall/winter was mirrored by reduced methane turnover times measured within the redox zone. Moreover, specific biomarkers indicative for aerobic methanotrophic bacteria implied an increase in the microbial population size from August 2011 until February 2012, indicating a methanotrophic community adapting to the variable methane flux. The deep water methane inventory of the EGB showed a seasonal pattern, with concentrations increasing during spring (May) and summer (August) and decreasing during fall (November) and winter (February) as a direct result of the seasonal varying vertical turbulent diffusivity. In contrast, the WGB showed no clear correlation between the seasons and the observed deep water methane variability. Here, the impact of lateral weak intrusions penetrating the deep water layer was identified as the main factor controlling the fluctuation of the methane inventory in the deep water. Moreover, methane concentrations and carbon stable isotopic data ($\delta^{13}\text{C CH}_4$) in the oxic water column demonstrate that the production of methane below the thermocline occurs in the entire central Baltic Sea from May through November, and despite the large methane pool in the underlying anoxic deep water, this might govern the moderate methane flux into the atmosphere in this area during the summer.

For the investigation of the methane-dependent denitrification (chapter 5) a water sample was gathered from the GD redox zone and the microorganisms contained therein were cultivated in a bioreactor under suboxic conditions over a period of 12 months. To enrich the microorganisms involved in the methane-dependent denitrification the bioreactor was continuously sparged with methane as the sole energy and carbon source and simultaneously supplied with a nutrient solution containing, compared to the environmental sample, considerably increased nitrate and nitrite concentrations. The enrichment experiment was monitored by different analytical methods such as nutrient analysis, cell counting, microbial activity measurements, and biomarker analysis. For the detection of responsible organisms, the enrichment culture was incubated with $^{13}\text{C CH}_4$ and $^{15}\text{N NO}_2^-$ and the cell-specific

incorporation of these „labels“ was analyzed using the NanoSIMS technique in combination with molecular biological methods. The bioreactor enrichment experiment showed a correlation between the turnover of methane and the temporal concentration pattern of nitrite and nitrate. Besides a mixture of uncultured microorganisms, type I methanotrophic and heterotrophic denitrifying bacteria were identified in the enrichment culture. The obtained results provide first indications for the occurrence of a methane-dependent denitrification under suboxic conditions in the marine realm supporting the assumption of a symbiotic interaction between methanotrophic and denitrifying bacteria as previously described for fresh water environments.

Zusammenfassung

Die vorliegende Arbeit soll die räumliche und saisonale Verteilung von Methan und dessen mikrobielle Oxidation in der Wassersäule der zentralen Ostsee untersuchen. Die zentrale Ostsee mit ihrer permanent dichtestratifizierten Wassersäule, die episodisch durch ozeanographische Ereignisse beeinflusst wird, bietet ein ideales Untersuchungsgebiet um Einflüsse auf das Methanverteilungsmuster und den mikrobiellen Umsatz von Methan zu verfolgen. In der vorliegenden Arbeit wurde ein multidisziplinärer Forschungsansatz durchgeführt, der Gaschemie, Methan-Oxidationsraten, und molekularbiologische Analysen vereinigt, um die pelagische Oxidation von Methan in Abhängigkeit von unterschiedlichen ozeanographischen Bedingungen zu untersuchen. Hierzu wurden zwei repräsentative Probenahme-Standorte ausgewählt (Gotlandtief (GD) und Landsorttief (LT), zentrale Ostsee), die sich durch unterschiedlich gestörte pelagische Redoxzonen sowie durch einen unterschiedlich vertikalen Transport von reduzierten Verbindungen zur Redoxzone auszeichnen (Kapitel 3). Zusätzlich zu diesen standortabhängigen Untersuchungen wurde die Verteilung sowie der mikrobielle Umsatz von Methan über einen Zeitraum von zwei Jahren (August 2011 – August 2013) entlang der Beckenachsen des östlichen und westlichen Gotlandbeckens (zentrale Ostsee) erforscht, um Einflussfaktoren auf die saisonale und räumliche Verteilung von Methan zu identifizieren sowie Veränderungen des damit einhergehenden mikrobiellen Methan-Umsatzes zu verfolgen (Kapitel 4). Ein weiteres Ziel dieser Arbeit war die Untersuchung der methanabhängigen Denitrifikation unter suboxischen Bedingungen in marinen Lebensräumen. Hierzu wurde ein mehrmonatiges Bioreaktor-Experiment durchgeführt, bei dem involvierte Mikroorganismen unter spezifischen Bedingungen angereichert wurden (Kapitel 5).

Die vergleichende Studie des GT und LT (Kapitel 3) zeigt, dass die Redoxzonen beider Becken einen ausgeprägten Methan-Konzentrationsgradienten zwischen dem Tiefen- und dem Oberflächenwasser aufweisen. Das Auffinden des Methangradienten zusammen mit der Anreicherung von ^{13}C CH_4 in der Redoxzone belegt den mikrobiellen Umsatz von Methan innerhalb dieses spezifischen Tiefenintervalls. Mit Hilfe der Gen-Expressionsanalyse der partikulären Methan-Monooxygenase konnte nur ein Phylotyp aerob Typ I methanotropher Bakterien in beiden Redoxzonen identifiziert werden. Die Untersuchungen zeigen weiterhin, dass die Methan-Umsatzzeit (turnover time) im LT um ein Vierfaches geringer ist als im GT.

Basierend auf den Methan-Konzentrationsprofilen und den Daten des Methan-Umsatzes innerhalb der Redoxzone wurde die vertikale turbulente Diffusivität für beide Standorte berechnet. Diese Berechnungen zeigen unter anderem, dass der vertikale Transport von Methan vom Tiefenwasser zur Redoxzone sowie unterschiedliche hydrographische Bedingungen (laterale Intrusionen) innerhalb der Redoxzonen beider Standorte wesentliche Faktoren darstellen, die den pelagischen Umsatz von Methan bestimmen.

Die zweijährige Studie entlang der Beckenhauptachsen der zentralen Ostsee (Kapitel 4) verdeutlicht, dass eine erhöhte vertikale turbulente Diffusivität im Herbst (November 2011) und Winter (Februar 2012) einen verstärkten Methanfluss vom anoxischen Tiefenwasser zur Redoxzone bedingt. Der erhöhte vertikale Transport von Methan im Herbst und im Winter wird durch verringerte Methan-Umsatzzeiten innerhalb der Redoxzone wiedergegeben. Weiterhin zeigen spezifische Biomarker, indikativ für aerobe methanotrophe Bakterien, eine Konzentrationszunahme zwischen August 2011 und Februar 2012, die wiederum einen Anstieg der mikrobiellen Populationsgröße impliziert und auf eine sich an variable Methanflüsse adaptierende methanotrophe Gemeinschaft hindeutet. Das Tiefenwasser des östlichen Gotlandbeckens zeigt ein saisonales Methanverteilungsmuster mit einem Konzentrationsanstieg während Frühling (Mai) und Sommer (August) und einer Abnahme während Herbst (November) und Winter (Februar) als unmittelbare Folge einer saisonal variierenden Diffusivität. Das westliche Gotlandbecken zeigt im Gegensatz hierzu keine Korrelation zwischen den Jahreszeiten und der beobachteten Variabilität der Methankonzentrationen im Tiefenwasser. Über die Langzeituntersuchungen zur Korrelation der Salz- und Methanverteilung im Tiefenwasser beider Becken konnten laterale Intrusionen als maßgebliche Ursache für die Fluktuation von Methan im Tiefenwasser des westlichen Gotlandbeckens identifiziert werden. Darüber hinaus zeigen die Methankonzentrationen und das Verhältnis der stabilen Kohlenstoffisotope ($\delta^{13}\text{C CH}_4$) im oxischen Wasserkörper, dass die Methanproduktion unterhalb der Thermokline in der gesamten zentralen Ostsee im Zeitraum von Mai bis November aufzufinden ist. Diese oberflächennahe Methanproduktion scheint, trotz des großen Methanpools im darunterliegenden anoxischen Wasserkörper, den moderaten Methanfluss zur Atmosphäre in den Sommermonaten zu steuern.

Zur Untersuchung der methanabhängigen Denitrifikation (Kapitel 5) wurde eine Wasserprobe aus der Redoxzone des GT gewonnen und die darin befindlichen Mikroorganismen in einem Bioreaktor über einen Zeitraum von 12 Monaten unter suboxischen Bedingungen kultiviert.

Über die kontinuierliche Einleitung von Methan als alleinige Kohlenstoff- und Energiequelle und der gleichzeitigen Zugabe eines mineralischen Mediums, das im Vergleich zur Umweltprobe deutlich erhöhte Nitrat- und Nitrit-Konzentrationen aufweist, sollten die an der methanabhängigen Denitrifikation beteiligten Organismen angereichert werden. Das Bioreaktor-Experiment wurde dabei mit verschiedenen analytischen Methoden überwacht: Nährstoffanalysen, Zellzahlbestimmung, mikrobielle Aktivitätsmessungen sowie Biomarker-Analysen. Zur Charakterisierung der an der methanabhängigen Denitrifikation beteiligten Mikroorganismen wurden Inkubationsexperimente mit ^{13}C CH_4 und ^{15}N NO_2^- durchgeführt und die zellspezifische Inkorporation dieser „Labels“ mittels NanoSIMS und molekularbiologischen Methoden verfolgt. Das Anreicherungs experiment im Bioreaktor zeigt eine Korrelation zwischen der Oxidation von Methan und dem zeitlichen Konzentrationsverlauf von Nitrit und Nitrat. Neben einem Gemisch aus unkultivierten Mikroorganismen konnten Typ I Methanotrophe und heterotrophe denitrifizierende Bakterien in der Anreicherungskultur nachgewiesen werden. Die gewonnenen Ergebnisse liefern erste Hinweise für das Auftreten einer methanabhängigen Denitrifikation unter suboxischen Bedingungen für den marinen Lebensraum. Die Abhängigkeit der Denitrifikation von der Oxidation von Methan ist vermutlich analog zu Frischwassersystemen auf eine symbiotische Wechselbeziehung zwischen methanotrophen und denitrifizierenden Bakterien zurückzuführen.

Motivation and Objective

Anoxic deep waters of silled basins such as the Black Sea, Cariaco Basin or the Baltic Sea are known as methane-rich environments. In the central Baltic Sea the strong permanent haline stratification leads to large vertical redox gradients in the water column with an upper oxic and deep anoxic water layer, which are separated by the redox zone. The water column of the central Baltic Sea is characterized by low methane concentrations in the oxic water layer and higher concentrations in the deep anoxic water layer with a large methane concentration gradient between both water bodies. The permanently stratified water column of the central Baltic Sea represents a brackish environment that is periodically disturbed by lateral intrusions and internal waves and that shows strong interactions with the basin boundaries. The Gotland Deep (GD) and Landsort Deep (LD) located in the eastern Gotland Basin and the western Gotland Basin (central Baltic Sea), respectively, differ considerably in their oceanographic conditions. As regards the LD it is known that the specific basin structure trigger an increased transport of deepwater towards the redox zone (vertical mixing). In the GD the vertical mixing is dominated by the energy input from the wind and is much lower compared to the LD. Furthermore, in the GD lateral intrusions and internal waves disturb the water column periodically. In contrast, the redox zone of the LD is characterized by less frequent and intense lateral intrusions leading to a more “undisturbed” situation of the redox zone. The redox zone appears to play a pivotal role in the local methane biogeochemistry as this specific depth interval is characterized by a pronounced methane concentration gradient indicating efficient microbial methane consumption. Only little is known about the apparent methane oxidation in the water column by microbially mediated processes preventing the escape of methane from the deep water into the atmosphere.

The present thesis investigating the “Spatial and seasonal distribution of methane and its microbial oxidation in the water column of the central Baltic Sea” was conducted within the framework of a multidisciplinary joint project funded by the DFG (Aerobic and anaerobic methane turnover in the water column of the central Baltic Sea) between the Leibniz Institute for Baltic Sea Research Warnemünde (IOW) and the Geoscience Center for Geobiology at the Georg-August-University of Göttingen.

The prevailing oceanographic conditions at the GD and LD lead to the assumption that the different characteristics of the water columns might have an impact on the pelagic methane turnover. Based on this hypothesis, the first aim of the present thesis focuses on the investigation of the pelagic methane turnover in dependence on the disturbance of the redox zone and the vertical mixing of the water column. For this scope, the turnover of methane and the composition of the methanotrophic community should be investigated at one time point in the GD and LD using a multidisciplinary approach that combines methane chemistry, methane oxidation rates and molecular biological analysis.

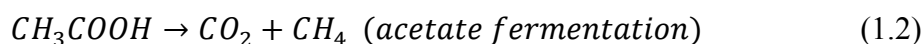
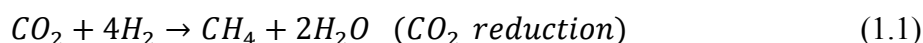
The second goal of this work is directed on the identification and the impact of controlling factors on the seasonal and spatial methane distribution as well as the seasonal variability of the microbial turnover of methane. In the central Baltic Sea little is known about the dynamic of methane within the deep anoxic basins and the microbial response to changing environmental conditions such as substrate availability. Therefore, data on the concentration of methane and physical parameters needed to be collected on a total of 11 cruises over a time period of two years (August 2011 – August 2013) along a transect from the eastern to the western Gotland Basin (central Baltic Sea). The microbial response on seasonal varying substrate availabilities within the redox zones of the GD and LD had to be analyzed for selected cruises in summer, autumn and winter using the data on stable carbon isotope ratios ($\delta^{13}\text{C CH}_4$), methane oxidation rates and biomarker concentrations.

As well as these field studies conducted within the central Baltic Sea, the significance of the aerobic methane oxidation coupled to nitrogen reduction also had to be investigated for the marine environment. For this purpose, the goal was to transfer an environmental water sample from the GD redox zone into a bioreactor to accumulate a microbial community under suboxic conditions. Analogous to fresh water environments, the feeding with specific substrates (methane, nitrite and nitrate) should favor the growth of methanotrophic bacteria and heterotrophic denitrifiers which use organic compounds released by methanotrophs as the electron donor for denitrification (methane-dependent denitrification). Moreover, the bioreactor experiment will help to estimate the transferability of the coupled process to other marine settings.

1 General Introduction

1.1 Generation and emission of methane

Methane (CH₄) is the most abundant organic molecule in the atmosphere. The global atmospheric concentration of methane (approximately 1800 ppbv) has been increased by a factor of 2.5 since pre-industrial times (Dlugokencky et al., 2011). Methane influences the earth's climate directly by absorbing infrared radiation (Cicerone and Oremland, 1988). Moreover, the atmospheric decomposition of methane via hydroxyl radicals leads to the formation of tropospheric ozone and stratospheric water vapor, which contribute additionally as greenhouse gases to the climate forcing (Dlugokencky et al., 2011). Methane can be emitted to the atmosphere by natural (e.g. wetlands, digestive tracts of wild ruminants and termites, oceans, and hydrates) and anthropogenic sources (e.g. agriculture, landfills, rice paddies, biomass burning, extraction of fossil fuels) (Wuebbles and Hayhoe, 2002). In the marine realm, methane is mainly generated by remineralization of organic matter within anoxic sediments. The biological production of methane (methanogenesis) is the final step of remineralization and is mediated by methanogenic archaea that require low-molecular substances for the production of methane that are provided by other microorganisms during the degradation of organic matter (Reeburgh, 2007). The most important molecules for methanogenesis are hydrogen (1.1) and acetate (1.2), which are used by the majority of methanogenic archaea (Heyer, 1990).



Besides methanogenesis the generation of methane can also occur by abiotic processes in the marine environment such as thermogenic generation of methane or serpentinization of olivine at hydrothermal systems (Berndt et al., 1996; Keir et al., 2008). Although shelf regions and marginal seas contribute about 75% to the oceanic methane flux into the atmosphere, the

global flux from marine regions is estimated to account for only 2% of all anthropogenic and natural sources (Bange et al., 1994). The most important reason for these low contributions from the oceans is that microbial methane oxidation in the sediments and water column effectively hampers the release of methane into the atmosphere (Reeburgh, 2007; Schmale et al., 2012; Valentine, 2011). Methane is oxidized in the aerobic marine environment by methanotrophic bacteria of type I, II and X (Hanson and Hanson, 1996), whereas in the anoxic waters this process is mediated by methanotrophic archaea (ANME I and II) (Schubert et al., 2006b). However, recent changes in global climate and near shore nutrient load suggest that the capacity of marine oxidation pathways might be challenged (Best et al., 2006). One of the regions particularly in the focus is the Arctic shelf because the current global situation shows that the progressive climate warming on earth could trigger the enhanced release of methane in Arctic shelf regions and thus trigger an abrupt climate warming (Shakhova et al., 2010).

1.2 Aerobic methane oxidation

According to their carbon assimilation that can either be performed by the ribulose monophosphate (RuMP) or serine pathway, aerobic methanotrophic bacteria are separated into the main groups type I and type II, respectively. Type I methanotrophic bacteria belong to the family *Methylococcaceae* and comprise the genera *Methylococcus*, *Methylomicrobium*, *Methylobacter*, and *Methylomonas*. Methanotrophic bacteria of type II contain species belonging to the genera *Methylocystis* and *Methylosinus* (Hanson and Hanson, 1996). Type X represents methanotrophs (e.g. *Methylococcus capsulatus*) that, similarly to type I, utilize the RuMP pathway for formaldehyde assimilation, but harbor also low enzyme levels of the serine pathway and grow at higher temperatures than type I and II methanotrophs. The biochemical pathway of aerobic methanotrophs was entirely revealed. Aerobic methanotrophs oxidize methane via oxygen using the key enzyme methane monooxygenase (MMO), which catalyzes the formation of methanol during the first step of methane oxidation (Fig. 1.1). Depending on the copper concentration of the respective habitat aerobic methanotrophs expresses two forms of MMO. Under low copper concentrations ($1 \mu\text{mol g}^{-1}$ dry cells), the soluble (sMMO, soluble in the cytoplasm) and under high copper concentrations the

particulate methane monooxygenase (pMMO, membrane-bound) is expressed (Hanson and Hanson, 1996).

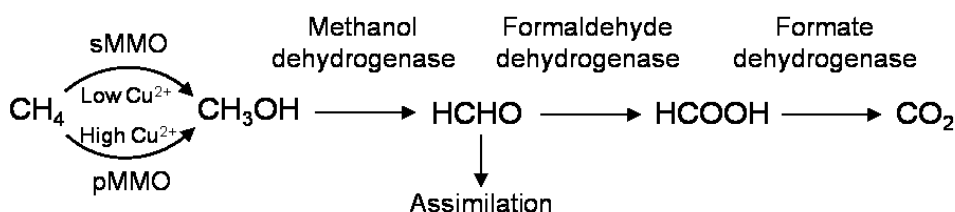


Figure 1.1. Pathway of aerobic methane oxidation after Modin et al. (2007), modified.

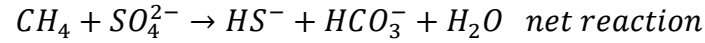
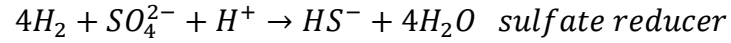
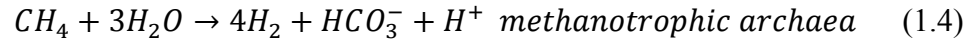
Only the particulate form (pMMO) is present in all three types of aerobic methanotrophs. The functional *pmoA* gene encoding the alpha subunit of the pMMO is used as marker to identify methanotrophs in different environments (Bourne et al., 2001; McDonald et al., 2008). In addition, the two groups of aerobic methanotrophic bacteria can be studied by biomarkers such as fatty acids and bacteriohopanepolyols. Type I methanotrophic bacteria contain predominantly 16-carbon fatty acids and type II 18-carbon fatty acids (Nichols et al., 1985). The bacteriohopanepolyols 35-aminobacteriohopane-31,32,33,34-tetrol (aminotetrol) and 35-aminobacteriohopane-31,32,33,34,35-pentol (aminopentol) are characteristic for analyzing aerobic methanotrophic bacteria, whereby the latter one is particularly specific for type I methanotrophs (Talbot et al., 2008).

Aerobic methanotrophs have also an important impact on the nitrogen cycle, because they are capable to oxidize ammonia to nitrite and nitrous oxide (N_2O). It was shown that this may be due to the evolutionary relationship between the MMO and ammonium monooxygenase (AMO), which is used by nitrifying bacteria for the oxidation of ammonia (Holmes et al., 1995). Furthermore, aerobic methanotrophs are able to promote denitrifiers in the presence of methane and low oxygen conditions (Knowles, 2005). In this process, denitrifiers utilize organic compounds as electron donors, which are released by methanotrophic bacteria during carbon assimilation. The consumption of methane and oxygen accompanied by the removal of nitrate as well as the formation of nitrous oxide and nitrogen (N_2) was observed in several studies (Amaral et al., 1995; Knowles, 2005; Thalasso et al., 1997). The clear evidence for the

synergetic interaction of methane oxidizing and denitrifying bacteria under oxic conditions was firstly provided by Waki et al. (2004), who showed the absence of denitrification by intended inhibition of methane oxidation using methyl fluoride. Biological studies investigating enrichment cultures of denitrifying methanotrophic consortia identified type I and II methanotrophic bacteria to be involved (Costa et al., 2000; Rhee and Fuhs, 1978). The compounds methanol, citrate, acetate, proteins, nucleic acids, or carbohydrates were suggested as intermediate organic substances that are released by the aerobic methanotrophic bacteria and consequently consumed by heterotrophic denitrifiers. The denitrification under oxygenated conditions represents an exception in the nitrogen conversion because it is known that molecular oxygen represses the enzymatic system for denitrification. Therefore, it can be assumed that the process of aerobic denitrification occurs in micro-anaerobic environments (e.g. central anoxic parts of particles) or even in the presence of oxygen (Modin et al., 2007). Jetten et al. (1997) presented an aerobic denitrifier (*Thiosphaera pantotropha*) which is capable to denitrify under oxygenated conditions. The most important factor controlling the aerobic methane-dependent denitrification seems to be oxygen. Several studies reported the absence of denitrification when the oxygen supply is stopped, indicating again the essential contribution of aerobic methanotrophic bacteria (Eisentraeger et al., 2001; Thalasso et al., 1997; Waki et al., 2005). Based on the theoretical model presented by Modin et al. (2007) the content of oxygen should be a compromise between suitable oxygen conditions to ensure aerobic methane oxidation and the suppression of denitrification by excessively high oxygen concentrations. Rönner and Sörensson (1985) proposed a threshold value of 9 μM O_2 for denitrification.

1.3 Anaerobic methane oxidation

The anaerobic oxidation of methane (AOM) in marine sediments converts approximately 80% of methane produced in the sedimentary environment before it is released into the water column (Reeburgh, 2007). AOM was proposed as a sulfate-dependent methane oxidation, which is mediated by a consortium of methanotrophic archaea and sulfate-reducing bacteria with a very low energy yield of $\Delta G^0 = -16.6 \text{ kJ/mol CH}_4$ (1.4) compared to the energy yield of $\Delta G^0 = -773 \text{ kJ/mol CH}_4$ obtained by the aerobic oxidation of methane (Boetius et al., 2000; Knittel and Boetius, 2009).



It was assumed that AOM is carried out by ANME using a reversal methanogenesis mechanism under low hydrogen concentrations (Hoehler et al., 1994). Moreover, genes encoding the methyl coenzyme M reductase (MCR) that catalyze the formation of methane in methanogenic archaea were also found in ANME (Hallam et al., 2003). Besides hydrogen also formate and acetate were suggested as possible electron shuttles between sulfate-reducing bacteria and archaea (Sørensen et al., 2001; Valentine and Reeburgh, 2000). However, the underlying mechanism of AOM is still under debate. Three groups of archaea (ANME I, II, III) were identified to be involved in AOM. ANME I and II can be assigned to the order *Methanosarcinales*, whereby ANME III belongs to the *Methanococcoides* sp. (Knittel et al., 2005). In contrast to the described syntrophic AOM process, Milucka et al. (2012) could provide first evidences that ANME II is able to perform methane oxidation and sulfate reduction in parallel. In this process, ANME II produces zero-valent sulphur (S^0) as the metabolic end product, which is finally converted to disulfide (HS_2^-). The released disulfide is assumed to be disproportionated by associated Deltaproteobacteria (e.g. sulfate-reducing bacteria) to sulfide (HS^-) and sulfate. The formed sulfate might be used again by the ANME II.

Apart from classical microbial processes to oxidize methane via electron acceptors such as oxygen and sulfate, different alternative pathways have been proven in different aquatic systems during the last decades (Modin et al., 2007; Reeburgh, 2007). In the sediments, oxidation processes by the reduction of nitrate, nitrite, iron and manganese could be shown, in the water column only by sulfate and oxygen (Reeburgh, 2007; Beal et al., 2009; Ettwig et al., 2010). Beal et al. (2009) provided first indications for a manganese- and iron-dependent AOM (MnO_2 and $Fe(OH)_3$) in sediment samples which were gathered from a methane seep site (Eel River Basin). The geochemical evidence under environmental conditions (mesocosm

studies) was demonstrated by Sivan et al. (2011), who showed an increase in anaerobic methane oxidation by adding of Fe (III)-oxide to intact sediment cores. Moreover, especially the reduction of nitrate together with methane as electron donor became particularly of interest during investigation of enrichment cultures which were inoculated with samples from fresh water environments (Modin et al. (2007) and references therein). The first evidence for anaerobic methane oxidation coupled to denitrification was provided in a bioreactor containing acetate degrading and denitrifying organisms (Islas-Lima et al., 2004). Sludge of this bioreactor was exposed to methane, which led to a decrease of nitrate as well as nitrogen production by the use of methane as sole electron donor. The involved microbial community was further described by Raghoebarsing et al. (2006), who enriched a microbial consortium consisting of bacteria and archaea, which was capable to oxidize methane anaerobically by the favored use of nitrite against nitrate. Further bioreactor studies could disprove the involvement of archaea and identified only one responsible bacterium named “*Ca. Methylomirabilis oxyfera*” that uses internally generated oxygen for the consumption of methane according to the pathway proposed by Ettwig et al. (2010) (Fig. 1.2).

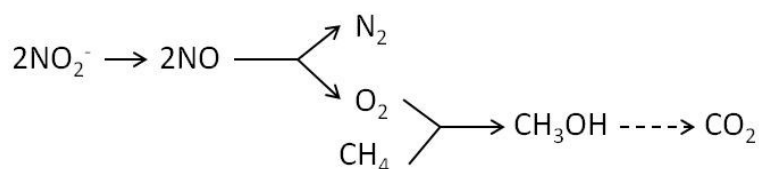


Figure 1.2. Proposed pathway of anaerobic methane oxidation in the presence of nitrite after Ettwig et al. (2010), modified.

Specific labeling experiments with “*Ca. Methylomirabilis oxyfera*” identified the incorporation of carbon which originated from bicarbonate instead of methane, providing evidence of a carbon dioxide fixing organism as well as the role of methane as the dominating energy source in the process (Rasigraf et al., 2014). These observations are in contrast to the metabolism of aerobic methanotrophic bacteria (MOB), which utilize exclusively methane as source for carbon and energy (Hanson and Hanson, 1996). Furthermore, incubation experiments with sediment samples from fresh waters demonstrated a stimulation of

anaerobic methane oxidation by adding of nitrate and thus indicate a significant influence on the sedimentary methane flux in nitrate-rich environments (Norði and Thamdrup, 2014).

1.4 Study area: central Baltic Sea

The Baltic Sea is a landlocked intracontinental sea in Northern Europe and constitutes one of the largest brackish environments on earth. The water balance in the Baltic Sea is driven by the freshwater runoff from the adjacent rivers and the episodic inflow of saline water from the North Sea (Fig. 1.3), resulting in an estuarine circulation (Lass and Matthäus, 2008). The bottom topography of the Baltic Sea consists of a series of sub-basins that are separated by submarine sills, which hamper the continuous water exchange with the North Sea. In the central and southern Baltic Sea, the less saline surface- and more saline deep water cause the formation of a permanent density boundary, the halocline, which has a crucial effect on the vertical exchange of matter and the renewal of deep water (Reissmann et al., 2009). Especially the downward diffusion of oxygen is affected by this density boundary, leading to a vertical biogeochemical zonation with oxygen-limiting conditions in the intermediate and deep water body and the microbial turnover of organic matter by electron acceptors such as nitrate or sulfate (Lass and Matthäus, 2008). The oxygenated surface water and the anoxic deep water are separated by the redox zone. This zone is a smooth transition between oxic and anoxic conditions with an occasional overlap of oxygen and hydrogen sulfide containing waters (Dellwig et al., 2012; Labrenz et al., 2010; Nausch et al., 2008). The pronounced chemical gradients in redox zones of stratified water columns are known to provide favorable conditions for different microbial processes such as ammonia oxidation, denitrification or methane oxidation (Brettar and Rheinheimer, 1992; Labrenz et al., 2010; Schubert et al., 2006a). Ventilation of the deep water by saline oxygenated water from the North Sea (so-called Major Baltic Inflows) has occurred irregularly over the last decades, leading to long periods of deep water stagnation in the central Baltic Sea (Matthäus et al., 2008; Reissmann et al., 2009); the last Major Baltic Inflow took place in 2003. The more frequent but less intense inflows contain water masses with a density too low to displace the old stagnant water in the deep basins and propagate laterally into intermediate water layers of the central Baltic Sea (Matthäus et al., 2008).

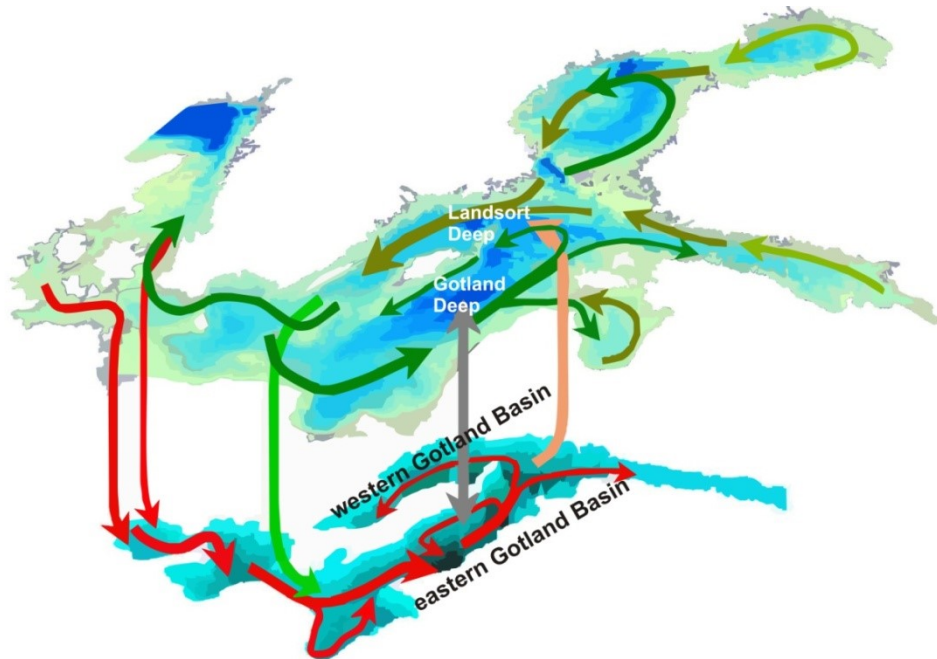


Figure 1.3. Large-scale circulation of the Baltic Sea after Matthäus et al. (2008), modified. Green and red arrows denote the surface and bottom layer circulation, respectively. The light green and beige arrows show entrainment. The gray arrow denotes diffusion.

1.5 Methane production in the Baltic Sea sediments

In the sediments of the Baltic Sea methane is generated through the process of methanogenesis. The upper sub-surface sediment layer is dominated by sulfate-reduction which represents a competitive microbial process to methanogenesis (Schmaljohann, 1996). Sulfate reducing bacteria and methanogenic archaea are dependent on the same substrates as energy sources, whereby sulfate reducing bacteria are able to degrade organic matter energetically more efficient than methanogenic archaea and thus suppressing the production of methane in the upper sediment layer. The competitive processes lead to steep methane and sulfate concentrations gradients in the upper sediment layer. The process of methanogenesis is situated below the so-called sulfate methane transition zone (SMTZ) where sulfate reducing bacteria and methanogenic archaea coexist (Parkes et al., 2007; Schmaljohann, 1996). An average sediment depth of 0.35 m was calculated for the SMTZ in muddy sediments such as present in the central Baltic Sea (Jørgensen and Fossing, 2011). Moreover, Piker et al. (1998)

could show for the Gotland Deep that the bulk production of methane occurs in the deeper sediments ($> 1\text{ m}$). In this sediment horizon, methane accumulates below the sulfate-containing sediment layer to high concentrations ($> 1\text{ mM}$) and diffuses upwards (e.g. average flux rate of the Gotland Deep sediments: $259\text{ }\mu\text{mol m}^{-2}\text{ d}^{-1}$) into the SMTZ where most of it is efficiently consumed by AOM (Treude et al., 2005), which hampers the release of methane into the water column (Iversen and Jørgensen, 1985; Piker et al., 1998). An important factor influencing the production rate of methane is the availability of organic substances. The amount of organic substances reaching the sediments depends again on the water depth and flow conditions. In contrast to the deep waters, shallow waters of coastal areas act as sediment traps and thus representing the most significant contribution to trigger enhanced methane production (Heyer, 1990). However, the production rate of methane in marine sediments is on average lower compared to limnic sediments, because most of the sedimented organic material is mineralized in the sulfate-rich surface sediments. Furthermore, the production rate of methane is strongly controlled by temperature (Bange et al., 1998; von Klein et al., 2002). Field studies in coastal areas of the Baltic Sea showed pronounced seasonal variations with increased methane production rates in summer compared to winter, which has been assigned to temperature changes of several degrees Celsius (Bange et al., 1998).

1.6 Water column distribution and oxidation of methane in the Baltic Sea

The vertical distribution of methane in the water column of the Baltic Sea strongly correlates with the vertical distribution of oxygen as well as the density stratification (Schmale et al., 2010). Below the halocline the concentrations of hydrogen sulfide and methane increase with increasing depth and show, compared to the upper oxygenated waters, enhanced methane concentrations in the deep saline water body. This particularly affects the permanent stratified basins in the southern and central Baltic Sea because these basins are characterized by an enhanced transport rate of organic matter into the deep anoxic waters (Reissmann et al., 2009). Therefore, the highest deep water methane concentrations were measured in the central Baltic Sea and the lowest in the northern basins of the Baltic Sea (Bothnian Bay and Bothnian Sea). However, the northern and western Baltic Sea (Belt Sea) is also characterized by a

widespread release of methane from the sediments, indicated by increasing methane concentrations towards the sediments (Laier and Jensen, 2007; Schmale et al., 2010). Although an active methane emission was observed in the whole Baltic Sea area, the flux of methane into the atmosphere remains relatively small with a higher flux in winter ($0.015\text{--}1.145\text{ nmol m}^{-2}\text{ s}^{-1}$) and a lower flux during summer ($0.008\text{--}0.162\text{ nmol m}^{-2}\text{ s}^{-1}$). Gülzow et al. (2013) identified wind, temperature, mixing depth and processes such as water column mixing and upwelling as controlling factors which determine the methane flux into the atmosphere. In this context, temporal variations of dissolved methane were also measured in the water column of the southwestern Baltic Sea (Eckernförde Bay) (Bange et al., 2010). These temporal methane fluctuations are triggered by changes in the sedimentary release of methane which, in turn, is caused by varying sedimentation rates of organic matter that originated from phytoplankton blooms. However, seasonal variations of the sedimentary methane emission are mainly regulated by temperature (Heyer and Berger, 2000). Furthermore, seasonal variations of the water column methane distribution were also identified in the western Baltic Sea (Arkona and Bornholm Basin) which are governed by the summer stratification of the water column, enhanced vertical mixing during winter and the frequent inflow of oxygenated saline water from the North Sea (Gülzow et al., 2014).

1.6.1 Central Baltic Sea

The central Baltic Sea (Gotland Basin) is characterized by strong methane enrichments in the stagnant anoxic water bodies (Fig. 1.3, eastern Gotland Basin (Gotland Deep) and western Gotland Basin (Landsort Deep); max. 504 nM and 1086 nM, respectively; Schmale et al. (2010)). Compared to the atmospheric equilibrium, only slightly elevated methane concentrations ($3\text{--}5\text{ nM CH}_4$) prevail in the surface waters (Bange et al., 1994; Gülzow et al., 2013; Schmale et al., 2010). Seasonal variations of these surface concentrations in the Gotland Basin were considered to be small (Gülzow et al., 2013). High-resolution gas chemistry studies in the water column of the Gotland Basins showed a pronounced methane concentration gradient and an enrichment of $^{13}\text{C CH}_4$ within the pelagic redox zone that indicates microbial activity related to aerobic oxidation of methane in that depth interval (Schmale et al., 2012). This finding is supported by earlier methane oxidation rate measurements, indicating that methane is preferentially oxidized under low oxygen

concentrations (16 to 63 $\mu\text{M O}_2$; Dzyuban et al. (1999)). Schmale et al. (2012) showed that aerobic methane oxidation within the pelagic redox zone of the Gotland Deep is performed by members of type I methanotrophic bacteria. Methane consumption being solely performed by type I methanotrophs was also supported by biomarker studies, which demonstrated a specific lipid pattern (i.e. the bacteriohopanepolyol 35-aminobacteriohopane-30,31,32,33,34-pentol (aminopentol) and the fatty acid C16:1 ω 8c together with the absence of C18:1 ω 8c (Berndmeyer et al., 2013; Schmale et al., 2012). Sediment studies in the Gotland Deep showed that the water column biomarker signal is transferred into the geological record, and that these biomarkers are useful for recording changes in the methanotrophic community throughout the Holocene (Blumenberg et al., 2013).

2 Materials and Methods

2.1 Material and methods used in conjunction with the field studies

The following chapter gives an overview on the analytical methods used in conjunction with the field studies conducted within the central Baltic Sea. These studies are about the comparison of the pelagic microbial methane oxidation within the redox zones of the Gotland Deep and Landsort Deep (chapter 3) and the seasonal and spatial methane dynamics and its associated microbial response in the water column of the central Baltic Sea (chapter 4). Water samples were taken using a rosette water sampler equipped with thirteen 5 L Free-Flow bottles (Hydro-Bios) and a CTD system (Seabird sbe911+ turbidity sensor ECO FLNTU, WET Labs) for continuous profiling of conductivity, temperature, water depth and turbidity.

2.1.1 Analysis of methane, oxygen and hydrogen sulfide concentrations

For the determination of methane concentrations, water samples were transferred from the rosette water sampler into 250 ml glass flasks and poisoned with 500 μ l of saturated mercury chloride solution. Methane concentrations were determined directly after the cruise using a modified purge and trap procedure (Michaelis et al., 1990; Thomas, 2011). This modified method includes the following process steps: the samples were stripped with helium to remove volatile constituents (purge step), dried using a Nafion[®] trap (Perma Pure LLC., USA), cryofocussed at -120°C (ethanol/nitrogen) on HayeSep D[®] (Valco Instruments Company Inc., Switzerland) desorbed by heating at 85°C and analyzed using a gas chromatograph (Shimadzu GC-2014), which was equipped with an activated aluminum oxide column (60/80 mesh) and a flame ionization detector. The oven temperature was 50°C and the carrier gas (helium) revealed a flow rate of 25 ml/min. A precision of $\pm 3.6\%$ was determined for the gas chromatographic analysis. The concentration of oxygen was determined by titration method (precision $\pm 0.9 \mu\text{M O}_2$) and the hydrogen sulfide concentrations were measured calorimetrically using the methylene blue method (precision $\pm 1.0 \mu\text{M H}_2\text{S}$)

(Grasshoff et al., 1999). Oxygen concentrations were only determined for samples virtually devoid of hydrogen sulfide.

2.1.2 Stable carbon isotope ratio of methane

Gas samples for stable carbon isotope analysis of methane ($\delta^{13}\text{C CH}_4$) were gained using a vacuum degassing system (described in detail in Keir et al. (2009)). Following this method, a water sample of 600 ml was directly transferred from the rosette water sampler into an 1100 ml pre-evacuated glass bottle, leading to a partial degassing (about 90% of the dissolved gas) of the water sample (Thomas, 2011). The extracted gas was decompressed to atmospheric pressure and subsequently transferred to a gastight burette. An aliquot of the extracted gas was conserved in a 10 ml pre-evacuated glass crimp vial containing a sodium chloride solution poisoned with mercury chloride and stored upside down to prevent the contact with the ambient air. The isotope ratio was determined using an isotope-ratio mass spectrometer (MAT 253, Thermo Electron, Germany) according to the method described by Schmale et al. (2012). $\delta^{13}\text{C CH}_4$ values are expressed versus VPDB (Vienna Pee Dee Belemnite) standard.

2.1.3 Methane oxidation rates

To determine the methane oxidation rates within the water column of the Gotland Deep and Landsort Deep (central Baltic Sea), a radio-labeling technique was applied. This labeling procedure involved the sampling and $^{14}\text{C CH}_4$ tracer preparation (chapter 2.1.3.1), and the processing of the samples (chapter 2.1.3.2). In this thesis, the applied radio-labeling technique was exclusively developed for the investigation of the microbial methane turnover within the water column of the Baltic Sea.

2.1.3.1 Sampling and ^{14}C CH_4 tracer preparation

According to Iversen and Blackburn (1981), the ^{14}C CH_4 tracer (Biotrend, Germany) used in this thesis was purified by a Mn-Cu hopcalite catalyst and sodium hydroxide (50 % w/w) to remove traces of ^{14}CO and $^{14}\text{CO}_2$, which both occur as by-products during microbial generation of ^{14}C CH_4 . Immediately before sampling, the sample bottles (transfusion bottles) were flushed with argon. According to the sampling procedure by Reeburgh et al. (1991), water samples were directly transferred from the rosette sampler into transfusion bottles and sealed air-free with aluminum screw caps and natural rubber septa. Three times the volume of the sample bottle (600 ml) was filled into the bottle in overflow to avoid any entry of oxygen into the water samples. In contrast to methods described by Reeburgh et al. (1991) and Durisch-Kaiser et al. (2005), a larger sample volume (600 ml) was chosen in order to account for the low specific ^{14}C CH_4 tracer activity (100 μl injection volume of ^{14}C CH_4 dissolved in sterile anoxic water, activity 3 kBq) used in this procedure and to obtain sufficient labeled oxidation products even in case of a low methane turnover. The final concentration of the injected tracer (each sample labeled with 5 nM ^{14}C CH_4) was lower than the *in situ* methane concentrations of the water samples (concentration range of the pelagic redox zone: approx. 8 – 800 nM CH_4) to prevent any artificial stimulation of microbial methane oxidation by increased methane concentrations. The ^{14}C CH_4 activity of the injected tracer was determined by stripping of the tracer liquid with synthetic air for at least 20 minutes and a following combustion step on a Cu(II)-oxide catalyst at 850°C (Treude et al., 2003). The resulting $^{14}\text{CO}_2$ was quantitatively trapped with a mixture of phenylethylamine and ethyleneglycolmonomethylether (1:7 v/v), and the activity was measured by liquid scintillation counting (Fig. 2.1).

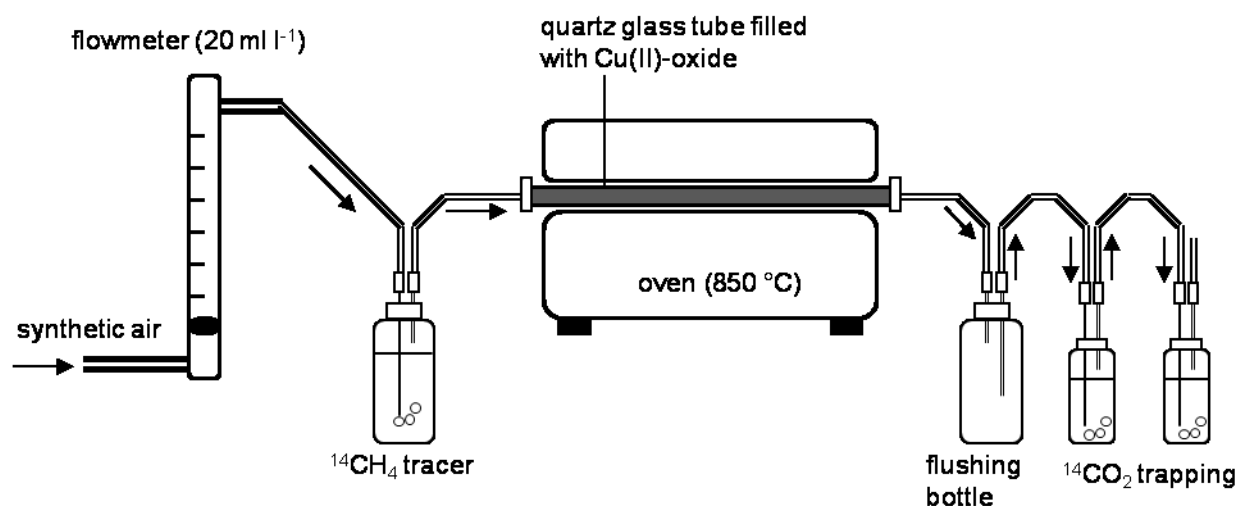


Figure 2.1. Schematic view of the combustion line.

2.1.3.2 Sample processing

After tracer injection, the bottles were incubated in the dark for 3 days near *in situ* temperature (~ 4 °C). The microbial activity was terminated by injection of sodium hydroxide (500 μ l, 50 % (w/w)), which led to the precipitation of dissolved inorganic carbon compounds ($\text{CO}_{2(\text{aq})}$, HCO_3^- , CO_3^{2-}). For trapping of the microbial-formed $^{14}\text{CO}_2$ a method described by (Treude et al., 2005) was used. Briefly, the samples were transferred into gastight bottles equipped with scintillation vials positioned in the gas headspace below the bottle cap. These vials contained a mixture of sodium hydroxide (2.5 % w/w) and phenylethylamine in equal amounts to capture the $^{14}\text{CO}_2$ released from the sample after acidification with hydrochloric acid (5 ml, 25 %) under stirring for 24 hrs. The activity of the scintillation vials was measured on a Tri-Carb 2910 TR (Perkin Elmer Inc., USA) liquid scintillation counter using a scintillation cocktail (Irga-safe Plus, Perkin Elmer). For selected water depths, incubation experiments were performed on triplicates to determine the standard deviation (s in percentage of the average, $n = 3$) of the measured oxidation rates for the upper oxic-, deep anoxic- and oxic-anoxic transition zone in intermediate water depth (80 – 145 m). For the Gotland Deep, the standard deviation for the oxic zone is 12.4 %, the oxic-anoxic transition zone 8.8 % and the anoxic zone 134.4 % derived from triplicates sampled in 70, 85 and 175 m water depth, respectively. For the Landsort Deep, the standard deviation for the oxic zone is

11.7 %, oxic-anoxic transition zone 11.2 % and the anoxic zone 173.2 % determined by triplicates sampled in 70, 80 and 175 m water depth, respectively. The amount of ^{14}C CH_4 tracer used in this thesis was optimized for oxidation processes in waters with low methane content, causing limitations in methane-rich waters, i.e. in the anoxic zone. Therefore, the measured oxidation rates within the anoxic zone cannot provide reliable values for anaerobic methane oxidation. Blank values were obtained by terminating with sodium hydroxide immediately after tracer addition and sample treatment as described above. Assuming a first-order kinetic during methane degradation, the methane oxidation rates (r_{ox}) were calculated according to Eq. (2.1),

$$r_{ox} = \frac{{}^{14}\text{CO}_2 * \text{CH}_4}{{}^{14}\text{CH}_4 * t * 0.9} \quad [\text{nM d}^{-1}] \quad (2.1)$$

where $^{14}\text{CO}_2$ is the radioactivity [dpm = disintegrations per minute] of the microbial-formed carbon dioxide, ^{14}C CH_4 is the radioactivity [dpm] of the injected tracer, CH_4 is the *in situ* methane concentration of the water sample [nM], t is the incubation time [d] and 0.9 the experimentally determined recovery factor (recovery factor of 1 indicates a quantitative release and capture of $^{14}\text{CO}_2$ produced by the turnover of CH_4). This factor was determined by a known amount of $\text{H}^{14}\text{CO}_3^-$ (Hartmann Analytik GmbH, Germany) dissolved in water, followed by acidification and the capture of $^{14}\text{CO}_2$ as described above. The turnover rate constant (k) in Eq. (2.2) expresses the fraction of ^{14}C CH_4 that is oxidized per unit time, whereby the turnover time of methane is represented by its reciprocal ($1/k$).

$$k = \frac{{}^{14}\text{CO}_2}{{}^{14}\text{CH}_4 * t * 0.9} \quad [\text{d}^{-1}] \quad (2.2)$$

The integrated methane oxidation rate over the oxic-anoxic transition zone (ir_{ox}) was calculated by subdividing the depth range of major methane consumption (redox zone and lower oxic zone) into individual depth intervals (Fig. 2.2). Eq. (2.3) describes the area calculation of one depth interval (A_i), with dz [m], the vertical distance of two consecutive

sampling depths, and $f(z)$ and $f(z + dz)$ the determined oxidation rates (r_{ox}) [$\mu\text{mol d}^{-1} \text{m}^{-3}$] of these sampling depths. The integrated oxidation rate (ir_{ox}) was finally obtained by summing up the areas of the individual depths intervals (A_i).

$$A_i = \frac{1}{2} (f(z) + f(z + dz)) dz \quad [\mu\text{mol d}^{-1} \text{m}^{-2}] \quad (2.3)$$

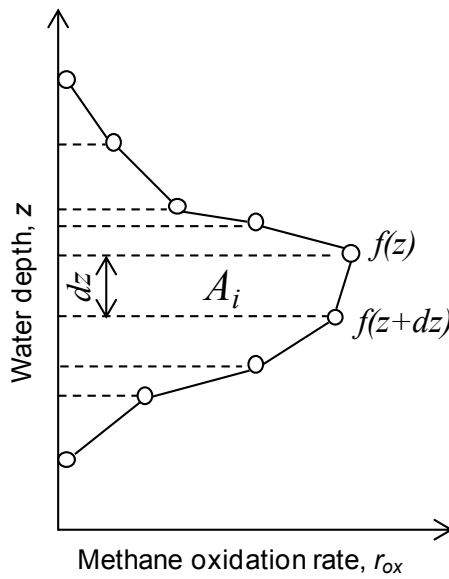


Figure 2.2. Graphical representation of the calculation of the integrated methane oxidation rate (ir_{ox}).

2.1.4 Vertical turbulent diffusivities

To estimate the vertical mixing in the water column based on the methane data set, vertical turbulent diffusivities (K_ρ) were calculated for the upper anoxic zone using the integrated oxidation rates (ir_{ox}) over the depth range of major methane consumption and the methane concentration gradients within the anoxic zone (GD: 150 – 200 m, LD: 150 – 300 m). Here, a constant flux of methane from the deep anoxic water and an almost complete and steady turnover of methane within the redox zone were assumed, i.e. the diffusive methane flux is assumed to match the integrated consumption in the redox zone. K_ρ was calculated according

to Eq. (2.4), where c [$\mu\text{mol m}^{-3}$] is the *in situ* concentration of methane, and z the water depth [m].

$$K_{\rho} = \frac{ir_{ox}}{dc/dz} \quad [m^2 d^{-1}] \quad (2.4)$$

2.1.5 *pmoA* gene and transcript analysis

Water samples for *pmoA* gene and transcript analysis were taken from the rosette water sampler and filled into PET flask. Of each water sample, 1000 ml was filtered on a Durapore filter (0.2 μm pore size, GVWP, Merck Millipore, USA), frozen in liquid nitrogen and stored at -80°C . DNA and RNA were extracted from frozen filters as described by Weinbauer et al. (2002). *pmoA* transcripts (abundance of active methanotrophs) were analyzed with reverse transcriptase PCR (30 – 33 cycles) using the primer system A189f/mb661r (Costello and Lidstrom, 1999; Holmes et al., 1995) followed by DGGE fingerprinting as described in Schmale et al. (2012). Visible bands were cut out of the gel, reamplified and sequenced by LGC Genomics GmbH (Berlin, Germany). Sequences were checked for quality using SeqMan software (DNASTAR Inc., USA). Phylogenetic affiliations of the partial sequences were initially estimated with the program BLAST (Altschul et al., 1990). In addition 50 ng DNA of each water sample was processed via PCR (30 – 35 cycles) and DGGE under the same conditions to determine the total methanotrophic assemblages (abundance of active and inactive methanotrophs) within the entire water column.

2.1.6 Biomarker analysis

Filter samples were taken at pre-defined water depths based on physical parameters and vertical methane distribution using an in-situ-pump on pre-combusted glass microfiber filters (\varnothing 30 cm; 0.7 μm pore size). The filters were kept frozen until analysis. Samples were treated as described in Berndmeyer et al. (2013). Briefly, the filters were repeatedly extracted with dichloromethane:methanol (3:1, v:v) using a microwave extraction device (CEM Mars 5,

Matthews, NC, USA). The extracts were combined to a final volume of 120 ml and an aliquot (40 ml) was acetylated using acetic anhydride:pyridine (1:1, v:v; 1 h at 50° C, overnight at room temperature). The aliquot was then dried under vacuum and analyzed for bacteriohopanepolyols (BHPs) using liquid chromatography-mass spectrometry (LC-MS). The BHPs 35-aminobacteriohopane-31,32,33,34-tetrol (aminotetrol) and 35-aminobacteriohopane-31,32,33,34,35-pentol (aminopentol), indicative for aerobic methanotrophic bacteria and the latter particularly for type I aerobic methanotrophic bacteria (Talbot et al., 2008), respectively, were analyzed to assess the abundance of these microorganisms within the redox zones.

2.2 Materials and methods used for the enrichment experiment

In the following chapter all specific methods are described which were used within the bioreactor enrichment experiment to investigate the methane-dependent denitrification under suboxic conditions within the redox zone of the central Baltic Sea (chapter 5). The applied methods in this study aimed on the characterization of involved microorganisms and the determination of the microbial substrate turnover during the enrichment experiment. A detailed description of the bioreactor set up is given in chapter 5.3.

2.2.1 DAPI staining

The bacterial morphology in the enrichment culture were examined using fluorescence staining after the method described by Porter (1980). Briefly, 20 ml of the enrichment culture was fixed with 1 ml Formalin (37% formaldehyde) and stored for 1h at 4°C in the dark. An aliquot (2 and 7 ml) of the fixed samples was filtered on a membrane filter (Whatman Cyclopore Membrane Polycarbonate Black, 0.2 µm, 25 mm). The filters were exposed to DAPI (4',6-diamidino-2-phenylindole) for 5 min in the dark and analyzed using fluorescence microscopy (ZEISS Axioskop 2 mot plus).

2.2.2 Cell counting

The cell number was analyzed using flowcytometrical measurements (FACS Calibur flow cytometer, Becton & Dickinson) as described by Jost et al. (2008). Briefly, subsamples of 1 ml were taken weekly from the enrichment culture and preserved with 100 μ l paraformaldehyde. Bacterial cells were stained with SYBR Green I DNA stain and measured for 3 minutes at a flow rate of 26.8 μ l min⁻¹. The measuring set up was adjusted to cover a bacterial size range of 0 – 2 μ m. The standard deviation of this method is < 5 %.

2.2.3 Nitrate and nitrite concentrations

The concentrations of nitrite and nitrate in the cultivation vessel were estimated weekly with test stripes (range: 0.0 – 1.7 mM NO₂⁻; 0.2 – 8.1 mM NO₃⁻, Merck, Germany). Additionally, accurate measurements of nitrite and nitrate were determined weekly after Grasshoff et al. (1999) using a continuous-flow-analyzer (Flowsys, Alliance Instruments, Germany).

2.2.4 Denitrification rates

¹⁵N-labeling experiments for the determination of denitrification rates were carried out after 7, 13, and 40 weeks of enrichment. According to the described method by Holtappels et al. (2011), a serum vial of 50 ml was filled in overflow with enrichment culture and immediately screw-capped with red butyl rubber septa. The serum vial was purged (50 ml min⁻¹) with helium for 10 min -under formation of a small helium headspace (5 ml)- to lower the N₂ background concentration and to decrease oxygen concentrations that accidentally contaminated the enrichment culture during sampling. This procedure reduces the concentrations of N₂ and O₂ to 20 % of their initial values (Holtappels et al., 2011). Subsequently, ¹⁵N-labeled nitrite and nitrate (purity > 98 atom% ¹⁵N, Cambridge Isotopes Laboratories, USA) were added to the serum vial under purging with helium to avoid the entry of oxygen and to ensure homogeneous mixing of the labeled sample. The final tracer concentration of the labeled samples was 200 μ M ¹⁵N NO₂⁻ and 287 μ M ¹⁵N NO₃⁻ at week 7, 385 μ M ¹⁵N NO₂⁻ and 245 μ M ¹⁵N NO₃⁻ at week 13, and 54 μ M ¹⁵N NO₂⁻ and 40 μ M ¹⁵N

NO_3^- at week 40. The labeled sample was subdivided into different Exetainers (4 ml liquid, 2 ml headspace). For each incubation time, two parallels were incubated in the dark at 25°C. The microbial activity was stopped after preassigned incubation times (^{15}N -incubations at week 7 after 17, 21 and 25 h; at week 13 after 7.5 h; and at week 40 after 23.5 and 47.5 h) by adding of saturated HgCl_2 solution. The linearity of nitrogen conversion during the incubations was verified by time series experiments in preliminary tests. To determine the production of labeled nitrogen ($^{29}\text{N}_2$ and $^{30}\text{N}_2$) a subsample from the Exetainer-headspace was injected into a GC-MS system (Porapak Q, 80/100 mesh, isotope-ratio mass spectrometer (Delta V plus Isotope Ratio MS (Thermo Fisher Scientific) at the University of Southern Denmark, Department of Biology). Assuming a first-order kinetic during nitrogen conversion, denitrification rates (r_d) were calculated according to Eq. (2.5), where $^{15}\text{N NO}_x^-$ is the tracer concentration of the ^{15}N -labeled nitrate and nitrite, t is the incubation time [h], $^{29}\text{N}_2$ and $^{30}\text{N}_2$ are the concentrations [μM] of the microbial-formed nitrogen and NO_x^- is the nitrate and nitrite concentration [μM] of the bioreactor sample.

$$r_d = \frac{{}^{29}\text{N}_2 + (2 \cdot {}^{30}\text{N}_2) \cdot 10^3}{{}^{15}\text{NO}_x^- \cdot t} \cdot \text{NO}_x^- \quad [\text{nM h}^{-1}] \quad (2.5)$$

2.2.5 Analysis of methane and oxygen concentration

The concentration of dissolved methane in the culture liquid was determined by gas chromatography. Briefly, a gas sample of 100 μl was taken with a gastight syringe (Hamilton) from the bioreactor headspace and transferred via on-column injection into a gas chromatograph (Shimadzu GC-2014), which was equipped with an activated aluminum oxide column (60/80 mesh) and a flame ionization detector. The oven temperature was 50°C and the carrier gas (helium) revealed a flow rate of 25 ml/min. A precision of $\pm 3.6\%$ was determined for the gas chromatographic analysis. The concentration of dissolved methane in the culture liquid was finally obtained by calculation after Weiss (1970) and Wiesenburg and Norman L. Guinasso (1979).

The concentration of dissolved oxygen in the culture liquid was determined by gas chromatography. Gas samples were directly transferred via capillary from the reactor

headspace into a gas chromatograph to avoid any contaminations with ambient air. The injection volume was ensured by a 100 µl sample loop. The gas chromatograph (Thermo Scientific, Trace GC Ultra) was equipped with a capillary column (80 m, molecular sieve) and a PDD detector. The oven temperature was 40°C and the carrier gas helium revealed a flow rate of 12 ml/min. A detection limit of 50 ppm O₂ was determined for this method. The concentration of dissolved oxygen in the culture liquid was finally obtained by calculation after Weiss (1970). Besides the gas chromatographic analysis dissolved oxygen in the culture liquid was continuously measured with an oxygen sensor (Clark-type, precision ± 0.1%, Applikon Biotechnology) to detect the entry of large oxygen quantities.

2.2.6 Methane oxidation rates

The methane oxidation rates measured during the bioreactor enrichment experiment (chapter 5) were determined using the method as described by Jakobs et al. (2013), see chapter 2.1.3. Different to this procedure, a sample volume of only 100 ml was chosen to account for the limited liquid volume of the enrichment culture (5.2 liter). The standard deviation (n = 3) of the measured samples amounted to 10.1 %.

2.2.7 Stable isotope probing and NanoSIMS analyses

2.2.7.1 ¹³C CH₄ and ¹⁵N NO₂⁻ incubations

Homogenous subsamples from the enrichment culture were taken anoxically and transferred into transfusions bottles (600 ml), sealed air-free with aluminium screw caps and natural rubber septa. The transfusion bottles were flushed with argon directly before sampling. Incubation experiments were performed on six subsamples. To determine the cell-specific incorporation of methane a headspace of 50 ml ¹³C CH₄ (99.9 atom % ¹³C, Campro Scientific GmbH, Germany) was applied for three subsamples. To define the cell specific incorporation of nitrogen, Na¹⁵NO₂ (dissolved in water) was additionally added to these subsamples, which revealed finally a concentration of 1.3 mM ¹⁵N NO₂⁻ (in situ conc. bioreactor: 1.1 mM NO₂⁻). The ¹⁵N-incubations were carried out only with ¹⁵N NO₂⁻ due to the low and/or non-

measurable denitrification rates of nitrate determined during the bioreactor runtime. The three residual subsamples served as unlabeled blanks. For these blanks a 50 ml headspace was applied, using the gas mixture that was used for the aeration of the bioreactor (CH_4/CO_2 , 95:5 v/v, purity 99.995 %, Linde gas, Germany). Moreover, the NO_2^- concentration of the blanks was adjusted to the ^{15}N NO_2^- concentration of the labeled subsamples by adding of NaNO_2 . All labeled and unlabeled subsamples were carefully shaken and incubated in the dark for 72 h at 25°C.

2.2.7.2 Stable isotope probing

To determine the phylogenetic affiliation of active methanotrophs the incubated subsamples (see 2.2.7.1) were processed for stable isotope probing as described below (Fig. 2.3). 500 ml of each sample were filtered on Durapore filter (0.2 μm pore size, GVWP, Merck Millipore, USA), frozen in liquid nitrogen and stored at -80°C. The filtered samples were processed according to the described method by Glaubitz et al. (2009) and references therein, which includes the following procedure: RNA extraction, DNase digestion, and isopycnic centrifugation. The gradients were fractionated and the density of each fraction was determined by refractometry. The 16S rRNA of each fraction was quantified by qPCR. Bacterial communities were analyzed with SSCP (Schwieger and Tebbe, 1998) using the primer systems com1f/com2rpH and w036f/w039rph. Bands were cut out off the gel, re-amplified and cloned in E.coli (Strataclone, Agilent). Sequencing was performed by LGC Genomics GmbH (Berlin, Germany). The quality of sequences was checked using SeqMan software (DNASTAR Inc., USA). Phylogenetic affiliations of the 16S rRNA gene sequences were initially estimated with the program BLAST (Altschul et al., 1990). The phylogenetic classification was calculated using the maximum-likelihood algorithms.

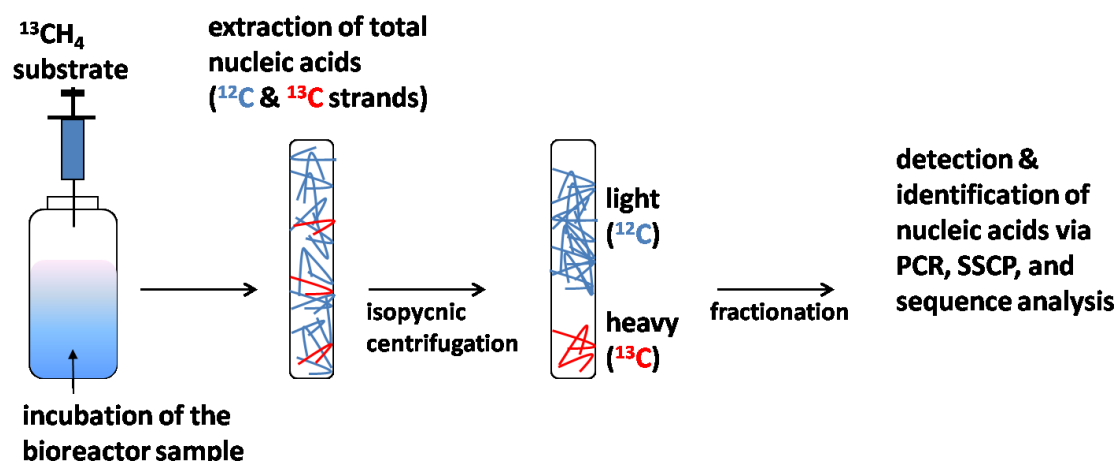


Figure 2.3. Principle procedure of Stable Isotope Probing.

2.2.8 NanoSIMS analysis

The abbreviation NanoSIMS stands for secondary ion mass spectrometry (SIMS) performing quantitative sample analysis of elemental and isotopic composition with a spatial resolution down to nanometer-scale (Nano). In the field of environmental microbiology, the NanoSIMS technique is applied to determine the metabolism of microbial cells using incubation experiments with labeled substrates (Musat et al., 2008). In this study, an aliquot of 3 ml from one labeled and unlabeled subsample (blank) was filtered on a Nucleopore filter (0.2 μm pore size, Nucleopore, Whatmann, USA), dried at RT and sputtered with a gold layer (~ 30 nm Au). Analyses were performed at the IOW using a NanoSIMS 50L instrument from Cameca (France). Images of ^{12}C -, ^{13}C -, $^{12}\text{C}^{14}\text{N}$ -, and $^{12}\text{C}^{15}\text{N}$ - were acquired simultaneously using double focalization mass spectrometry at following conditions: 16 keV energy, $^{133}\text{Cs}^+$ primary ion beam with a current of 4 pA, mass resolving power >7000 . 9 – 45 planes were acquired during scanning from 25 different spots (areas from of 5 x 5 μm to 13 x 13 μm , 512 x 512 pixels, dwelling time 250 μs per pixel). The obtained planes were processed using the software Look@NanoSIMS (Polerecky et al., 2012) based on MATLAB (The MathWorks, Inc.). Briefly, the planes were accumulated after correction of temperature-dependent shifts from plane to plane. Bacteria were defined as regions of interest (ROIs) and the isotopic ratios were calculated for each ROI. In this study, the isotopic enrichment is expressed as atom percent enrichment (APE) according to Eq. (2.6), with the isotopic ratios of the unlabeled (R_i) and $^{15}\text{N}/^{13}\text{C}$ -labeled bacteria (R_f).

$$APE = \left[\frac{R_f}{(R_f + 1)} - \frac{R_i}{(R_i + 1)} \right] * 100 \% \quad (2.6)$$

2.2.9 *pmoA* gene analysis

The abundance of active and inactive methanotrophs was determined using the *pmoA* gene encoding the alpha subunit of the particulate methane monooxygenase (pMMO). The method for the detection of *pmoA* genes was performed in the same manner as applied for the water column studies (see chapter 2.1.5).

2.2.10 Biomarker

The cell material of the enrichment culture was centrifuged and the resulting pellet was subsequently lyophilized. About 7 mg was extracted using a modified Bligh & Dyer extraction method (White and Ringelberg, 1998). Details are described in Berndmeyer et al. (2014). Briefly, about 35 ml of MeOH/DCM/phosphate buffer (2:1:0.8; v:v; phosphate buffer: 8.7 g K₂HPO₄ in 1 l nanopure water, adjusted to pH 7.4 with 6 N HCl) were added to the samples and shortly sonicated. Samples were then shaken and after centrifugation (30 min, 2000 rpm) the supernatant was decanted into a separatory funnel. DCM and water were added to a final ratio of MeOH/DCM/phosphate buffer (1:1:0.9, v:v). The separatory funnel was shaken and the aqueous (MeOH and water) and organic phases (DCM) separated for 6h. The lower DCM phase was obtained and dried as above.

An aliquot (20%) was hydrolyzed using 6% KOH in methanol (2 h at 80 °C in ultrasonication bath), in order to release ester-bound lipids and to extract free lipids. The resulting solution was extracted with n-hexane (3×), yielding the neutral lipid fraction. This fraction was treated with N,O-bis(trimethylsilyl)trifluoroacetamide (BSTFA) for 2 h at 80 °C to silylate alcohols. Fatty acids (FA) were obtained by acidification of the residue of the alkaline reaction solution to a pH of 1 and subsequently extracted using n-hexane (3×). Fatty acids were then converted to their methyl esters by adding trimethylchlorosilane in methanol (1:9; v:v; 2 h, 80 °C) and

were subsequently extracted with *n*-hexane. Silylated neutral lipids and methylated fatty acids were analysed with coupled gas chromatography-mass spectrometry (GC-MS) using a Varian CP-3800 chromatograph equipped with a fused silica column (Phenomenex Zebron ZB-5MS, 30 m ID 0.32 mm, 0.25 μ m film thickness) coupled to a Varian 1200L mass spectrometer (He as carrier gas). The temperature program was 80°C (3 min) to 310°C (held 25 min) at 6°C min⁻¹. Samples were injected splitless into a PTV. Compounds were identified by comparing mass spectra and retention times with published data.

3 Comparative studies of pelagic microbial methane oxidation within the redox zones of the Gotland Deep and Landsort Deep (central Baltic Sea)

3.1 Introduction

Anoxic marine basins are fields of great interest, because they are characterized by high methane concentrations in the deep waters compared to the prevailing concentrations in the upper oxygenated water layer (Reeburgh et al., 1991; Schmale et al., 2010). The emission of methane into the atmosphere has been considered to be small in these marine environments (Gülzow et al., 2013; Schmale et al., 2011). Although microbial oxidation of methane in the water column represents an important sink of methane before it escapes into the atmosphere, the impact of dynamic drivers and environmental conditions, such as methane source strength and hydrodynamic forces, on the efficiency of that particular mechanism is still insufficiently described (Reeburgh, 2007; Schmale et al., 2012). With its distinct oxic and anoxic stratified zones that are episodically perturbed by oceanographic events, the Baltic Sea provides an ideal field to investigate these effects on the methane cycle. The following work focuses on the influence of different oceanographic conditions on the methane turnover within the pelagic redox zone. For this scoping, a comparative interdisciplinary study was carried out in the Gotland Deep and Landsort Deep (central Baltic Sea) in August 2012. These sampling sites differ considerably in the disturbance of the redox zone and the vertical transport of reduced compounds (vertical mixing) towards the redox zone. The combined data on methane chemistry, methane oxidation rates and molecular biological analysis allow first insights on the impact of differing oceanographic settings and regional transferability of microbial processes related to pelagic microbial methane consumption.

3.2 Methods

The methods applied for this and the following field study (chapter 4) are introduced in chapter 2.1 of this thesis. An overview of the conducted field studies and the analytical approach is shown in Fig. 3.1.

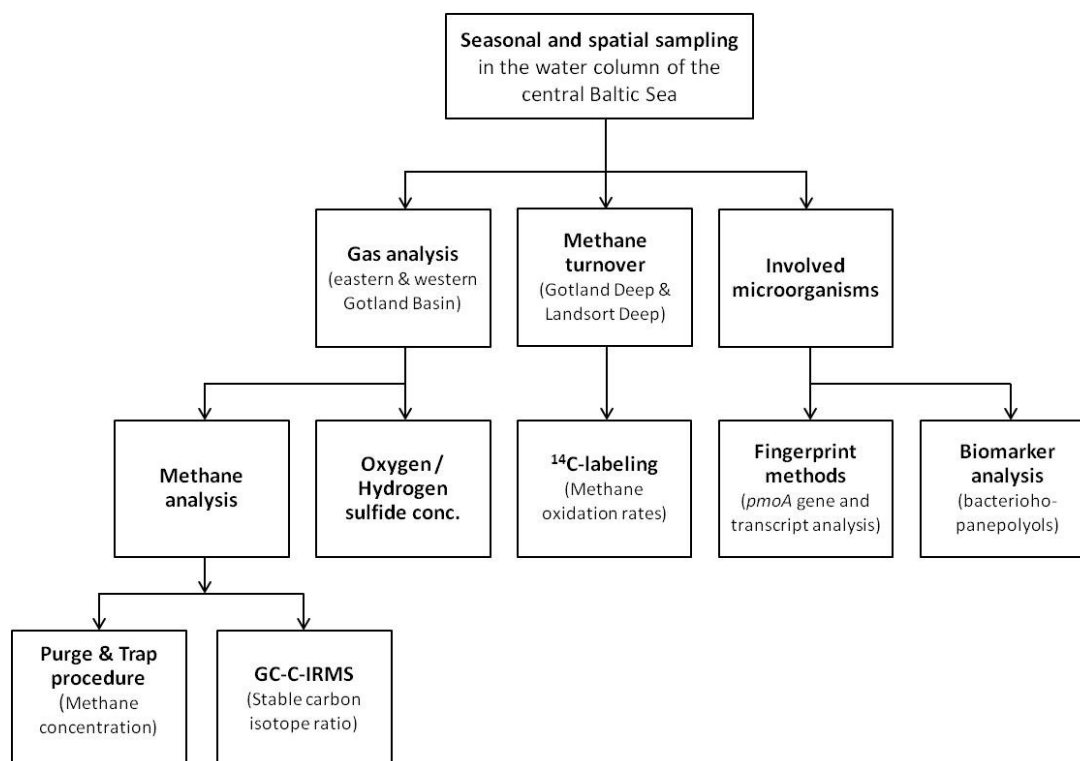


Figure 3.1. Flow diagram of the methods used in conjunction with the field studies conducted in the central Baltic Sea. Details to the different methods are given in chapter 2.1.

3.3 Study area

Investigations were carried out in the water column of the Gotland Deep (57°19.2'N 20°03.0'E; water depth 223 m) and Landsort Deep (58°35.0'N 18°14.0'E; water depth 422 m) located in the central Baltic Sea (Fig 3.2). Both sampling sites are characterized by different basin structures and hydrographic conditions (see cross section through the central Baltic Sea, Fig. 3.2.C). The Landsort Deep represents the deepest areal in the western Gotland Basin

(max. depth 460 m) with a relatively small spatial dimension. In contrast, the eastern Gotland Basin represents the largest basin of the Baltic Sea, with a maximum water depth of about 250 m at the Gotland Deep.

During an inflow of saline waters from the North Sea towards the central Baltic Sea, this water mass propagates first into the eastern Gotland Basin. Depending on the strength of the inflow, the deep water mass can continue its path via a northern passage towards the western Gotland Basin. The travel of inflowing saline water from the North Sea along different basins and sills promotes the mixing between saline bottom water and less saline overlying water masses, resulting in a decreasing salt content of the intruding water along its way into the central Baltic Sea. Accordingly, the Landsort Deep is characterized by less frequent and weaker lateral intrusions, resulting in a more stable oxic-anoxic transition zone (redox zone) and a lower deep water salinity compared to the Gotland Deep (Matthäus et al., 2008).

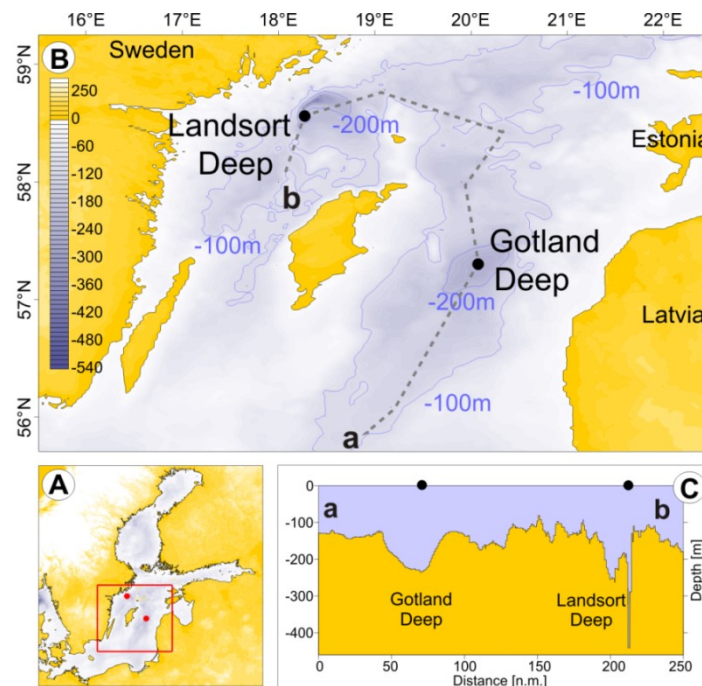


Figure 3.2. (A) Sampling sites in the central Baltic Sea (red dots). (B) Bathymetric map of the central Baltic Sea with the Gotland Deep in the eastern Gotland Basin and the Landsort Deep in the western Gotland Basin. (C) Cross section from the eastern (a) to the western Gotland Basin (b).

3.4 Sampling strategy

Samples were taken during cruise 06EZ/12/13 on RV *Elisabeth Mann Borgese* in August 2012. Sampling for molecular biological analysis and radiotracer experiments were performed after first inspection of the physical parameters of the water column (e.g. salinity, turbidity) using a CTD probe (CTD system Seabird sbe911+ and a turbidity sensor ECO FLNTU, WET Labs) and methane concentration analysis onboard to identify the most relevant depths intervals for methane oxidation. To obtain enough sample volume for all analysis, water samples were taken within five casts on two consecutive days at each sampling site. Methane, oxygen and hydrogen sulfide analysis were performed on the first day of sampling. Water samples for determination of methane oxidation rates and molecular biological analysis were obtained on the following day. Between these two samplings the physical parameters of the water column showed no significant differences.

3.5 Results

3.5.1 Gotland Deep

During the field study the temperature and salinity profiles (Fig. 3.3A) demonstrated strong vertical gradients, revealing thermohaline stratification with pronounced density differences of individual water bodies. The thermocline extended from 15 to 30 m water depth and the halocline was located in a depth interval from 60 to 80 m. The vertical turbidity profile showed two maxima – one in the surface water and the other in around 127 m water depth. According to the content of oxygen (O_2 , Fig. 3.3B), the water column can be separated into different depths intervals (Rabalais et al., 2010; Tyson and Pearson, 1991), an oxic zone from 0 to 81 m ($349 - 9 \mu M O_2$), a redox zone from 81 to 143 m ($< 9 \mu M O_2$) and an anoxic zone below 143 m with no detectable O_2 concentrations. Hydrogen sulfide concentrations (H_2S , Fig. 3.3B) build up slightly between 93 and 127 m ($3 - 17 \mu M H_2S$) but show a stronger increase below that depth interval (max. $172 \mu M H_2S$). The turbidity anomalies covered a depth interval of approximately 62 m (81 – 143 m), reflecting the redox zone and the subsequent transition to anoxic conditions (chemocline) (Kamyshny et al., 2013). For the Gotland Deep it is known that O_2 and H_2S can co-occur at the redox zone (Labrenz et al.,

2010). However, since O_2 concentrations were only measured until first detection of H_2S , the co-occurrence of O_2 and H_2S is not documented in the dataset. Assuming that the suboxic water layer is mirrored by the depth interval of turbidity anomalies (Kamysny et al., 2013), the redox zone is positioned between 81 m and 143 m water depth (Fig. 3.3A).

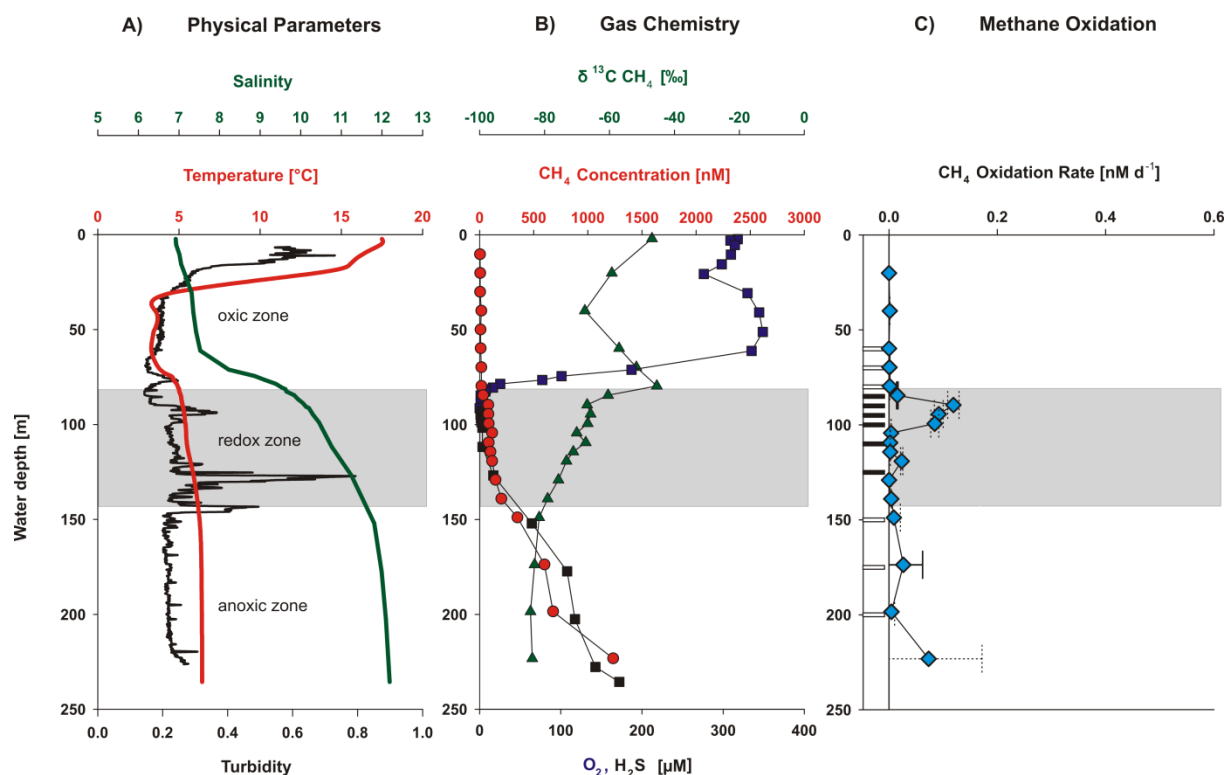


Figure 3.3. Gotland Deep. **(A)** Vertical profiles of salinity (green), temperature (red) and turbidity (black); **(B)** Oxygen (blue squares), hydrogen sulfide (black squares), methane (red circles) and $\delta^{13}C$ values of methane (green triangles); **(C)** Methane oxidation rates (light-blue diamonds) and sampling depths of *pmoA* gene expression analysis (black bars denote the occurrence and white bars the absence of active type I methanotrophs). To obtain the standard deviation (s) for methane oxidation rates, triplicates were taken in three water depths (70, 85, 175 m). The solid error bars indicate the standard deviation from these triplicates, whereas the dashed error bars show the standard deviation calculated from these triplicates for the single water samples. The redox zone is indicated by the gray-shaded area.

The methane profile (Fig. 3.3B) revealed concentrations lower than 10 nM CH_4 in the surface water. Below 80 m water depth, the methane concentration increased with increasing water depth with a methane maximum of 1233 nM CH_4 in the bottom water at 223 m water depth.

The stable carbon isotope ratios in the deep water body are characterized by relatively low $\delta^{13}\text{C}$ CH_4 values (-84 ‰ at 223 m water depth) and a continuous enrichment of ^{13}C CH_4 towards the redox zone with strongly increasing $\delta^{13}\text{C}$ CH_4 values between 90 and 80 m water depth ($\delta^{13}\text{C}$ CH_4 from -67 to -45 ‰). Above the redox zone the isotopic ratio shifted back to more negative values ($\delta^{13}\text{C}$ CH_4 from -45 to -68 ‰) and showed values at the sea surface that are close to atmospheric $\delta^{13}\text{C}$ ratios of methane (-47.6 ‰, <http://www.esrl.noaa.gov/gmd/dv/iadv/>) measured in the Baltic Sea.

Methane oxidation rates were measured in the oxic, suboxic and anoxic part of the water column. The major consumption of methane occurred in a depth interval between 80 and 130 m (Fig. 3.3C). The highest rate was measured within the redox zone (0.12 nM d⁻¹ at 90 m water depth) with a methane turnover time of 455 days ($k = 0.0022 \text{ d}^{-1}$, Fig. 3.5).

Expression of the *pmoA* gene was restricted to only one type I methanotroph in a depth interval from 85 to 125 m. Sequence analysis revealed a similarity of 100 % to an uncultured bacterium named Uncultured GotDeep_pmoA1 (accession number KC188735), which had already been detected earlier in the central Baltic Sea (Schmale et al., 2012). *pmoA* genes could not be detected in the Gotland Deep.

3.5.2 Landsort Deep

Water column data from the Landsort Deep display thermohaline stratification similar to that observed in the Gotland Deep (Fig. 3.4A). The thermocline extended from 10 to 30 m water depth, and the halocline was located in a depth interval from 50 to 80 m. Apart from the turbidity signal in the surface water, a pronounced signal was present in a depth interval between approximately 91 and 130 m (Fig. 3.4A). The oxic zone extended from 0 to 84 m (351 – 9 μM O_2 ; see Sect. 3.5.1 above). Again following the assumption, that turbidity anomalies can be used as an indicator for the depth interval of O_2 – H_2S transition zone (Kamyshny et al., 2013), the redox zone is positioned between 84 and 130 m water depth (Fig. 3.4B). H_2S concentrations increased only slightly within the lower redox zone and remained relatively constant towards the sediment. The deep water revealed maximal H_2S concentrations of about 14 μM .

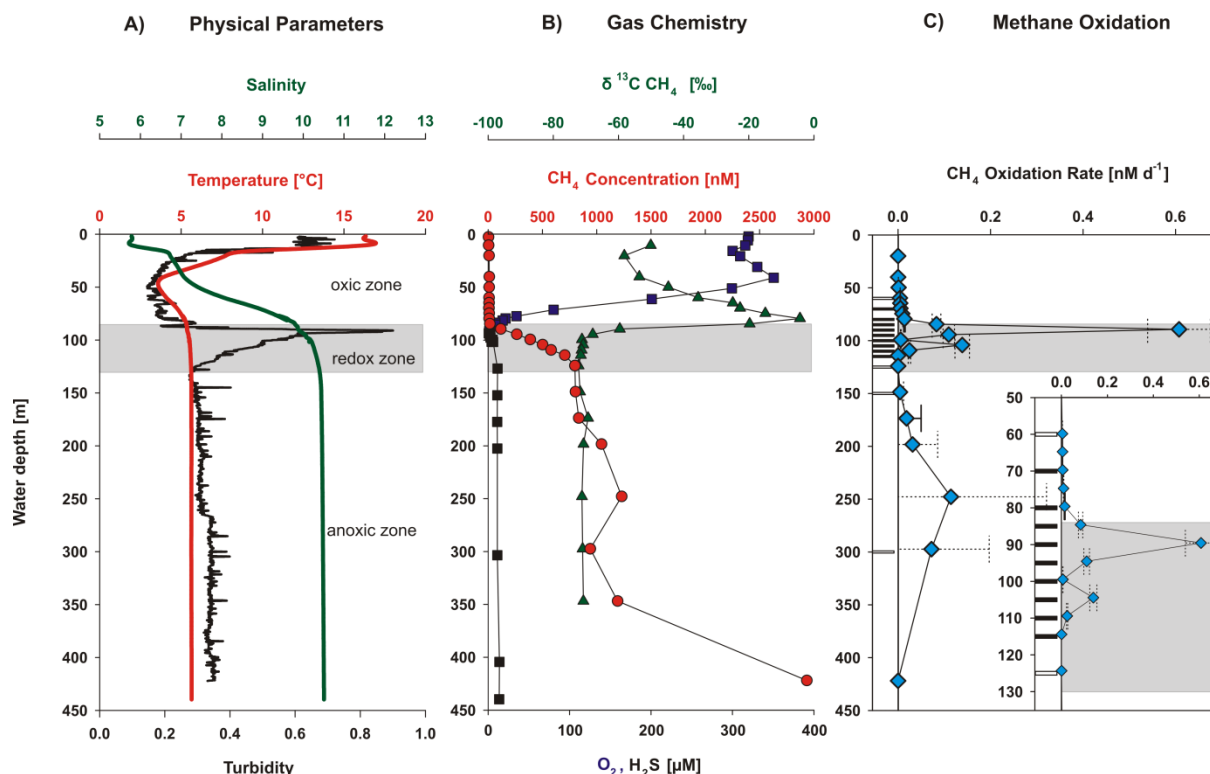


Figure 3.4. Landsort Deep. **(A)** Vertical profiles of salinity (green), temperature (red) and turbidity (black); **(B)** Oxygen (blue squares) and hydrogen sulfide (black squares), methane (red circles) and $\delta^{13}\text{C}$ values of methane (green triangles); **(C)** Methane oxidation rates (light-blue diamonds) and sampling depths of *pmoA* gene expression analysis (black bars denote the occurrence and white bars the absence of active type I methanotrophs). To obtain the standard deviation (*s*) for methane oxidation rates, triplicates were taken in three water depths (70, 80, 175 m). The solid error bars indicate the standard deviation from these triplicates, whereas the dashed error bars show the standard deviation calculated from these triplicates for the single water samples. The redox zone is indicated by the gray-shaded area. The insert in **C**) illustrates the depth interval of the redox zone in higher vertical resolution.

The methane concentration profile showed a strong enrichment close to the bottom (2935 μM CH₄ at 422 m), a pronounced methane gradient within the redox zone (from 80 to 124 m) and methane concentrations lower than 10 nM CH₄ in the surface water. At the redox zone, a sharp stable carbon isotopic shift was found between 99 and 85 m ($\delta^{13}\text{C}$ CH₄, from -71 to -20 ‰ in the upper part of the redox zone).

Methane oxidation was detected throughout the water column, where the major consumption of methane took place between 80 and 115 m water depth (Fig. 3.4C). The highest rate was measured within the redox zone (0.61 nM d^{-1} at 90 m water depth) with a methane turnover time of 127 days ($k = 0.0079 \text{ d}^{-1}$, Fig. 3.5).

As determined for the Gotland Deep, the expression of the *pmoA* gene was restricted to the Uncultured GotDeep_pmoA1 in a depth interval from 70 to 115 m (Fig. 3.4C). *pmoA* genes were detected between 80 and 115 m water depth.

Table 3.1. Result summary.

Parameter	Gotland Deep	Landsort Deep
depth interval of the redox zone	81 – 143 m	84 – 130 m
$\delta^{13}\text{C CH}_4$ (redox zone)	-60 – -79 ‰	-20 – -72 ‰
max. CH_4 conc. (bottom water)	1233 nM, 223 m	2935 nM, 422 m
$\delta^{13}\text{C CH}_4$ (bottom water)	-84 ‰, 223 m	-71 ‰, 422 m
max. methane oxidation rate (r_{ox})	0.12 nM d^{-1} , 90 m	0.61 nM d^{-1} , 90 m
max. turnover rate constant (k)	0.0022 d^{-1}	0.0079 d^{-1}
min. methane turnover time ($1/k$)	455 d	127 d
integrated methane oxidation rates in the redox zone (ir_{ox})	$1.77 \mu\text{mol d}^{-1} \text{ m}^{-2}$	$4.85 \mu\text{mol d}^{-1} \text{ m}^{-2}$
vertical turbulent diffusivities (K_p , upper anoxic zone)	$2.5 \cdot 10^{-6} \text{ m}^2 \text{ s}^{-1}$	$1.6 \cdot 10^{-5} \text{ m}^2 \text{ s}^{-1}$
<i>pmoA</i> detection (DNA analysis)	not achieved	80 – 115 m
<i>pmoA</i> gene expression (mRNA analysis)	85 – 125 m	70 – 115 m

3.6 Discussion

The physical, chemical and microbiological results (summarized in Tab. 3.1) show considerable differences between both deeps. In the following chapter, we will discuss the

different factors controlling the fate of methane in the Landsort Deep (LD) and Gotland Deep (GD) based on data of the methane dynamics and the hydrodynamic situation.

3.6.1 Microbial methane consumption in the Gotland Deep and Landsort Deep

3.6.1.1 Concentration and stable isotope pattern

The measured $\delta^{13}\text{C}$ CH_4 values (GD: -84 ‰, 223 m; LD: -71 ‰, 347 m) in the anoxic waters of both deeps are in the range of those which are representative for a biogenic origin of methane (Whiticar, 1999). This stable isotope signature is modified by microbial methane turnover in the overlain water column as this consumption impacts the concentration distribution of methane and its stable carbon isotope pattern (Reeburgh, 2007; Schmale et al., 2010; Whiticar, 1999). The dataset points to prominent microbial methane consumption within the redox zones in both deeps (Figs. 3.3 and 3.4). The significance of this specific depth interval is emphasized by a constant methane concentration decrease and a pronounced change of the $\delta^{13}\text{C}$ CH_4 values. Here, the observed enrichment of ^{13}C CH_4 within the redox zone in both deeps can be explained by isotopic discrimination during microbial methane oxidation due to the kinetic isotope effect that leads to an enrichment of ^{13}C CH_4 in the residual methane pool (Whiticar, 1999). In the LD, the steeper methane gradient within the redox zone together with the stronger ^{13}C CH_4 enrichment in the lower oxic zone indicates more pronounced and efficient methane consumption compared to the GD assuming similar eddy diffusion.

3.6.1.2 Methane oxidation rates

The outstanding position of the redox zone in the LD and GD as an important depth interval for microbial methane oxidation is also supported by measured elevated oxidation rates in this specific depth. However, remarkable differences are obvious between both deeps. Compared to the redox zone of the LD, which is characterized by the highest oxidation rates (max. rate

0.61 nM d⁻¹), the rates in the GD (max. rate 0.12 nM d⁻¹) were much lower. Oxidation rates measured in the suboxic zone of anoxic basins like the central Black Sea: $1 \times 10^{-3} - 1.6$ nM d⁻¹ (Durisch-Kaiser et al., 2005; Reeburgh et al., 1991) or the Cariaco Trench: 0.4 – 0.8 nM d⁻¹ (Scranton, 1988) are on the same order of magnitude as the data obtained in this study. Also, the integrated oxidation rates (ir_{ox}) calculated for the depth interval along the redox zone of the LD (4.85 $\mu\text{mol d}^{-1} \text{m}^{-2}$, 84 – 130 m) is almost three times as high as the integrated rate in the GD (1.77 $\mu\text{mol d}^{-1} \text{m}^{-2}$, 81 – 143 m). At this zone the maximum turnover rate constant (k) calculated for the LD (0.0079 d⁻¹) is nearly four times as high as the constant in the GD (0.0022 d⁻¹, Fig. 3.5). Assuming that the turnover rate constant is reflecting the population size of methanotrophic microorganisms (Kessler et al., 2011), the growth of these organisms is possibly stimulated by the stronger stability of the intermediate water body that is less perturbed by lateral intrusions in the LD compared to the GD (see Sect. 3.6.2.2). Furthermore, elevated turnover rate constants were also detected in the oxic zone of the LD and not only within the redox zone as it was observed in the GD. This is in accordance with the transcript analysis, which could confirm the expression of the *pmoA* gene above the redox zone of the LD, indicating active methanotrophs also in the oxic zone.

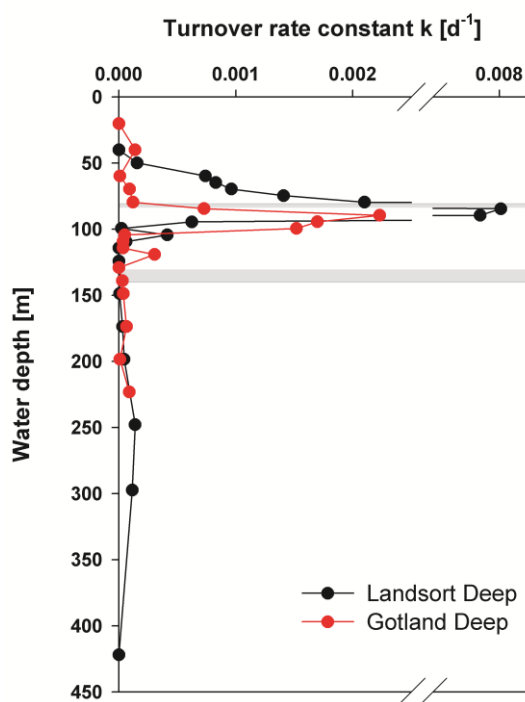


Figure 3.5. Turnover rate constants (k) from the Gotland Deep (red) and Landsort Deep (black). Indicated are the redox zones of the Gotland Deep (grey-shaded area) and the Landsort Deep (white rectangle).

In addition to these perturbations, the concentration of methane also influences the abundance of the microorganisms involved in the turnover of CH₄ within the redox zones of both deeps. Previous studies showed that increased substrate availability results in a dynamic adaption of the population size of the aerobic methanotrophic community (Kessler et al., 2011; Valentine et al., 2001). In conjunction with the present study, this would imply that in comparison to the GD the higher methane concentrations within the redox zone of the LD (GD: 200 nM CH₄, 139 m; LD: 799 nM CH₄, 124 m) promote microbial methane oxidation and the growth of the methanotrophic community. The different population sizes within the redox zones are also supported by the DNA analysis. In contrast to the GD, where no *pmoA* genes could be amplified in PCR reaction and thus probably were below the detection limit, DNA analysis for the identification of *pmoA* genes on the samples obtained in the LD yielded in PCR products. Thus, the *pmoA* gene copy number at GD was below the detection limit of the used approach. In this study, it was not feasible to determine this limit directly. But for soil methanotrophs it ranged between 10¹ and 10² copies of the *pmoA* gene per reaction (Kolb et al., 2003), which could be a realistic number also for the present study.

To determine the kinetic fractionation factor (α) of microbial methane oxidation within the redox zones a plot of $\delta^{13}\text{C CH}_4$ versus $1/\text{CH}_4$ (Fig. 3.6) was created according to Mau et al. (2012). To avoid any side effects in these calculations, which could be caused by lateral intrusions (i.e. input of CH₄ from other regions with a different $\delta^{13}\text{C CH}_4$ signature), the dataset obtained in the LD was used in a first step, which is compared to the GD characterized by a less disturbed intermediate water layer (Dellwig et al., 2012). Motivated by the apparent restriction of methane oxidation within the redox zone, as observable from the methane concentration gradient and $^{13}\text{C CH}_4$ enrichment in the LD redox zone (Fig. 3.4B), a closed-system Rayleigh fractionation approach was applied according to Coleman et al. (1981). The methane oxidation trend between the deep water (1192 nM CH₄, $\delta^{13}\text{C CH}_4$: -71 ‰) and the water depth, which is characterized by the strongest $^{13}\text{C CH}_4$ enrichment within the redox zone ($\delta^{13}\text{C CH}_4$: -20 ‰ at 85 m water depth), fitted best with a fractionation factor (α) of 1.012 (Fig. 3.6A). In a second step, this derived α was used to calculate the oxidation trend in the GD, which is characterized by a more disturbed intermediate water layer (Dellwig et al., 2012). The assumption of a similar α is justified because of comparable temperatures and chemical conditions, and in particular by the identification of the same single methanotrophic bacterium in both deeps (see Sect. 3.6.1.3). The calculated theoretical oxidation trend can be

used to classify each CH_4 data point into three main groups: below the mixing line (CH_4 affected by mixing processes), between the mixing line and oxidation trend (CH_4 influenced by mixing and partly influenced by oxidation) and above the oxidation trend (CH_4 clearly related to oxidation processes). The results show that the CH_4 data points in both basins fit reasonably well in the ^{13}C CH_4 -depleted part of the oxidation trend. However, within the redox zone of the eastern Gotland Basin a deviation is visible in the ^{13}C CH_4 enriched part (Fig. 3.6B). Based on oceanographic studies, which indicated a stronger perturbation of the redox zone in the eastern compared to the western Gotland Basin (Dellwig et al., 2012; Kamysny et al., 2013), it is assumed that the observed deviation from the oxidation trend results from enhanced mixing within the redox zone of the eastern Gotland Basin.

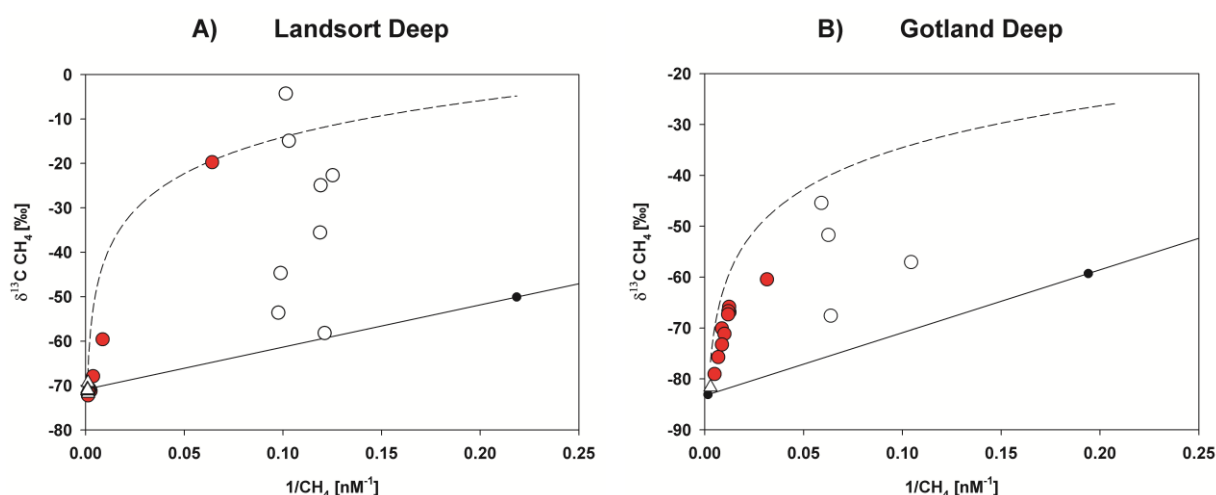


Figure 3.6. Landsort Deep (A) and Gotland Deep (B). $\delta^{13}\text{C CH}_4$ versus $1/\text{CH}_4$. Please note different scales for $\delta^{13}\text{C CH}_4$. The solid lines denote mixing between deep and surface water, the dashed lines represent the oxidation trends based on a fractionation factor of $\alpha = 1.012$, the open triangles indicate the anoxic zone, the red circles the redox zone and the open circles the oxic zone.

3.6.1.3 Aerobic methanotrophs in the redox zone

Sequence analysis revealed that in both deeps, methane oxidation in the redox zone is restricted to type I methanotrophic bacteria, indicating that the different environmental

settings (i.e., methane concentrations and disturbances within the redox zone by lateral intrusions) did not influence the microbial diversity of aerobic methanotrophs. The exclusive detection of type I methanotrophs confirms recently published biomarker analysis, which indicates the absence of type II methanotrophic bacteria in the water column of the GD (Berndmeyer et al., 2013; Schmale et al., 2012). The restricted diversity of type I methanotrophs in the central Baltic Sea is in agreement with studies conducted by Schubert et al. (2006c) in the Black Sea, who identified type I methanotrophic bacteria as the most important methane consumer in the redox zone. However, other studies conducted in the oxic zone as well as in the redox zone of the Black Sea also proved the existence of type II and X methanotrophs (Blumenberg et al., 2007; Durisch-Kaiser et al., 2005). The methanotrophic bacteria identified in the GD and LD is restricted to the phylotype Uncultured GotDeep_pmoA1 (Schmale et al., 2012). A phylogenetically affiliated phylotype of the Uncultured GotDeep_pmoA1 was also detected in a meromictic crater lake (Lake Pavin) that is characterized by a permanently stratified water column (Biderre-Petit et al., 2011). Apart from the identified phylotype in the present study, two main phylotypes of type I methanotrophs have been found in the meromictic lake. It can be assumed that the reduced diversity in the Baltic Sea redox zone is related to an overlap of sulfide- and oxygen-containing waters as a result of lateral intrusions (Dellwig et al., 2012). The influence of sulfide-containing waters on the microbial diversity has been shown by Labrenz et al. (2010). Based on this relation it is assumed that the toxicity of sulfide to many organisms may inhibit the activity of other methanotrophs than the detected phylotype (Schmale et al., 2012). However, a higher diversity of active aerobic methanotrophic bacteria in the compared to the GD less disturbed redox zone of the LD could not be detected.

The detection of the *mcrA* gene for analyzing anaerobic methanotrophs was not performed in the studies due to the main focus on aerobic methane oxidation. From a theoretical point of view, sulfate-dependent methane oxidation (AOM) in the anoxic water layer should be possible as the ambient sulfate concentrations (LD: 0.81 g kg⁻¹ and GD: 0.93 g kg⁻¹; derived from the averaged salinity in the anoxic water layer; calculated after Bruland (1983) would enable this process (Reeburgh, 2007). This assumption is supported by the methane oxidation rate measurements, which indicate anaerobic turnover of methane in both basins. However, the determined oxidation rates are significantly affected by high standard deviations and a potential underestimation due to the chosen ¹⁴C CH₄ tracer amount. The method developed

for this study was designed to analyze microbial methane oxidation within the oxic and redox zone, and as such these oxidation rates cannot provide clear evidence for the existence of AOM processes.

3.6.2 Hydrodynamic controls on the fate of methane in the Gotland Deep and Landsort Deep

3.6.2.1 Vertical mixing

The vertical transport of matter (e.g., nutrients, gases, particles) in the central Baltic Sea is strongly influenced by vertical mixing processes. The different intensities of mixing directly impact the concentration distribution pattern of chemical species in the water column (Holtermann et al., 2012; Nausch et al., 2008). Especially the transport across the chemocline influences important biogeochemical processes as reduced and energy-rich chemical species like CH_4 , H_2S , iron (Fe^{2+}) and manganese (Mn^{2+}) are abundant in high concentrations within the deep water and can drive microbial reactions at the redox zone (Dellwig et al., 2012; Labrenz et al., 2005; Schmale et al., 2012).

Between 300 m water depth and the lower edge of the redox zone (130 m) the LD is characterized by a uniform methane profile, whereas the methane concentrations in the GD decrease constantly with decreasing depth. The same relationship is also reflected by the H_2S profiles and the $\delta^{13}\text{C}$ CH_4 distribution in the anoxic water bodies. The shapes of the methane profiles are related to the different vertical turbulent diffusivities (K_ρ , see also Eq. 4) between the two basins, which are increased nearly 6 times in the LD compare to the GD (K_ρ : GD $1.1 \cdot 10^{-5} \text{ m}^2 \text{ s}^{-1}$, LD $6.2 \cdot 10^{-5} \text{ m}^2 \text{ s}^{-1}$, annual mean at 150 m water depth; (Axell, 1998). The uniform shape of the LD methane profile in a depth range between approximately 150 m and 300 m as well as the increase towards the bottom can be nicely explained by the vertical structure of K_ρ , which shows a maximum (K_ρ : $9.5 \cdot 10^{-5} \text{ m}^2 \text{ s}^{-1}$) in the depth range between 200 and 300 m and a decrease (K_ρ : $1.0 \cdot 10^{-5} \text{ m}^2 \text{ s}^{-1}$) to the bottom.

Assuming that the flux of methane from the anoxic deep water to the redox zone and the consumption of methane within the redox zone are in steady state, the dataset can be used to

calculate vertical turbulent diffusivities (K_ρ) for the upper anoxic zone (GD: 143-200 m, LD: 130-250 m). Using the integrated methane oxidation rates (ir_{ox}) in the redox zones (see Sect. 3.6.1.2) and the methane concentration gradients within the upper anoxic zone, K_ρ can be calculated according to Eq. (4), where c is the *in situ* concentration of methane [$\mu\text{mol m}^{-3}$] and z the water depth [m].

$$K_\rho = \frac{ir_{ox}}{dc/dz} \quad [m^2 d^{-1}] \quad (4)$$

The vertical turbulent diffusivity calculated by this method for the LD are one order of magnitude higher than those for the GD (GD: $2.5 \cdot 10^{-6} \text{ m}^2 \text{ s}^{-1}$, LD: $1.6 \cdot 10^{-5} \text{ m}^2 \text{ s}^{-1}$). This higher vertical turbulent diffusivity in the LD is in accordance with the observations of Axell (1998), who reported a 6 times larger K_ρ for the LD than for the GD at the 150 m depth level. However, the vertical turbulent diffusivity calculated within the present study are 4 times lower compared to the values reported by Axell (1998). The enhanced vertical transport of methane implies a higher supply of substrate to the methanotrophic community within the redox zone of the LD.

3.6.2.2 Lateral intrusions

The turbidity in anoxic basins is often used as a marker to determine the depth of the chemocline. Turbidity anomalies near the chemocline reflect an incompletely understood phenomenon. It is often explained by the diffusion of reduced chemical species across the redox zone, which lead to the precipitation of metal oxides (e.g., oxides of Fe and Mn) or the oxidation of H_2S to elemental sulfur S^0 (Dellwig et al., 2010; Kamyshny et al., 2013). Another theory is that the energy-rich compounds transported from the anoxic zone across the chemocline increase microbial turnover of matter and thus the abundance of bacteria in a discrete depth interval (Dellwig et al., 2010; Labrenz et al., 2010; Prokhorenko et al., 1994). However, the distribution pattern can also be used to discuss the stability of that chemical boundary as lateral intrusions of external water masses into the redox zone will perturb the

established chemical stratification (Kamyshny et al., 2013) and may inject O₂/H₂S enriched water into this specific depth interval (Dellwig et al., 2012). The turbidity profile of the GD (Fig. 3.3A) reveals different distinct peaks along the redox zone. Previous studies in the GD indicate that these turbidity anomalies are related to lateral intrusions into the redox zone (Dellwig et al., 2012; Lass et al., 2003). Therefore, lateral intrusions or internal waves produce perturbations in the intermediate water column and prevent the formation of a clearly defined redox zone. In contrast, the LD reveals only one pronounced turbidity signal on top of the redox zone with a constant decrease with increasing water depth (Fig. 3.4A). Even if this decrease cannot currently be explained, the clear trend without turbidity spikes (in contrast to the observation in the GD) point to a more undisturbed situation in the LD redox zone (Dellwig et al., 2012; Kamyshny et al., 2013). Temperature-salinity diagrams (T-S) are useful approaches to identify the strength of intrusions in the central Baltic Sea (Dellwig et al., 2012). Signatures of intrusions can be identified in the GD by slight variations in the T-S profiles across the entire redox zone (see insert Fig. 3.7A). The LD is characterized by a relatively smooth T-S pattern, indicating the undisturbed situation of this intermediate water layer (see insert Fig. 3.7B).

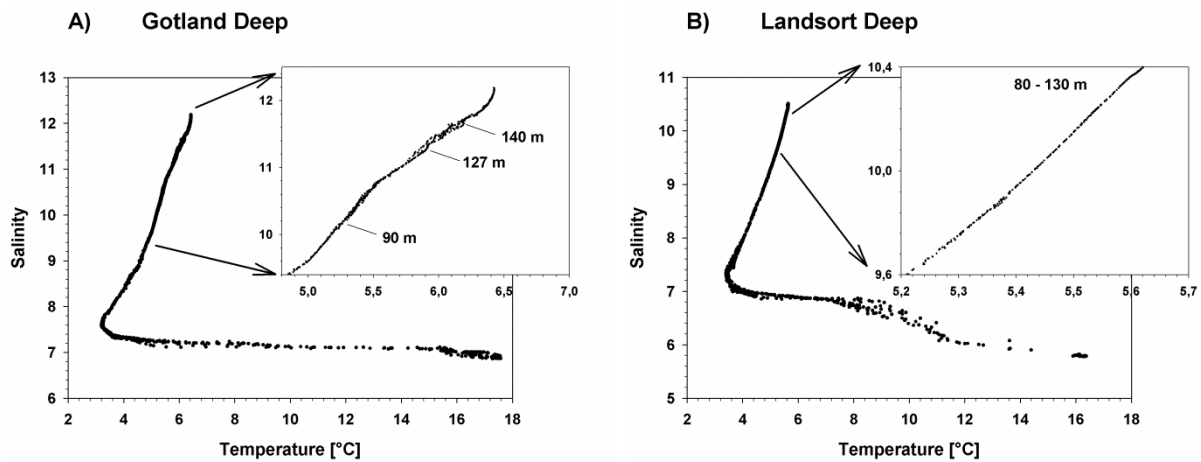


Figure 3.7. Temperature-salinity diagrams. The inserts denote the depth interval where the redox zone is located.

3.7 Conclusions

In the present study, methanotrophic processes within the stratified water columns of the Gotland Deep and Landsort Deep (central Baltic Sea) were investigated to reveal their dependence on different hydrographic conditions. Within the redox zones of both deeps, microbial consumption of methane was identified by the distribution patterns of the concentration of methane, ^{13}C CH_4 and elevated methane oxidation rates. In this intermediate depth interval one potentially active type I methanotrophic bacterium was identified at both sampling sites, indicating that the different hydrographic conditions apparently do not impact the diversity of methanotrophic communities. In contrast, the microbial turnover of methane in the redox zones reveals considerable differences with lower methane oxidation rates in the Gotland Deep compare to the Landsort Deep. The intensity of lateral intrusions and the vertical transport rate of methane from the anoxic zone into the redox zone are different between both deeps, and seem to represent the key processes that control the turnover of methane within the redox zone. The results confirm that pelagic microbial methane oxidation within redox gradients represent an efficient methane sink that prevents the escape of methane from the deep anoxic zone into the atmosphere. The comparative investigations in the Gotland Deep and Landsort Deep also indicate that this microbially mediated process can react on different environmental conditions by adapting the population size of methanotrophs and/or the rate of methane oxidation.

4 Seasonal and spatial methane dynamics in the water column of the central Baltic Sea (Gotland Sea)

4.1 Introduction

Despite the recent progress in gaining a better understanding of methane turnover in the oceans, little is known about the response of the pelagic methane sink to changing environmental conditions such as substrate availability. So far, the few field studies and model developments aimed at that crucial question suggest a dynamic adaptation of the pelagic methanotrophic community on changing methane concentrations (Crespo-Medina et al., 2014; Kessler et al., 2011; Schmale et al., 2011; Valentine et al., 2001; Valentine et al., 2010). Based on these rare studies, the main goal of the present work is directed at the identification and impact of controlling factors on the seasonal and spatial methane distribution as well as the seasonal variability of the microbial turnover of methane. Therefore, data on the concentration of methane and physical parameters was collected on a total of 11 cruises over a two year time period (August 2011 – August 2013) along a transect from the eastern to the western Gotland Basin (central Baltic Sea, see Fig. 4.1). The microbial response on seasonal varying substrate availabilities was analyzed within the redox zones of the GD and LD for selected cruises in summer, autumn and winter using the data on stable carbon isotope ratios ($\delta^{13}\text{C CH}_4$), methane oxidation rates and biomarker concentrations.

4.2 Methods

The methods applied for this study are introduced in chapter 2.1 of this thesis. An overview of the conducted field studies and the analytical approach is shown in Fig. 3.1.

4.3 Study area

The central Baltic Sea (Fig. 4.1) consists of two deep main basins, the eastern (EGB) and the western Gotland Basin (WGB). The EGB comprises the Gotland Deep (GD, 57°19.2'N, 20°03.0'E), which represents the largest sub-basin (max. 250 m), and the adjacent Fårö Deep (FD, 58°00.0'N, 19°54.0'E, max. 205 m). In the WGB, the Landsort Deep (LD, 58°35.0'N, 18°14.0'E) is the major basin and is also the deepest spot (max. 460 m) in the Baltic Sea (Fig. 4.1). In the central Baltic Sea, the strong stratification at the halocline efficiently suppresses the vertical exchange of the surface waters with the deeper water masses. The most efficient way to renew the water masses below the halocline is due to so-called major Baltic Inflows. These inflows, entering from the North Sea, are characterized by a relatively high density and oxygen concentrations compared to the deeper Baltic Sea water. The pathway of the inflowing dense water into the central Baltic Sea follows the basin structure, coming from the western Baltic, reaching first the EGB and continuing its transport route via a northern passage either counterclockwise around the island of Gotland into the north-western Gotland Basin or north-eastwards into the Gulf of Finland, Fig. 4.1 (Meier, 2007). Such an inflow event takes 4 – 6 months to reach the central Baltic Sea (Matthäus et al., 2008). The transport of saline water along its transport route promotes mixing with less saline overlying water masses, leading to a decreasing salt content of the intruding water towards the WGB. Accordingly, the salinity in the deep sub-basins continuously decreases from the EGB to the WGB. During the past two decades, only three (1993, 1997 and 2003) major Baltic Inflows led to a complete ventilation of the deep water layer by the introduction of saline oxygenated water (Matthäus et al., 2008), whereas weaker Baltic Inflows happen more frequently and can renew parts of the deeper water masses (Feistel et al., 2003). In between these strong inflow events, during the so-called stagnation periods, inflowing water masses are not dense enough to replace the water at the bottom and thus, propagate laterally into intermediate water levels of the easterly located Gotland Basin. In the EGB these lateral weak intrusions have a strong effect on the physical and chemical stratification of the intermediate water layer and cause a more perturbed redox zone compared to the prevailing conditions in the same depth level in the WGB (Dellwig et al., 2012).

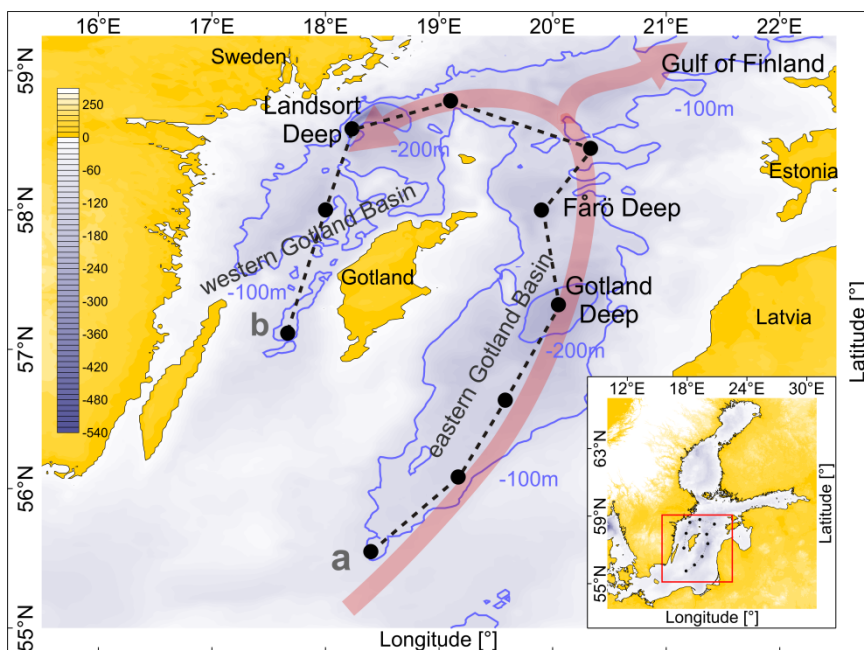


Figure 4.1. Sampling sites (black circles) along the transect (dashed line) crossing the eastern (EGB) and the western Gotland Basin (WGB). The general circulation of inflowing saline water into the central Baltic Sea is illustrated by the red arrows. The insert shows the position of the central Baltic Sea (red square) and the sampling sites (black circles).

4.4 Sampling

Investigations were carried out over a time frame of two years (August 2011 until August 2013) on a transect from the EGB to the WGB, central Baltic Sea (Fig. 4.1). Along this transect water samples for measurements of methane, oxygen and hydrogen sulfide concentrations were collected (Tab. 4.1) in predefined depths at 10 sampling stations on a total of 11 cruises (performed within the monitoring program of the Leibniz Institute for Baltic Sea Research Warnemünde, IOW). At the Gotland Deep and Landsort Deep additional water samples were gathered for methane oxidation rates, $\delta^{13}\text{C}$ CH_4 isotope analyses, and biomarker studies. During these cruises the corresponding physical parameters (salinity, temperature and turbidity) were obtained using a CTD system (Sea-Bird sbe911+ and turbidity sensor ECO FLNTU, WET Labs). The sampling depths for methane oxidation rates and biomarker studies were selected after observation of physical parameters and onboard methane concentration analyses to evaluate the relevant depth interval for pelagic methane

oxidation. On the main cruises where the turnover of methane was investigated (Tab. 4.1), water samples were obtained within five casts: the first three casts were used to determine the depth interval most relevant for methane oxidation (onboard methane, oxygen and hydrogen sulfide analysis), and the remaining two casts to obtain water samples for the determination of methane oxidation rates. The physical parameters of the water column showed no significant changes between these casts.

Table 4.1. Overview of analyzed parameters along the transect from the eastern to the western Gotland Basin. Samples for methane oxidation rates, $\delta^{13}\text{C}$ CH_4 isotope analyses, and biomarker studies were only gathered at the Gotland Deep and Landsort Deep.

Measured parameters	Time of cruise										
	Aug. '11	Nov. '11	Feb. '12	Mar. '12	May '12	Aug. '12	Nov. '12	Feb. '13	Mar. '13	May '13	Aug. '13
methane, oxygen & hydrogen sulfide concentrations	X	X	X	X	X	X	X	X	X	X	X
methane oxidation rates	X	X	X			X					
$\delta^{13}\text{C}$ CH_4 isotope analyses	X		X			X					
biomarker	X		X								

4.5 Results

In the following chapter, the illustration of the results are restricted of the first sampling year (Aug. 2011 – Aug. 2012) to visualize the general physical and gas chemical conditions of the water column. Seasonal and spatial variations of both sampling years (Aug. 2011 – Aug. 2013) will be described subsequently and further discussed in chapter 4.6. The results of the Gotland Deep and Landsort Deep are described in more detail due to the higher vertical sample resolution at these stations and the additional data on $\delta^{13}\text{C}$ CH_4 values, methane

oxidation rates and biomarker analysis (Tab.4.2). The presented data from the Gotland Deep and Landsort Deep collected in August 2012 were already published in Jakobs et al. (2013) and is here embedded into the comprehensive data set of this study.

4.5.1 Salinity and temperature distribution and temporal variations in the central Baltic Sea

During the sampling campaigns between August 2011 and August 2013 the salinity and temperature profiles showed pronounced gradients along the transect, indicating a stable thermohaline stratification of the water column (Fig. 4.2). In the summer time (August) the thermocline was situated in 30 m water depth, separating the warm surface water (max. 16 – 19°C) from the intermediate cold layer located in the 30 – 60 m depth interval. The fall (November) and winter periods (February) were characterized by seasonal cooling (down to 3°C) and complete homogenization of the upper 50 – 60 m of the water column, resulting in a sharp separation of the upper cold from the underlying warmer layer in 60 m water depth. The halocline was located in 60 – 80 m water depth (Fig. 4.2). Salinity decreased continuously in the deep water over time until March 2013. In May 2013 a slight increase of salinity was measured in the EGB as well as in the WGB. The temperature evolved in time similarly to salinity: decreasing slightly until March 2013, and increasing in May 2013.

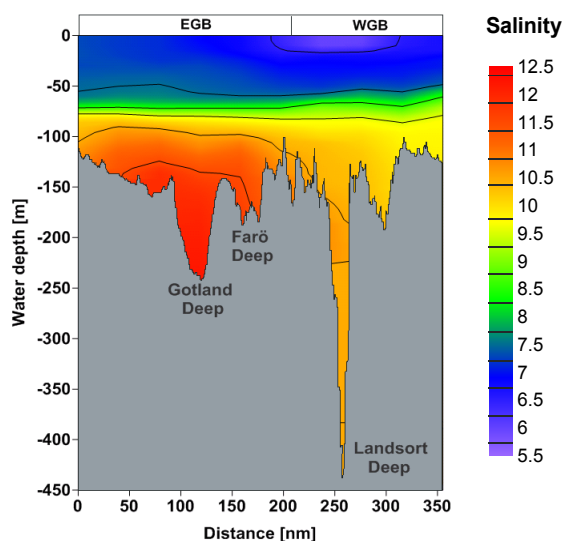


Figure 4.2. Salinity distribution (August 2012) along the transect from the eastern (EGB) to the western Gotland Basin (WGB).

4.5.2 Oxygen and hydrogen sulfide distributions and temporal variations in the central Baltic Sea

Along the transect, the vertical concentration patterns of oxygen (O_2) and hydrogen sulfide (H_2S) were mainly governed by salinity and temperature. Above the halocline the O_2 distribution showed a temperature correlation (Fig. 4.3) with high O_2 concentrations in February/May and lower concentrations in August. Below the halocline, O_2 concentrations decreased rapidly towards the redox zone. The water column can be separated according to the O_2 content into an oxic zone ($> 9 \mu M O_2$), an anoxic zone without detectable O_2 concentrations, and the intermediate redox zone (Jakobs et al., 2013). H_2S concentrations built up slightly below the redox zone and increased towards the bottom water (max. H_2S conc., GD: $176 \mu M$; LD: $41 \mu M$). Seasonal variations of the deep water H_2S concentrations were detected in the EGB as well as in the WGB (Fig. 4.3). O_2 and H_2S can co-occur in the redox zone (Dellwig et al., 2012; Kamyshny et al., 2013; Labrenz et al., 2010). In this study, O_2 concentrations were only measured until the first detection of H_2S , which restricted the exact localization of the lower boundary of the redox zone (chemocline). Another approach to define the lower boundary of the redox zone (i.e. the complete absence of oxygen) is the inspection of water column turbidity anomalies (Jakobs et al., 2013; Kamyshny et al., 2013; Yakushev et al., 2007). Turbidity anomalies are attributed to the precipitation of metal oxides and sulfur caused by the transport of their reduced species (e.g. iron II, manganese II and hydrogen sulfide) across the redox zone (Dellwig et al., 2010; Kamyshny et al., 2013). Moreover, the increase of the bacterial abundance within the redox zone supported by the supply of reduced chemical species from the anoxic deep water has been identified as the reason for the observed turbidity anomalies (Berg et al., 2013; Prokhorenko et al., 1994). In the present study, the chemocline was defined as the depth level where the turbidity dropped down almost to the initial values observed above the redox zone (Figs. 4.4A and 4.8A).

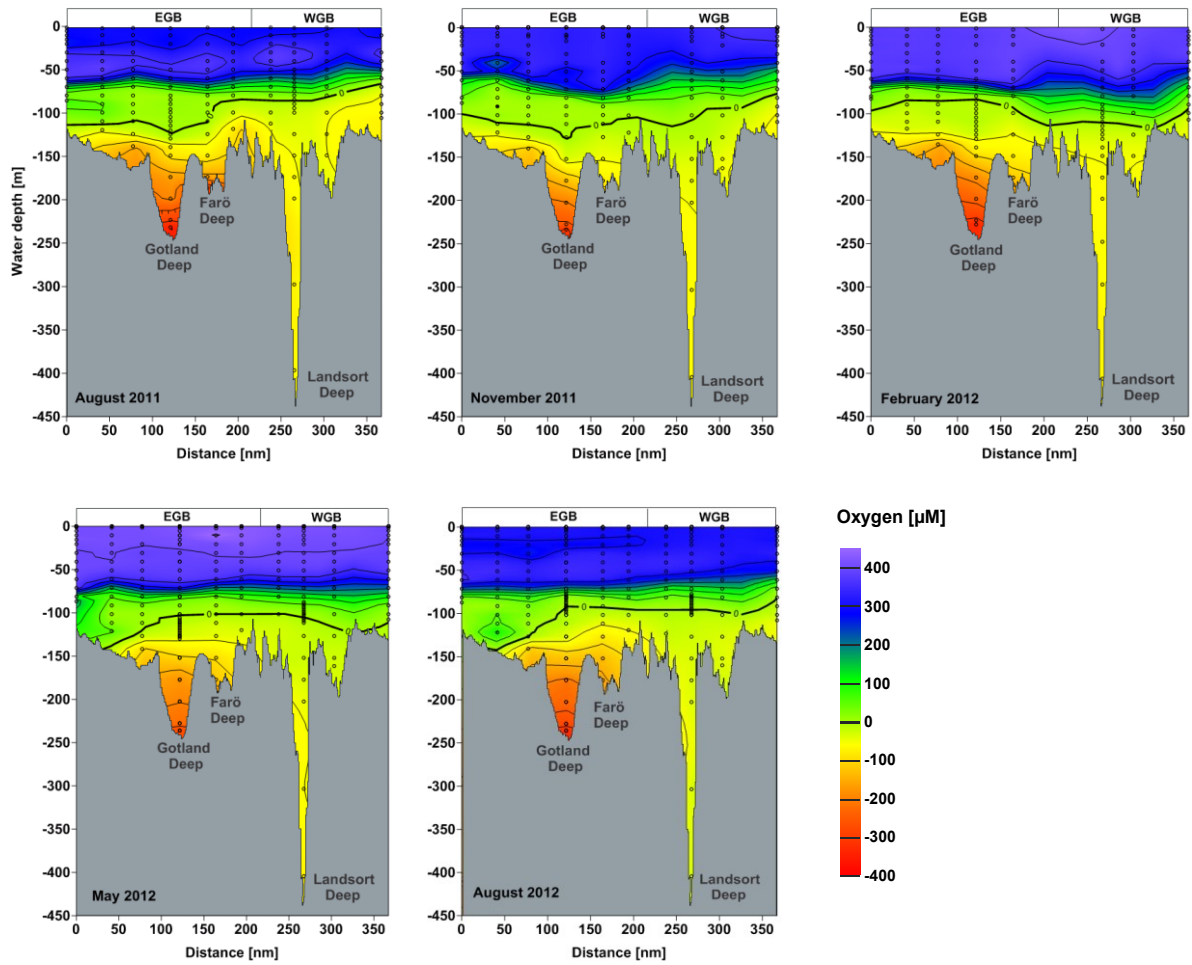


Figure 4.3. Contour plots of oxygen and hydrogen sulfide along the transect from the eastern Gotland Basin (EGB) to the western Gotland Basin (WGB). Hydrogen sulfide is given as negative oxygen equivalents. The bold black lines emphasize the shallowest detection of hydrogen sulfide.

4.5.3 Mid- and deep water methane distributions, isotopic compositions and microbial turnover

4.5.3.1 Eastern Gotland Basin

In the sampling period, maximum methane concentrations were determined in the bottom water of the GD (1518 nM CH₄, May 2013) and FD (1919 nM CH₄, August 2012). The deep water was characterized by a continuous methane decrease towards redox zone. $\delta^{13}\text{C}$ ratios of

methane remained stable over time with relatively low values in the deepest waters in February and August (Fig. 4.4B).

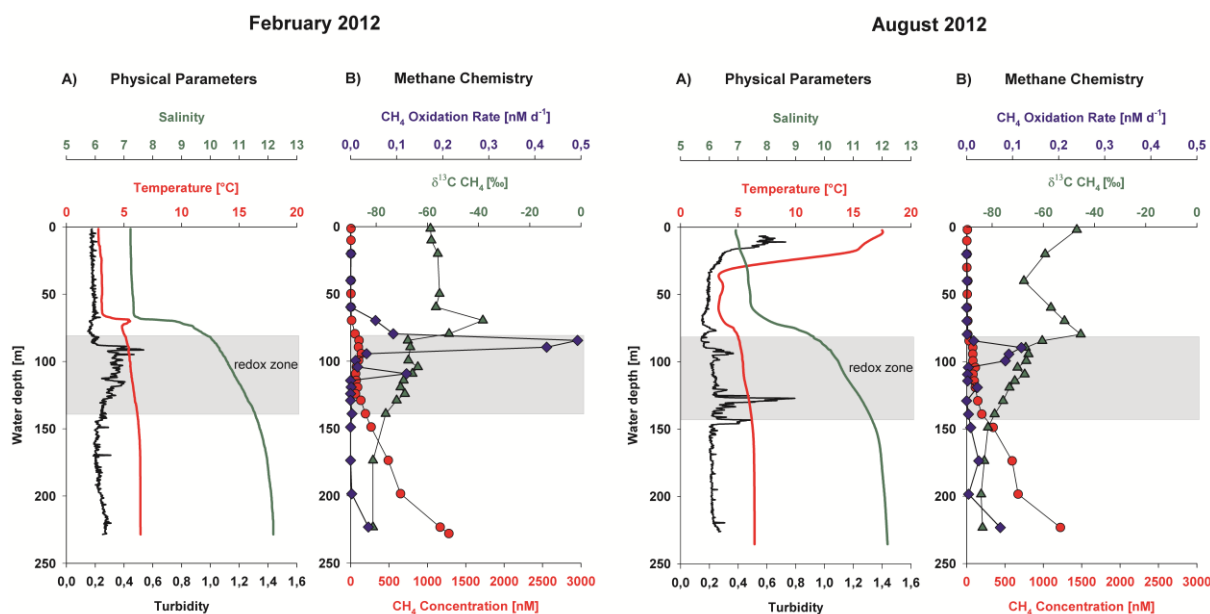


Figure 4.4. Gotland Deep. February and August 2012. **A)** Vertical profiles of temperature (red line), salinity (green line), and turbidity (black line). The redox zone is denoted by the gray shaded area. **B)** Methane concentrations (red circles), $\delta^{13}\text{C}$ values of methane (green triangles), and methane oxidation rates (blue diamonds). The data of August 2012 were taken from Jakobs et al. (2013).

In contrast, the contour plots (Fig. 4.5) of the methane concentration show considerable seasonal variations in the deep water of the EGB. The deep water was characterized by a pronounced methane concentration decrease from August 2011 towards November 2011. Within this period, the deep water methane concentrations decreased by approximately 500 nM CH_4 . This concentration decrease became particularly apparent in the FD, where the water layer characterized by concentrations lower than 300 nM CH_4 expanded almost down to the bottom water. However, from November on, the deep water methane concentrations of the EGB increased to initial levels by August 2012. An identical seasonal trend for the EGB was observed in the following year, with lowest methane concentrations in November 2012, which

mostly recovered until February 2013 and further increased towards August 2013, data shown in chapter 4.6.1.

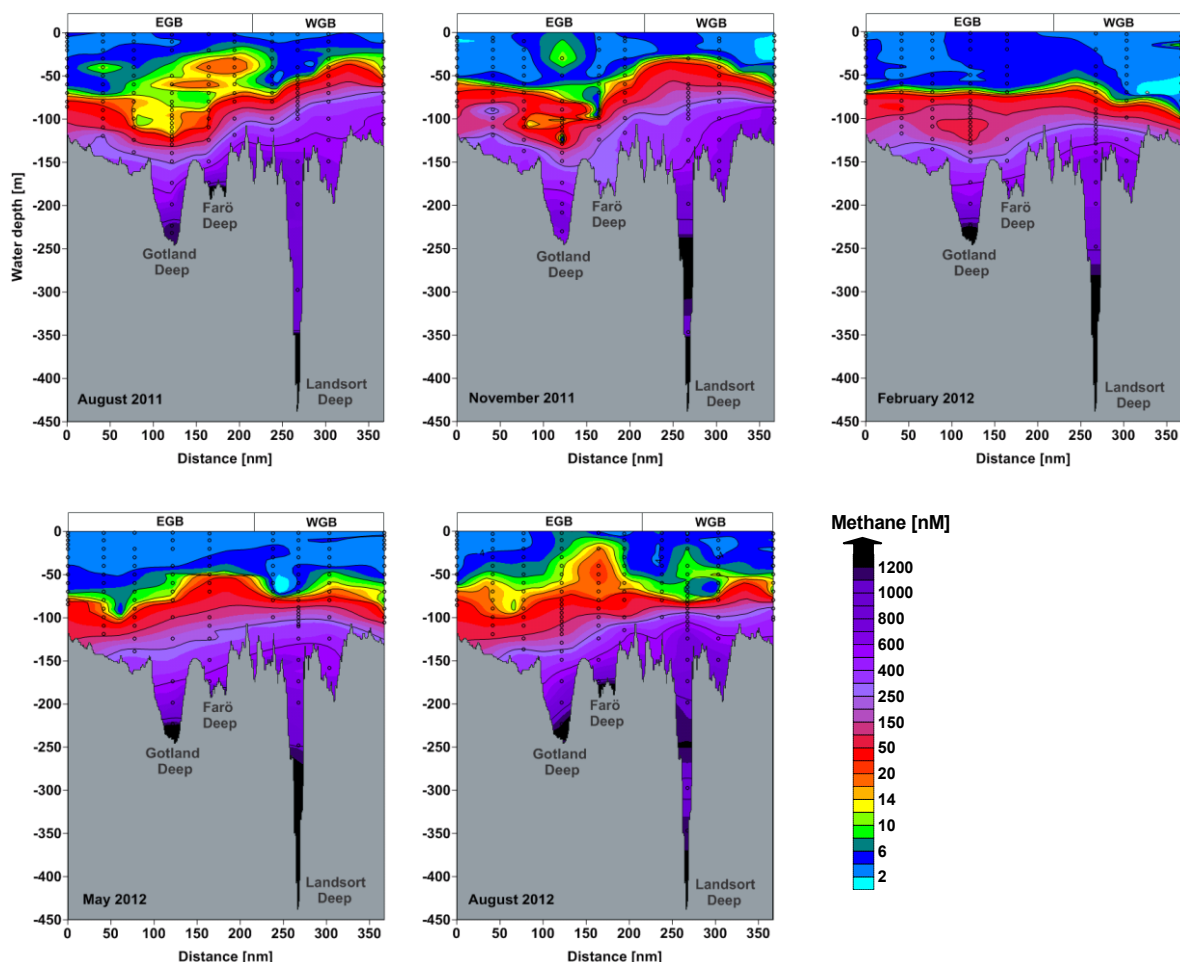


Figure 4.5. Contour plots of the vertical methane distribution along the transect from the eastern (EGB) to the western Gotland Basin (WGB). Please note the non-uniform color coding for the methane concentrations.

The redox zone of the GD was characterized by strongly decreasing methane concentrations towards the oxic water layer and a pronounced ^{13}C CH_4 enrichment within the redox zone (Fig. 4.4B). At this sampling station microbial methane oxidation was detected throughout the whole water column, whereby elevated methane oxidation rates were measured within the depth interval of the redox zone (Fig. 4.4B). Methane oxidation rates in this zone were highest

in February 2012 (max. 0.49 nM d^{-1}) with lowest turnover times of 159 days in November 2011 and 222 days in February 2012 (Tab. 4.2).

The vertical distribution pattern of specific biomarkers, indicative for aerobic methanotrophic bacteria, showed a pronounced concentration increase of aminotetrol and aminopentol between August 2011 and February 2012 within the redox zone (Fig. 4.6, GD).

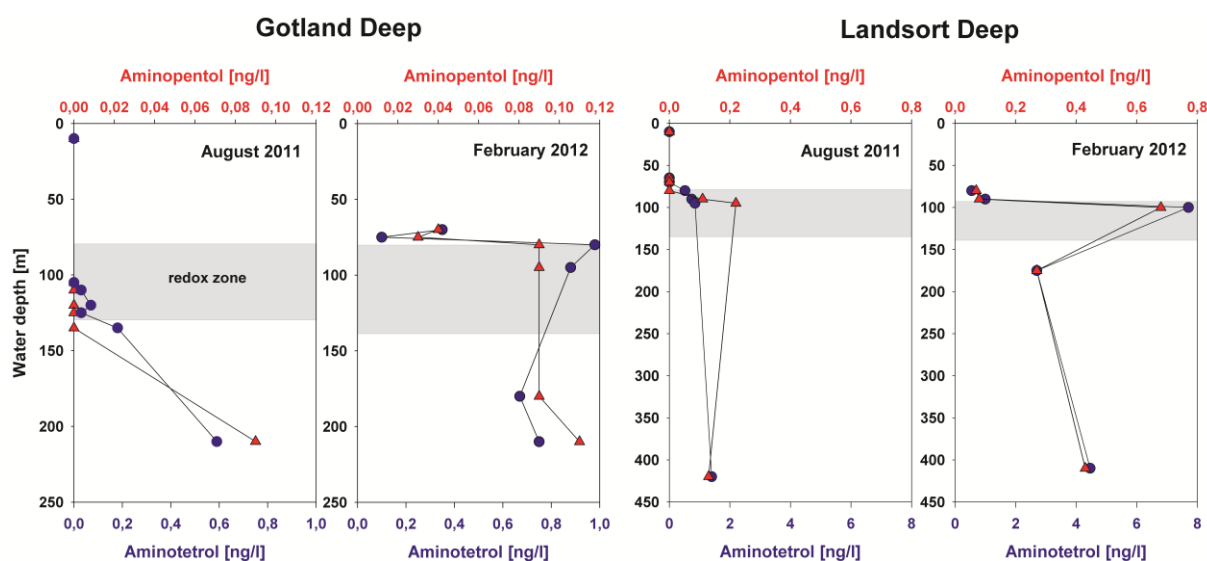


Figure 4.6. Gotland Deep and Landsort Deep. Vertical distribution of aminotetrol (blue circles) and aminopentol (red triangles) in August 2011 and February 2012. Gray shaded areas denote the redox zones.

In the oxic water layer (20 – 70 m) of the EGB slightly elevated methane concentrations (max. 17 nM CH_4) were detected annually below the thermocline in the time frame from May to November (surrounding water: $< 10 \text{ nM CH}_4$, see Fig. 4.7). This methane anomaly was accompanied by an isotopic shift towards lower $\delta^{13}\text{C}$ values between the redox zone and thermocline (Fig. 4.7). However, the water layer above the thermocline was characterized by lower methane concentrations and increasing $\delta^{13}\text{C CH}_4$ values towards the surface water (Fig. 4.7, $\delta^{13}\text{C CH}_4$, August 2012: from -68 ‰ , 40 m to -47 ‰ , 2 m; atmosphere: -47.6 ‰ , <http://www.esrl.noaa.gov/gmd/dv/iadv/>).

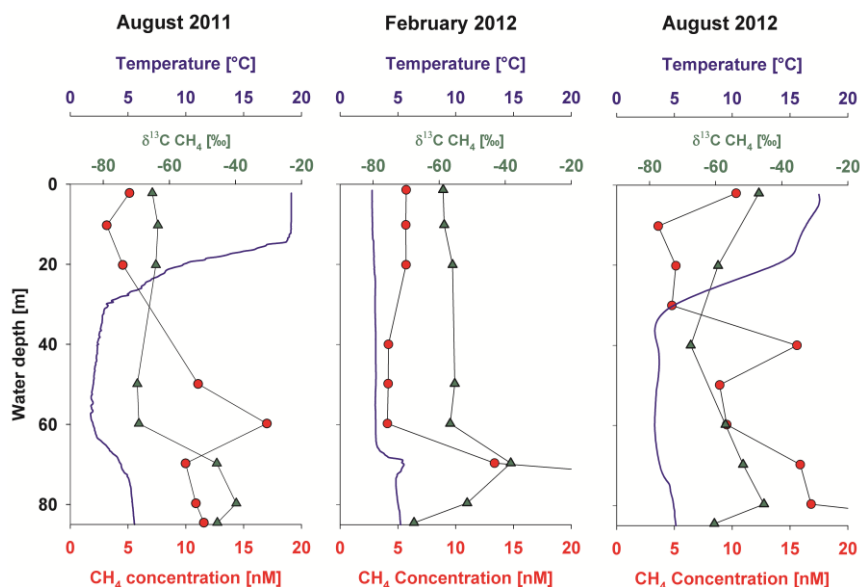


Figure 4.7. Gotland Deep. Vertical profiles of methane concentrations (red circles), $\delta^{13}\text{C}$ values of methane (green triangles), and temperature (blue line) for the upper water column.

4.5.3.2 Western Gotland Basin

The vertical methane distribution in the WGB showed strong methane enrichments with relatively low $\delta^{13}\text{C}$ CH_4 values in the deep water (Fig. 4.8B). The methane concentration pattern in the deep water was characterized by strong temporal variations (Fig. 4.5). Unlike in the EGB, a correlation of the deep water methane variability and the seasonal cycle was not observed.

The redox zone revealed a pronounced methane gradient together with increasing $\delta^{13}\text{C}$ CH_4 values towards the oxic water layer (Fig. 4.8B). The methane oxidation rates showed relatively low values in the oxic and anoxic zone of the water column, whereas elevated methane oxidation rates were detected within the redox zone (Fig. 4.8B). At this zone, methane oxidation rates were highest in February 2012 with lowest turnover times of 63 days in November 2011 and 18 days in February 2012 (Tab. 4.2). As determined for the GD, the highest concentrations of aminotetrol and aminopentol were measured in February 2012 within the redox zone (Fig. 4.6).

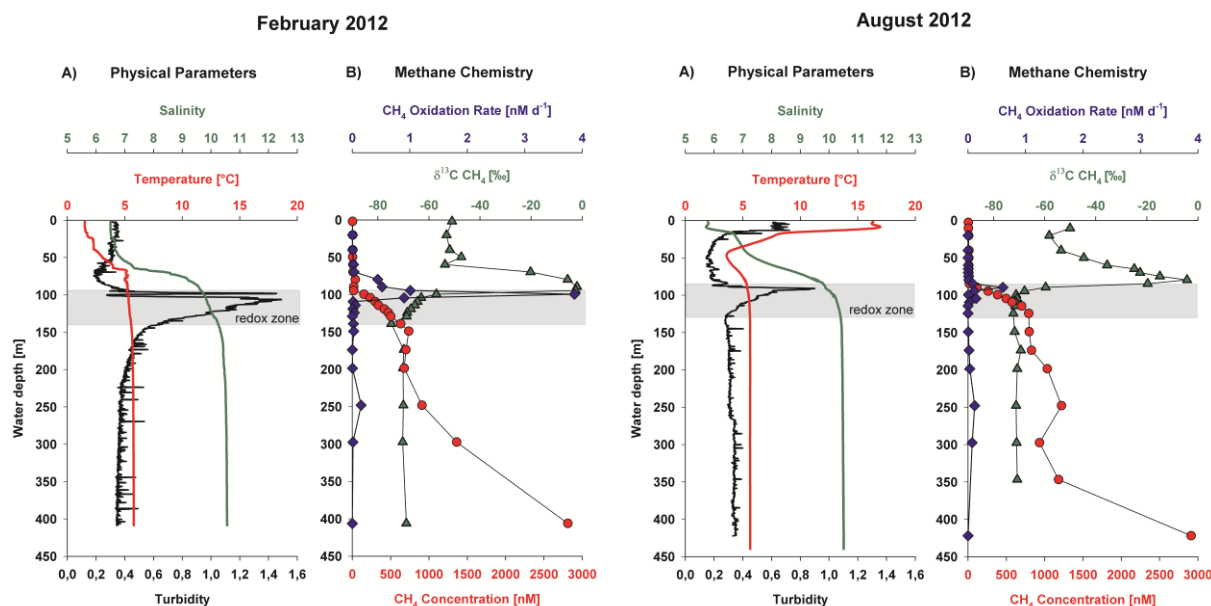


Figure 4.8. Landsort Deep. February and August 2012. **A)** Vertical profiles of temperature (red line), salinity (green line), and turbidity (black line). The redox zone is denoted by the gray shaded area. **B)** Methane concentrations (red circles), $\delta^{13}\text{C}$ values of methane (green triangles), and methane oxidation rates (blue diamonds). Please note different scales for methane oxidation rates in comparison to Figure 4.4. The data of August 2012 were taken from Jakobs et al. (2013).

The oxic water layer of the WGB was characterized by methane concentrations lower than 17 nM CH₄. Similar to summer methane concentrations in the EGB, a methane maximum accompanied by an isotopic shift could be observed in the oxic water layer below the thermocline (Fig. 4.9). The water layer above the thermocline was characterized by lower methane concentrations and increasing $\delta^{13}\text{C}$ CH₄ values towards the surface water (Fig. 4.9), which were close to values measured in the atmosphere of the Baltic Sea (-47.6 ‰, <http://www.esrl.noaa.gov/gmd/dv/iadv/>).

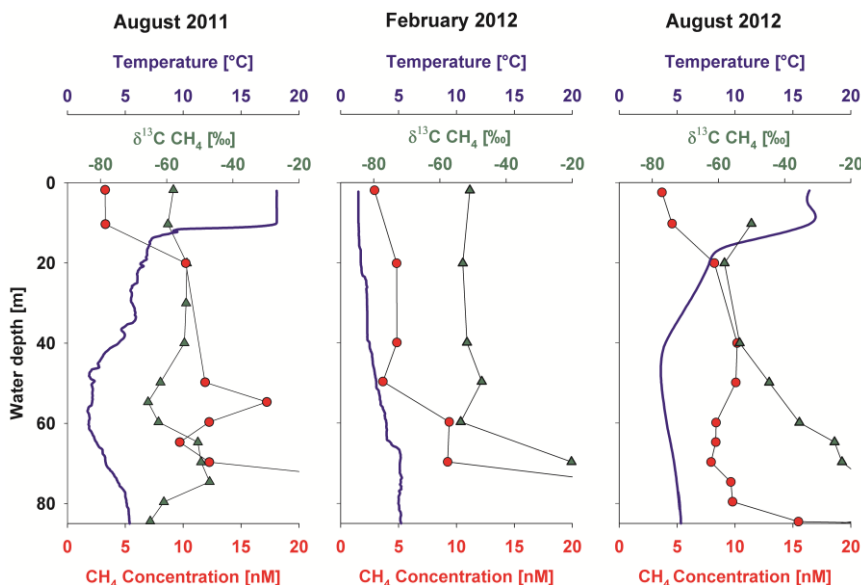


Figure 4.9. Landsort Deep. Vertical profiles of methane concentrations (red circles), $\delta^{13}\text{C}$ values of methane (green triangles), and temperature (blue line) for the upper water column.

Table 4.2. Methane oxidation rates, turnover rate constants, and methane turnover times in the Gotland Deep and Landsort Deep. The data of August 2012 were taken from Jakobs et al. (2013).

Parameter	Gotland Deep (GD)			Landsort Deep (LD)				
Time	Aug. '11	Nov. '11	Feb. '12	Aug. '12	Aug. '11	Nov. '11	Feb. '12	Aug. '12
max. methane oxidation rates [nM d^{-1}] in the redox zone	0.07	0.37	0.49	0.12	1.03	3.65	3.86	0.61
integrated methane oxidation rates, $i_{r_{ox}}$ [$\mu\text{mol d}^{-1} \text{m}^{-2}$] in the redox and lower oxic zone	1.72	6.29	6.45	1.77	8.95	147.26	37.63	4.85
max. turnover rate constant, k [d^{-1}] in the redox zone	0.0028	0.0063	0.0045	0.0022	0.009	0.016	0.056	0.008
min. methane turnover time, k^{-1} [d] in the redox zone	357	159	222	455	111	63	18	125

4.6 Discussion

4.6.1 Influence of vertical mixing on the deep water methane distribution

In the central Baltic Sea, vertical mixing directly impacts the vertical transport of reduced compounds (e.g. iron II, manganese II, ammonia or methane) from the deep anoxic water towards the redox zone (Dellwig et al., 2010; Jakobs et al., 2013; Reissmann et al., 2009). Since the halocline efficiently decouples the surface from the deeper waters, vertical mixing processes in the EGB below the halocline are triggered by wind events, which excite several types of deep water motions (e.g. internal waves). These motions, through dissipation of energy, lead to vertical mixing, which can be quantitatively described by vertical turbulent diffusivities (Holtermann et al., 2014; Holtermann and Umlauf, 2012). In addition, the close distance to the coastline, which can cause coastal-trapped waves, may also influence the intensity of vertical mixing (Axell, 1998).

Seasonal studies conducted by Axell (1998), at the 150 m depth level, indicate a seasonal variability with increased vertical mixing in the EGB in November and February compared to August and May (GD, K_p : August: $0.8 \cdot 10^{-5} \text{ m}^2 \text{ s}^{-1}$, November: $2.4 \cdot 10^{-5} \text{ m}^2 \text{ s}^{-1}$). Calculations for the depth range below 150 m showed even a slight increase of K_p towards the bottom water (Axell, 1998). In the EGB, these K_p strongly correlate with the periodic decrease in methane concentrations in November as well as with the increase in methane concentrations between February and August (Fig. 4.5). These seasonal variations are also visible in the deep water H_2S concentration distribution (Fig. 4.3), which reflected the same fluctuation trend as observed for methane concentrations. The contribution of decomposing organic matter to pronounced seasonal shifts of H_2S concentrations has not been observed in the water column of the Baltic Sea (Nausch et al., 2012). The occurring significant changes of H_2S concentrations are rather described as a result of hydrodynamic events within the deep anoxic water column (e.g. inflow events, turbulent diffusion) (Fonselius, 1981).

Although the vertical turbulent diffusivities calculated for the GD (Fig. 4.10A) are somewhat lower than values determined by Axell (1998), the seasonal difference between August 2011 and November 2011 is of the same order of magnitude. When comparing the magnitude of the calculated K_p with the seasonal variations of the deep water (230 m) methane concentrations (Fig. 4.10A), the pronounced methane decrease in November 2011 correlated with the

enhanced K_p , reflecting an upward transport of deep water methane into the redox zone, where most of it is microbially consumed. In contrast, the decreasing K_p from November 2011 until August 2012 led to an increase in the deep water methane concentrations. Therefore, the highest methane concentrations in the bottom water of the GD were detected in May in both years. Similar to the GD, an even more pronounced fluctuation trend was found in the FD, which can also be attributed to the enhanced vertical mixing during the time period from November until February and lower mixing between May and August. The influence of deep water mixing on the methane concentrations indicates that the observed methane accumulations in the EGB can only occur during time periods of weak vertical mixing. Furthermore, the annual wind-induced increased vertical mixing in November prevents the continuing enrichment of methane even during periods of deep water stagnation.

As described for the EGB, the K_p determined in the WGB are also highest in November and February (e.g. LD, 150 m water depth: November: $7.0 \cdot 10^{-5} \text{ m}^2 \text{ s}^{-1}$; LD, August: $5 \cdot 10^{-5} \text{ m}^2 \text{ s}^{-1}$, Axell (1998)) with considerably elevated values in the WGB compared to the EGB. However, according to the determined depth variations of K_p (Axell, 1998), the influence of vertical mixing is strongly reduced below 350 m water depth in the WGB and showed a maximum within the upper anoxic zone (200 – 300 m, K_p : $9.5 \cdot 10^{-5} \text{ m}^2 \text{ s}^{-1}$). In this study, the vertical structure of K_p was reflected by the measured methane concentrations as well as the vertical distribution of $\delta^{13}\text{C CH}_4$ values (Fig. 4.8). The depth range between approx. 150 and 300 m is directly affected by the enhanced intensity of vertical mixing, leading to the homogenization of the water column and thus to relatively uniform and temporally stable methane concentrations within the upper anoxic zone (e.g. CH_4 conc. in 200 m water depth, Fig. 4.10B). In contrast to the EGB, the bottom water of the WGB was characterized by much higher methane concentrations. The reason for this methane accumulation may be the strong decrease of K_p below 350 m water depth, which can efficiently suppress the turbulent vertical methane flux in these depths. This assumption is further supported by the calculated K_p , showing no clear correlation with the temporal methane concentration profile of the deep water (Fig. 4.10B, 430 m).

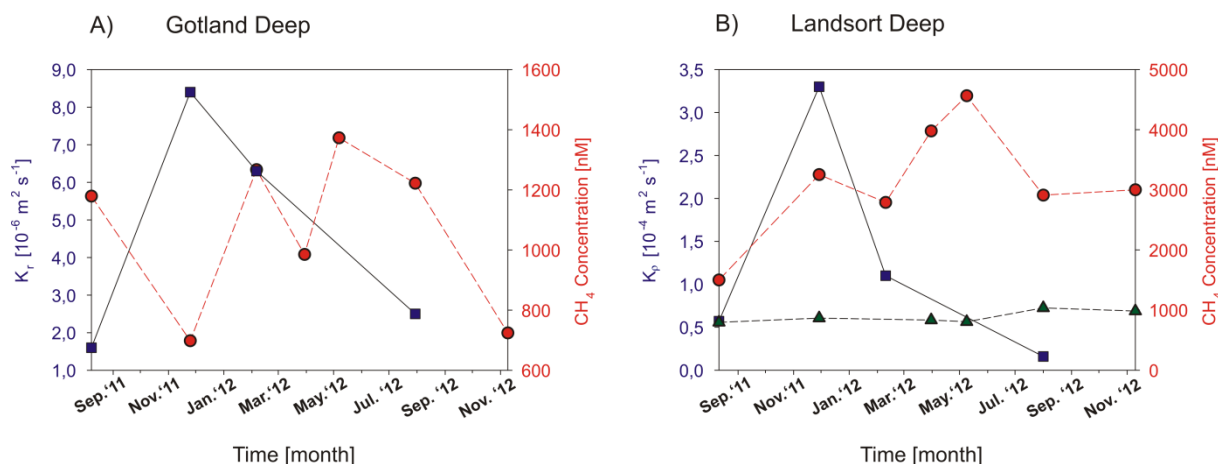


Figure 4.10. Calculated vertical turbulent diffusivities K_p (blue squares) and bottom water methane concentrations between August 2011 and November 2012. **A)** Gotland Deep. Methane concentrations in 230 m water depth (red circles). **B)** Landsort Deep. Methane concentrations in 200 m (green triangles) and 430 m water depth (red circles).

However, the deep water methane concentrations in the WGB (e.g. in the LD) were characterized by considerable temporal variations (Figs. 4.10B and 4.11C). The hydrodynamic impact of mixing processes on the deep water layer can be derived from the vertical salinity distribution, as vertical mixing causes a decrease in salinity due to mixing with less saline overlying water masses. In February 2012 and 2013, enhanced vertical mixing is illustrated by a pronounced salinity decrease in the deep water layer of the LD (Fig. 4.11F). This also implies that in February 2013, the deep water of the LD was significantly more affected by mixing processes compared to February 2012, which is indicated by a strongly decreased salinity below 250 m water depth during the second year. Therefore, methane could only accumulate in that part of the water column (Fig. 4.11C, >300 m, February–May 2012), which was not affected by enhanced vertical mixing. Summarizing, the intensity of vertical mixing as well as the extent of the mixing depth are clearly crucial factors influencing the deep water methane distribution in the central Baltic Sea.

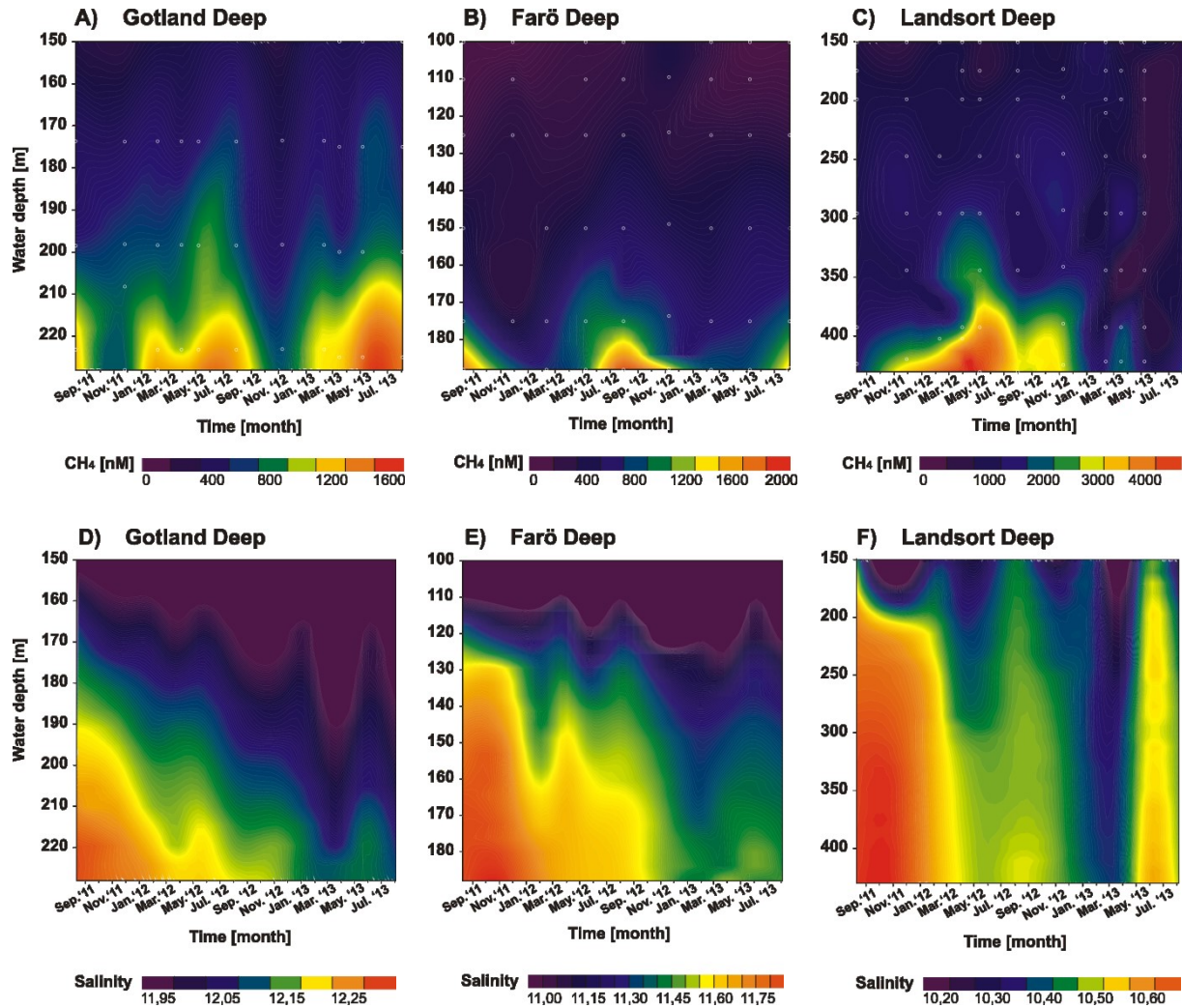


Figure 4.11. Gotland Deep, Farö Deep and Landsort Deep. **A)**, **B)** and **C)** Temporal development of the methane distribution in the deep water. **D)**, **E)** and **F)** Temporal development of the salinity distribution in the deep water. Please note different scales for methane and salinity distribution.

Besides seasonal variations of vertical mixing, potential seasonal changes of the sedimentary methane source (methanogenesis) may impact the methane flux into the redox zone as well. An important factor influencing the methane production is the availability of organic substances. Gustafsson and Stigebrandt (2007) demonstrated for the GD that sinking particulate organic matter has a short residence time in the water column and is thus mainly decomposed in the sediment. Changes in the methane flux caused by seasonal variations of the sedimentation rate of organic material are considered to be insignificant due to the

negligible production of methane within the upper sediment layer (Piker et al., 1998). Piker and co-authors (1998) could show that the bulk production of methane occurs in the deep sediment ($> 1\text{ m}$) below the sulfate-containing sediment layer ($0 - 20\text{ cm}$). In addition changes in the temperature, which can influence the methane production (Bange et al., 1998), cannot explain differences in the methane production rates and sedimentary methane flux since the temperature showed no significant changes (e.g. GD: $\pm 0.01\text{ }^{\circ}\text{C}$) in the deep anoxic water during the sampling campaign. However, even if methane production rates are not available for the time frame presented in this study, it is assumed that the two main drivers for the seasonal modulation of methane production in the sediment are expected to have a minor effect in the deeper basins of the Baltic Sea.

4.6.2 Intrusions of saline water

The salinity and temperature trends of the deep water indicate a stagnation period during the entire sampling time without any ventilation by saline oxygenated water (Nausch et al., 2012, 2013; Reissmann et al., 2009). Besides strong intrusions of saline water from the North Sea, which impact the physical, chemical and biological conditions in the deep water (e.g. major Baltic Inflows), lateral weak intrusions also have the potential to influence the intermediate water layer of the central Baltic Sea (Meier, 2007). The horizontal salinity gradient from the EGB towards the WGB (Fig. 4.2) illustrates that most of these lateral weak intrusions will bypass the GD and further propagate into the deep water layers of the WGB, provided that the transport route is not blocked by any topographic obstacles. This assumption is supported by the density distribution in both basins, which shows that the density measured in the GD at 95 m is similar to the one found in the bottom water (430 m) of the LD.

The seasonal patterns of salinity and methane in the deeper water column (Fig. 4.11) clearly indicate the impact of saline intrusions on the seasonal methane distribution in the WGB. Intrusions of saline water masses most likely directly influenced the deep water methane concentration by dilution with less methane-enriched water. An intrusion of saline water into the LD and a successive methane decrease could be identified in August 2012 and May 2013 (Figs. 4.11C and 4.11D). The penetration of saline water into the WGB was also documented by the measured H_2S concentrations in the deep anoxic waters, which also showed apparent

decreases in the LD from May 2012 (41 $\mu\text{M H}_2\text{S}$) until August 2012 (14 $\mu\text{M H}_2\text{S}$) and from March 2013 (29 $\mu\text{M H}_2\text{S}$) until May 2013 (18 $\mu\text{M H}_2\text{S}$).

The minor influence of lateral weak intrusions on the deep water methane distribution in the EGB is reflected in the data set obtained at the GD. Although slight increases of salinity could be detected in May 2012 and 2013 (Fig. 4.11D), these changes are explained by the variability of the salinity and temperature profile due to deep water motions within the basin. The motions can create reversible changes of about 0.1°C and 0.1 g/kg on time scales of 14 hours to 3 days (Holtermann et al., 2014; Holtermann and Umlauf, 2012). The measured deep water methane concentrations in May 2012 and 2013 even showed an increase (Fig. 4.11A), supporting the notion that waters from deeper areas, which have a higher salinity and methane concentration, have been advected by the deep water motions. The sediment in the GD are characterized by a high turnover of organic matter, resulting in enhanced methane generation and the release of methane into the water column, respectively (Piker et al., 1998). Therefore, it is assumed that the sedimentary methane production in the EGB represents the dominant methane source. Methane-enriched waters intruding from sub-basins upstream from inflowing saline water are a minor additional methane source. In contrast to the hydrodynamic situation in the GD, the northerly situated FD (Fig. 4.1B) shows indications of the impact of lateral weak intrusions on the deep water methane distribution at least at the end of the time series. At this sampling station, the pronounced salinity increase in May 2013 can be attributed to a saline intrusion, and may have thus prevented the accumulation of methane (Figs. 4.11B and 4.11E). In summary, the areas more closely located towards the WGB and characterized by less dense bottom water will be stronger affected by lateral weak intrusions than those in the EGB.

4.6.3 Microbial response on varying substrate availability in the redox zone

The obtained data set in this study together with the embedded data from Jakobs et al. (2013) clearly emphasize the oxidation of methane within the redox zone by significant changes of the $\delta^{13}\text{C CH}_4$ values, a pronounced methane gradient, elevated oxidation rates, and the presence of lipid biomarkers indicative of aerobic methanotrophic bacteria (Figs. 4.4B, 4.6

and 4.8B). In this study, the integrated methane oxidation rates within the redox zone demonstrated the apparent response of the methanotrophic community on seasonally varying substrate (CH_4) conditions (Tab. 4.2). At both locations (GD and LD), the integrated oxidation rates were much larger in November 2011 and February 2012 than in August 2011/2012 (Tab. 4.2). Based on the accelerated methane transport towards the redox zone during November 2011 and February 2012 an adaption of the methanotrophic community can be expected (Mau et al., 2013). Assuming that the turnover rate constant (k) is an indirect proxy for the population size and/or cell activity (Kessler et al., 2011; Valentine et al., 2001), the measured k -values indicated an effective adaption of the methanotrophic community depending on the variable upward supply of methane from the deep anoxic waters.

Apart from k as an indirect proxy, the microbial response was further reflected in the concentration pattern of bacteriohopanepolyols (Fig. 4.6). Within the redox zones at both sampling sites, aminotetrol and aminopentol, together indicative for aerobic methanotrophs and the latter for type I aerobic methanotrophic bacteria (Talbot et al., 2001) showed a pronounced concentration increase from August 2011 to February 2012, indicating a positive adaptation of the methanotrophic community to the increasing substrate supply during this time period (Fig. 4.6). The analysis of biomarkers demonstrated that the enhanced methane turnover in November 2011 and February 2012 (Tab. 4.2) are mainly caused by the increase in population size. However, an increase in biomarker concentrations due to enhanced cell activity cannot be completely excluded since changes in the enzyme activity can influence the metabolism of bacterial cells and the concentration of metabolites and effectors (Röling (2007) and references therein). Interestingly, the aminotetrol and aminopentol were also detected in the anoxic water below the redox zone (Fig. 4.6). Berndmeyer et al. (2013) and Blumenberg et al. (2013) demonstrated that the biomarker signal of aerobic methanotrophs within the GD redox zone is also transferred into the sedimentary geological record. The presence of BHPs in the anoxic water column may thus reflect water column transport between the redox zone and sediment. However, in the deep water, the contribution of other bacteria to these bacteriohopanepolyols cannot be excluded, because sulfate-reducing bacteria (SRB, e.g. genus *Desulfovibrio*), that are abundant in the anoxic waters of the Baltic Sea (Gast and Gocke, 1988), were also identified as producers of aminotetrol and aminopentol (Blumenberg et al., 2012; Blumenberg et al., 2006). However, both compounds were reported

to be only trace compounds in SRB and thus methanotrophic bacteria are considered as the main contributors of aminotetrol and aminopentol in the central Baltic Sea water column.

4.6.4 Methane production in the oxic water layer

In addition to methane oxidation, methanogenesis takes place in the oxic water layer of the central Baltic Sea. First indications for methanogenesis within the water column of the Gotland Deep (GD) were provided by Schmale et al. (2012), who observed a methane anomaly during summer 2008. Similar methane anomaly was also detected in this study. In the oxic water layer, the carbon isotope ratio of methane showed a considerable ^{13}C CH_4 depletion and a pronounced increase of methane (Figs. 4.7 and 4.9) indicating microbial methane production. The isotopic backshift to more negative $\delta^{13}\text{C}$ CH_4 values is caused by the isotope discrimination against ^{13}C during methanogenesis (Whiticar, 1999). As $\delta^{13}\text{C}$ CH_4 values were only determined in the GD and LD, the influence on the stable isotope pattern of methane can only be shown for these two sites. However, during the two-year sampling period, the methane concentration maximum in the oxic water column was detected in a large spatial extension through the EGB and the WGB in a time frame from May until November (Fig. 4.5).

The formation of a temporal thermocline at the beginning of summer separates the oxic water layer into two physically different sub-layers which hamper vertical mixing and the transport of methane towards the surface water (Figs. 4.7 and 4.9, temperature profiles). It is assumed that the observed methane anomaly results from a continuous microbial methane production in the oxic waters, which cannot be compensated by microbial methane oxidation or ventilation into the atmosphere. This leads to an accumulation of methane in the oxic water layer between 20 and 70 m water depth (see Fig. 4.5, August). Wind-induced water column mixing at the beginning of November promotes the deepening of the mixing depth and thus, the upward transport of the accumulated methane to the sea surface and an enhanced release of methane into the atmosphere (see Fig. 4.5, February 2012). In the central Baltic Sea significant differences in the methane fluxes during summer and winter were confirmed by Gölzow et al. (2013), who reported higher methane fluxes in February compared to July/August. The sedimentary methane source apparently does not significantly contribute to

the steady methane enrichment in the oxic water layer during summer and early fall because the isotopic signature within the oxic water layer cannot be explained by the upward transport from the deep methane pool. The pronounced pelagic methane oxidation in the redox zone results in an isotopic shift to more positive $\delta^{13}\text{C}$ CH_4 values. The $\delta^{13}\text{C}$ CH_4 value within the sub-thermocline oxic water layer is lighter than below (governed by methane oxidation in the redox zone) and above (governed by exchange with the atmospheric methane pool), thus clearly pointing to biogenic production within this zone.

Methane anomalies under oxic conditions are well known as the “ocean methane paradox” (Reeburgh, 2007). The accumulation of methane in oxic waters has been observed in different marine environments like the Mediterranean Sea, North Atlantic Ocean (Tragana et al., 1979) or the Gulf of Mexico (Brooks et al., 1981) demonstrating that the process of methanogenesis is not restricted to anoxic sediments. Previous studies postulated that pelagic methane production in the presence of oxygen may result from the metabolisms of methylated compounds (e.g. methylphosphonates (MPn) Karl et al. (2008), dimethylsulfoniopropionate (DMSP) Damm et al. (2010)) or the activity of methanogenic archaea in the presence of photoautotrophs (Grossart et al., 2011). Other theories proposed that the production of methane is related to anoxic micro-niches within organic particles or fecal pellets (Karl et al., 2008; Karl and Tilbrook, 1994). Zooplankton grazing experiments conducted by De Angelis and Lee (1994) showed zooplankton methane production rates depending on the grazing zooplankton species and the phytoplankton diet. Mesozooplankton (copepods) can create local anoxic microenvironments in their guts in an otherwise oxic water column (Tang et al., 2011). These studies demonstrate that the different mechanisms of methane formation have also to be considered as important potential methane sources in the oxic water column of the Baltic Sea.

The data suggest that biogenic methane production within the oxic water column is a general feature of the central Baltic Sea in the summer period, potentially driving the moderate methane flux towards the atmosphere during that part of the year, as well as the enrichment of methane in upwelled waters during summer upwelling reported by Gölzow et al., (2013).

4.7 Conclusion

The present study in the central Baltic Sea shows that seasonal and episodic temporal hydrographic events impact the water column methane distribution and the associated methanotrophic response within the pelagic redox zone. In the eastern Gotland Basin, deep water methane concentrations are regulated by seasonally occurring mixing events, whereas those in the western Gotland Basin are mainly regulated by infrequent episodic lateral weak intrusions. The methane oxidizing community at the redox zone reacts effectively to changes in methane supply, which is determined by the transport from the deep anoxic methane pool. In addition to methane oxidation, methane in the central Baltic Sea is produced in the oxic water layer below the thermocline, in agreement with studies on the “ocean methane paradox” in other marine regions.

5 Bioreactor studies to investigate the methane-dependent denitrification under suboxic conditions within the redox zone of the central Baltic Sea

5.1 Introduction

The evidence of aerobic methane oxidation coupled to denitrification was provided for different freshwater environments, whereas the significance of this process for the marine realm has not been adequately investigated. The goal of this study aims at the investigation of methane-dependent denitrification under suboxic conditions in the marine environment. The stratified water column of the central Baltic Sea with its oxygen-depleted intermediate depth interval (redox zone), which is continuously supplied with methane from the sediments and characterized by pronounced nitrate and nitrite gradients, provides an ideal study area to investigate the link between methane oxidation and nitrogen conversion. In the present study, an environmental water sample from the Gotland Deep redox zone (central Baltic Sea) was gathered as inoculum to accumulate microorganisms under suboxic conditions in a bioreactor consisting of methanotrophic and denitrifying bacteria, which perform methane oxidation coupled to denitrification under suboxic conditions. During the enrichment experiment the culture was monitored by different analytical methods (Fig. 5.1) such as nutrient analysis, cell counting, microbial activity measurements (^{15}N and ^{14}C labeling experiments), biomarker analysis, fingerprint methods, and further characterized by phylogenetic analysis (stable isotope probing) and NanoSIMS measurements.

5.2 Methods

The methods applied for this study are introduced in chapter 2.2 of this thesis. An overview of the analytical approach of the conducted bioreactor enrichment experiment is shown in Fig. 5.1.

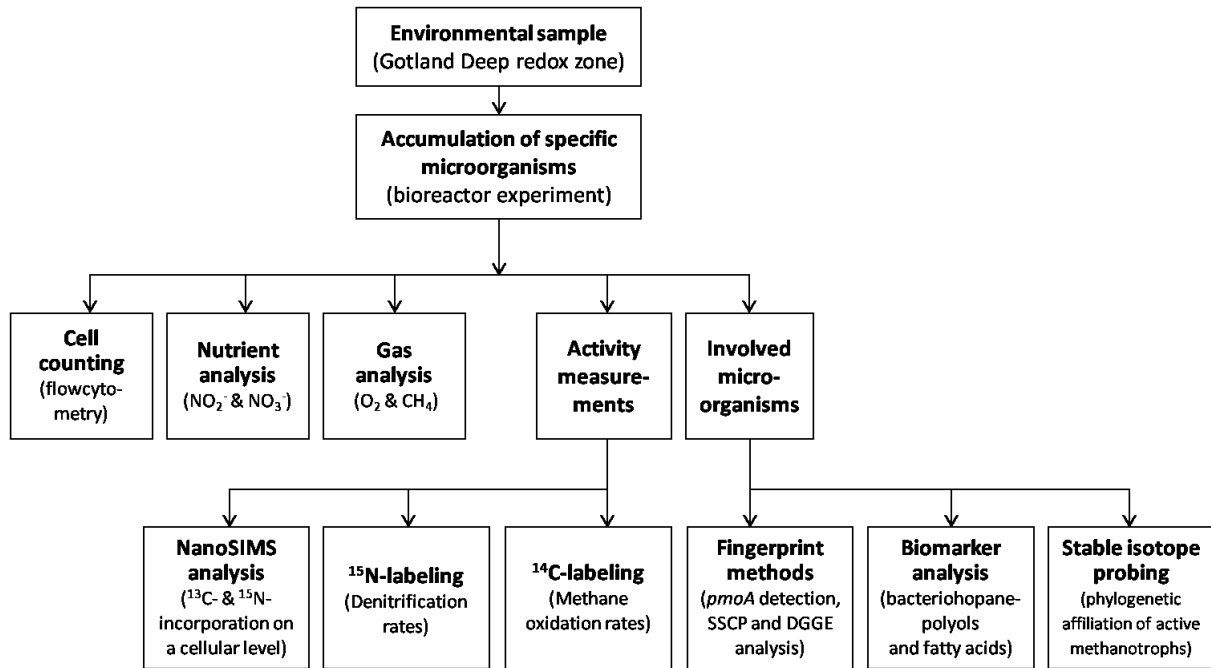


Figure 5.1. Flow diagram of the analytical approach of the conducted enrichment experiment. The methods applied for the enrichment experiment are described in chapter 2.2.

5.3 Sampling strategy at the Gotland Deep redox zone

A water sample of 4.2 liter was taken using a rosette sampler in 86 m water depth from the Gotland Deep redox zone in August 2012. The sampling depth was chosen exactly at the depth where the profiles of nitrate and nitrite revealed pronounced concentration gradients accompanied by strongly decreasing methane concentrations towards the upper water body (Fig. 5.2). Moreover, the sampling depth was characterized by oxygen limiting conditions (2.7 $\mu\text{M O}_2$), representing suitable conditions for aerobic methane oxidation as well as the potential of co-occurring denitrification (Modin et al., 2007; Thalasso et al., 1997).

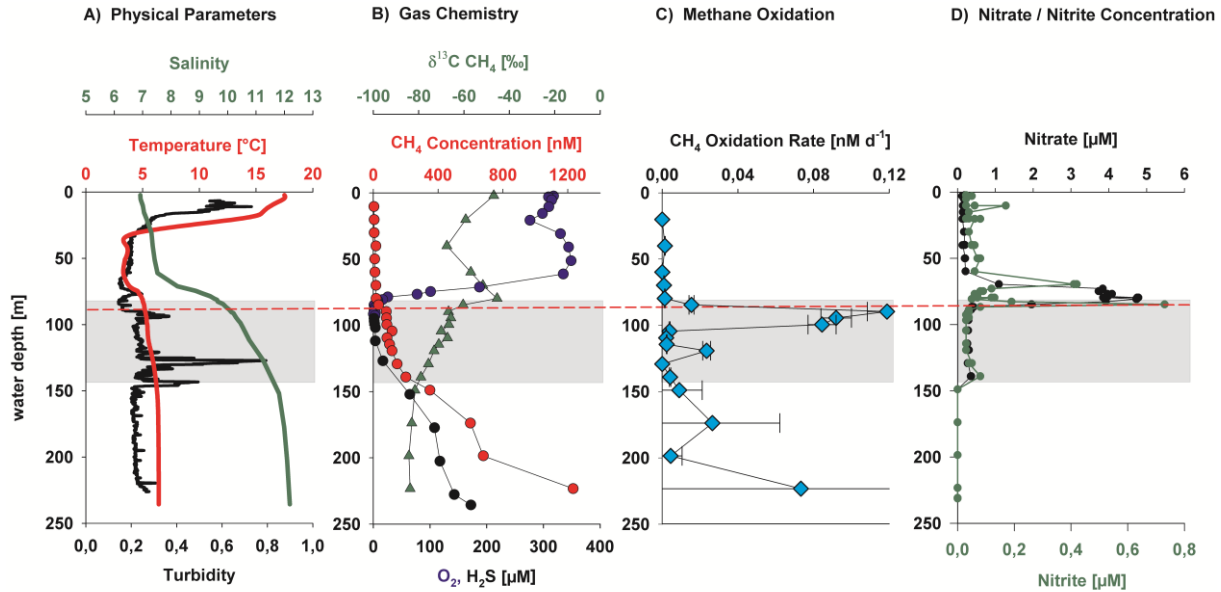


Figure 5.2. Gotland Deep. **A)** Vertical profiles of temperature (red line), salinity (green line), and turbidity (black line). **B)** Methane (red circles), $\delta^{13}\text{C}$ values of methane (green triangles), oxygen (blue circles) and hydrogen sulfide (black circles) **C)** Methane oxidation rates (light-blue diamonds). **D)** Nitrate (black circles) and nitrite (green circles). The redox zone is denoted by the gray-shaded area. The red dashed line illustrates the sampling depth of the bioreactor inoculum.

5.4 Cultivation procedure

The water sample was directly transferred into an autoclaved bioreactor (Fig. 5.3, Applikon Biotechnology, Netherlands, total volume 7 liter, max. working volume during enrichment 5.2 l). Before filling the bioreactor with the water sample, the culture vessel was flushed with argon to avoid the entry of additional oxygen to the enrichment culture. The cultivation procedure was immediately started directly on board after filling the bioreactor and later continued at the IOW. The bioreactor was sparged with a mixture of CH_4/CO_2 (95:5 v/v, purity 99.995 %, Linde gas, Germany) with a flow rate of 10 ml min^{-1} . The CO_2 concentration in the gas supply maintained a relatively constant pH range (6.8 – 7.0) in the enrichment liquid, which was monitored by a pH electrode. A nutrient solution (Tab. 5.1) was continuously supplied (0.1 ml min^{-1}), consisting of an artificial brackish water medium (Bruns et al., 2002), which was modified by addition of nitrite and nitrate, trace elements (Widdel et al., 1983), vitamins (Balch et al., 1979), selenite and tungstate (Widdel and Bak, 1992). The

nutrient solution was prepared with demineralized water ($\geq 18 \text{ M}\Omega \text{ cm}^{-1}$) and analytical-grade reagents. Moreover, during the supply the nutrient solution was continuously sparged with a mixture of Ar/CO₂ (95:5 v/v) to maintain anoxic conditions. To prevent the growing of photosynthetic organisms, the bioreactor was covered with aluminium foil. In addition, all tubings (Norprene[®], Saint Gobain, France) for gas- and nutrient-supply were light-proof and revealed a low oxygen permeability. The culture was continuously stirred (250 r.p.m.) and temperature controlled at 25°C. The gas outlet of the bioreactor was equipped with a gas cooler to condensate evaporated culture liquid, which would be exhausted with the gas stream. The liquid volume of the culture vessel was maintained with a level controller and an effluent pump. Dissolved oxygen in the culture liquid was continuously measured with an oxygen sensor (Clark-type, precision $\pm 0.1\%$) to detect the entry of large oxygen quantities. For more sensitive measurements, oxygen was determined periodically via gas chromatography in the headspace of the culture vessel.

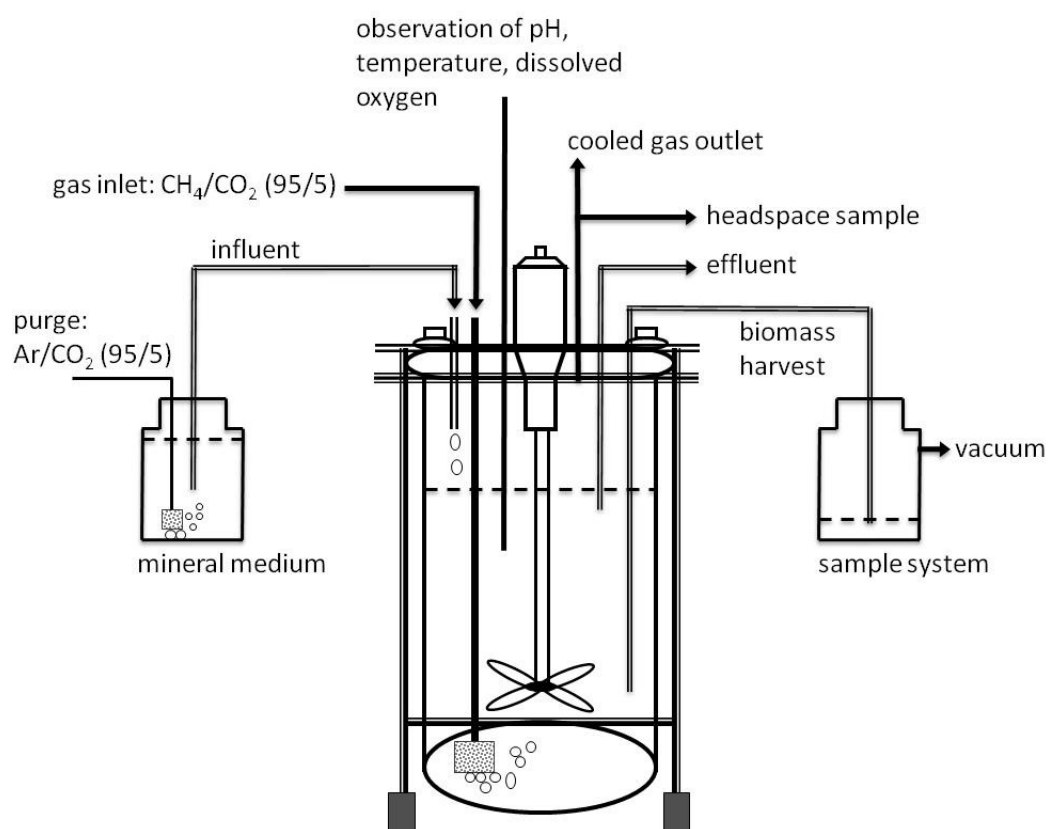


Figure 5.3. Bioreactor set up for the evaluation of the methane-dependent denitrification.

Table 5.1. Compound concentrations of the nutrient solution.

Artificial brackish water medium [mM]			
NaCl	95.0	Na ₂ SO ₄	6.4
MgCl ₂ *6 H ₂ O	11.2	KHCO ₃	10.0
CaCl ₂ *2 H ₂ O	2.3	KBr	0.192
KCl	2.0	H ₃ BO ₃	0.092
SrCl ₂	0.034	KH ₂ PO ₄	0.009
NH ₄ Cl	0.092	NaF	0.016
Nitrate / Nitrite [mM]			
NaNO ₃	5.0	NaNO ₂	1.0
Trace elements [μM]			
FeCl ₂ x 4 H ₂ O	7.54	Na ₂ MoO ₄	0.18
CoCl ₂ x 6 H ₂ O	0.79	NiCl ₂	0.19
MnCl ₂ x 2 H ₂ O	0.62	CuCl ₂	0.015
ZnCl ₂	0.51	HCl (solvent)	33
Vitamins [nM]			
p-Aminobenzoic acid	1820	Thiamin HCl	29.64
Folic acid	9.08	Pyridoxine HCl (Vit B6)	97.2
Biotin	16.4	Cyanocobalamine (Vit B12)	0.15
Nicotinic acid	81.2	Lipoic acid	48.4
Cacium-Pantothenate	45.6	Riboflavin	26.56
Selenite and tungstate [nM]			
Na ₂ SeO ₃ x H ₂ O	6.94	Na ₂ WO ₄ x 2 H ₂ O	5.44
NaOH (solvent)	2000		

The bioreactor was supplied with nutrient solution over a time period of 7 days. Afterwards, the gas influent and gas outlet were closed and the stirrer was stopped to allow for the settling of microbial biomass on the bottom of the culture vessel. After settling for one hour, 1 liter of the supernatant was removed using the effluent pump. During pumping, the gas outlet was connected to a 2 liter flask, which was filled with the exhaust gas and continuously flushed with argon (50 ml min^{-1}), to ensure pressure equalization and to prevent the entry of large amounts of oxygen. This weekly cycle of filling and liquid removal was maintained during the whole time of enrichment.

5.5 Results

5.5.1 Microscopy inspection and cell counting

The enrichment culture contained cocci and rods, whereby rod-shaped bacteria were dominating the culture (Fig. 5.4, week 6 and 15). In the further time course changes in the microbial community were observable, e.g. by the occurrence of flagellates (Fig. 5.4, see luminous dots at week 19).

At the beginning of the enrichment experiment the cell number increased continuously (Fig. 5.5) and showed a maximum of $1.7 \cdot 10^7 \text{ cells ml l}^{-1}$ at week 4 (environmental sample: $8.3 \cdot 10^5 \text{ cells ml l}^{-1}$). This cell number maximum was accompanied by the formation of macroscopically visible particles (particle diameter: $\sim 1 \text{ mm}$). In the following time course the cell number dropped down by 73% from week 4 until week 7 and remained on a relatively stable level afterwards (approximately $4.6 \cdot 10^6 \text{ cells ml l}^{-1}$) with some minor variations until week 40. The end of the enrichment experiment was characterized by two obvious maxima of $1.6 \cdot 10^7$ and $1.4 \cdot 10^7 \text{ cells ml l}^{-1}$, which were observed in week 43 and 53, respectively.

5.5.2 Oxygen concentration

The gas chromatographically measured oxygen content in the culture liquid amounts on average to $0.5 \text{ } \mu\text{M O}_2$. No indications for huge oxygen amounts in the bioreactor were

detected via the Clark-Electrode (detection limit: 45 $\mu\text{M O}_2$) during the whole time of enrichment.

5.5.3 Nitrate and nitrite concentrations

According to the continuous supply of nutrient solution (5 mM NO_3^- and 1 mM NO_2^-), the concentrations of nitrate and nitrite increased steadily within the first weeks of enrichment (Fig. 5.5, I) and reached a concentration plateau at week 10 (0.93 mM NO_2^- nitrite and 4.87 mM NO_3^-). An apparent decrease of nitrite (Fig. 5.5, II) was observed from week 12 (0.93 mM) until week 18 (0.54 mM). In this time frame the nitrate concentrations showed also a pronounced decrease (from 5.12 to 4.79 mM NO_3^-). In the following time period (Fig. 5.5, III) the concentrations increased significantly and reached values (max. 6.54 $\mu\text{M NO}_3^-$ and 1.13 $\mu\text{M NO}_2^-$), which exceeded the nitrite and nitrate concentrations of the added nutrient solution. The end of the enrichment experiment (Fig. 5.5, IV) was characterized by nitrite and nitrate concentrations, comparable to those, which were adjusted for the nutrient solution.

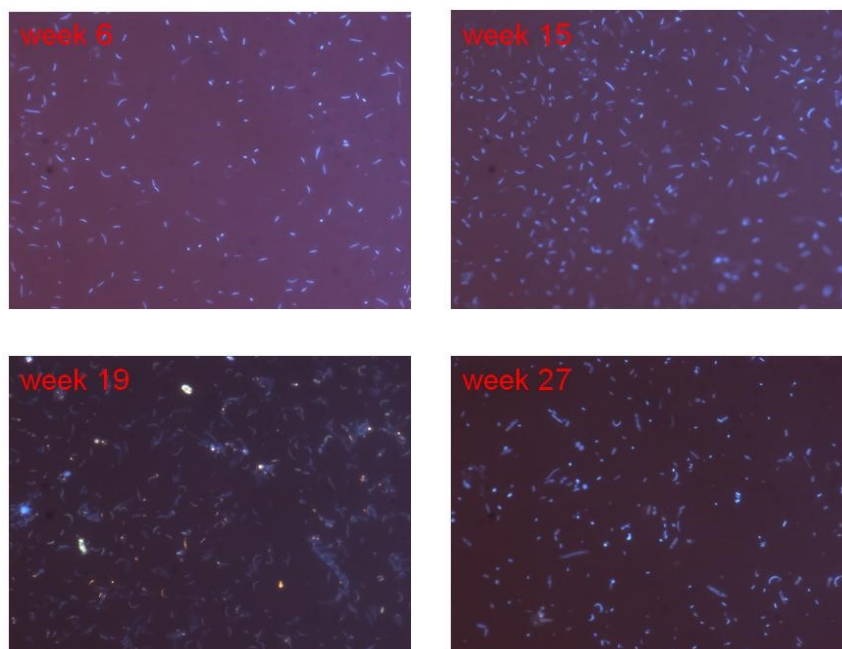


Figure 5.4. Microscopy examination (1000-fold magnification) of DAPI stained cells showing coccoid- and rod-shaped bacteria. Please note the microscopy pictures were obtained with varying filtration volumes (week 6 and 27: 2 ml; week 15 and 19: 7 ml).

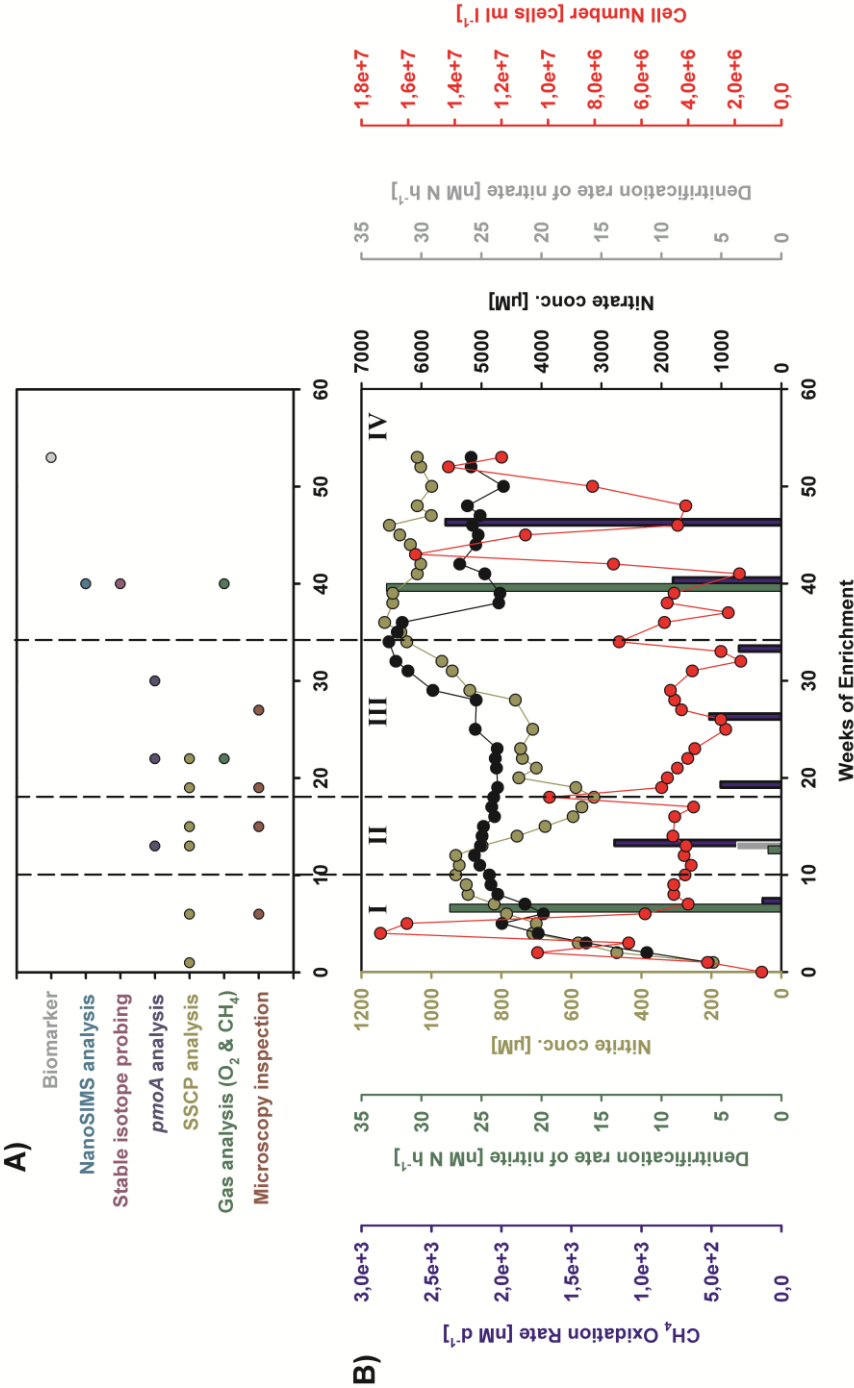


Figure 5.5. A) Chronological overview of the applied analytical methods during the enrichment experiment. B) Result overview of the temporal development of the cell number (red circles), concentrations of nitrate (black circles) and nitrite (light green circles), denitrification rates of nitrate (green bars) and nitrite (grey bars), and methane oxidation rates (blue bars). Roman numerals denote the different development stages of the enrichment culture.

5.5.4 Denitrification rates

The determined reduction of nitrite at the beginning and at the end of the enrichment experiment was on the same order of magnitude (Fig. 5.5, I and IV). Compared to these measured rates the nitrite reduction was strongly decreased at week 13 (Fig. 5.5, II). However, the conversion of nitrate was only observed at week 13.

5.5.5 Methane oxidation rates

The measured methane oxidation rates showed significant temporal variations over the course of the enrichment. The lowest oxidation rate (132 nM d^{-1}) was measured at the beginning of the experiment at week 7 (Fig. 5.5, I). However, already the following measurement at week 13 (Fig. 5.5, II) showed a strongly increased oxidation rate (1191 nM d^{-1}). Compared to this oxidation rate, the intermediate period of the enrichment experiment (Fig. 5.5, III) was characterized by lower oxidation rates, which amounted on average to 416 nM d^{-1} . The determined oxidation rates at the end of the enrichment (Fig. 5.5, IV) showed a strong steady increase from week 33 until week 46 (from 302 to 2398 nM d^{-1}).

5.5.6 SSCP analysis

The temporal development of the bacterial abundance showed substantial changes during the enrichment experiment. Especially at week 13 (Fig. 5.5, II), the abundance of specific bacteria changed, clearly visible by the variations of the band pattern (Fig. 5.6). Sequence analysis of the dominant bands revealed sequences which cannot be assigned phylogenetically to methanotrophic bacteria. Interestingly, the sequence analysis of band 8 (Tab. 5.2) at week 19 and 22 (Fig. 5.5, II and III) show evidence for the occurrence of bacteria belonging to the *Hyphomonas* sp..

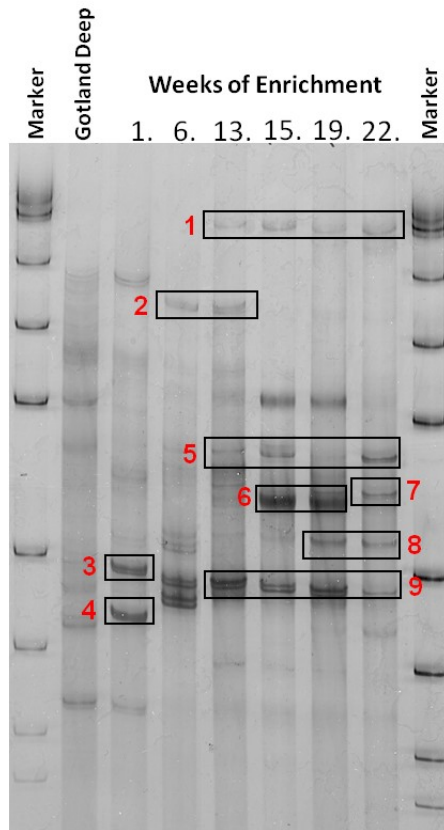


Figure 5.6. SSCP analysis. Black squares illustrate sequenced bands, the numbers in red denote the phylogenetic affiliations listed in Table 5.2.

Table 5.2. SSCP sequence analysis. The phylogenetic affiliations of the sequenced bands are listed according to the numbering in Fig. 5.6.

Band	Phylogenetic affiliation	Sequence similarity	Accession number
1	<i>Acidovorax</i> sp.	100 %	KF556688
2	uncultured bacterium delta proteobacterium	99 %	GU567808
3	uncultured bacterium clone	100 %	FJ354442
4	<i>Cafeteria roenbergensis</i> mitochondrial	100 %	AF193903
5	Bacterium BW3PHG	100 %	KC012867
6	uncultured bacterium clone	100 %	KC287100
7	uncultured bacterium clone	100 %	HQ190478
8	<i>Hyphomonas</i> sp.	100 %	AY690716
9	uncultured deep-sea bacterium clone	99 %	JF973643

5.5.7 *pmoA* detection and DGGE analysis

pmoA genes could be detected randomly at week 13, 22 and 30. DGGE analysis of the *pmoA* gene (DNA level) at these times showed only one involved methanotrophic species. Sequence analysis revealed a similarity of 100 % to an uncultured type I methanotrophic bacterium (uncultured *Methylococcus* sp., accession number KF757070).

5.5.8 Stable isotope probing

Two groups of ^{13}C -enriched uncultured bacteria could be identified using the incubation with ^{13}C CH_4 (chapter 2.2.7.1): the first group phylogenetically affiliated to type I methanotrophic bacteria (Gammaproteobacteria), the second group belonging to Deltaproteobacteria (red rectangles, Fig. 5.7). The detected unlabeled organisms can be assigned to denitrifying (Betaproteobacteria) and sulfur oxidizing bacteria (Gammaproteobacteria) as well as to the group of Alphaproteobacteria.

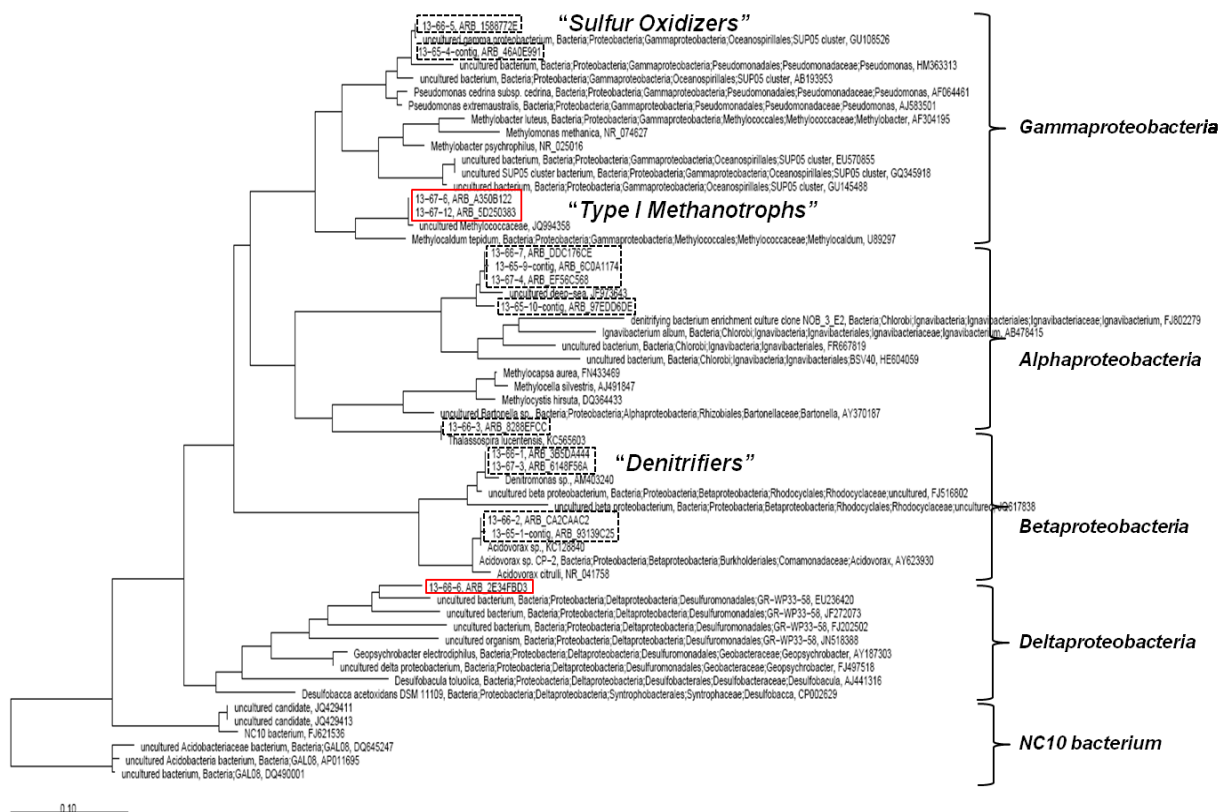


Figure 5.7. Phylogenetic analysis based on stable isotope probing. Enriched organisms are denoted by red rectangles. Black dashed rectangles denote "unlabeled" organisms.

5.5.9 NanoSIMS analysis

The analyzed bacteria of the labeled sample (chapter 2.2.7.1) can be clearly differentiated by their isotopic signature from those measured in the unlabeled sample (Fig. 5.8). Almost all measured bacteria of the labeled sample showed an enrichment of ^{15}N , of which a fraction of $\sim 9\%$ revealed simultaneously an incorporation of ^{13}C . Therefore, the average enrichment of ^{15}N was much higher than the measured ^{13}C enrichment (average values of the atom percent enrichment of all measured bacteria, coccoid bacteria: ^{13}C 0.009 %, ^{15}N 0.06 %; rod bacteria: ^{13}C 0.015 %, ^{15}N 0.06 %).

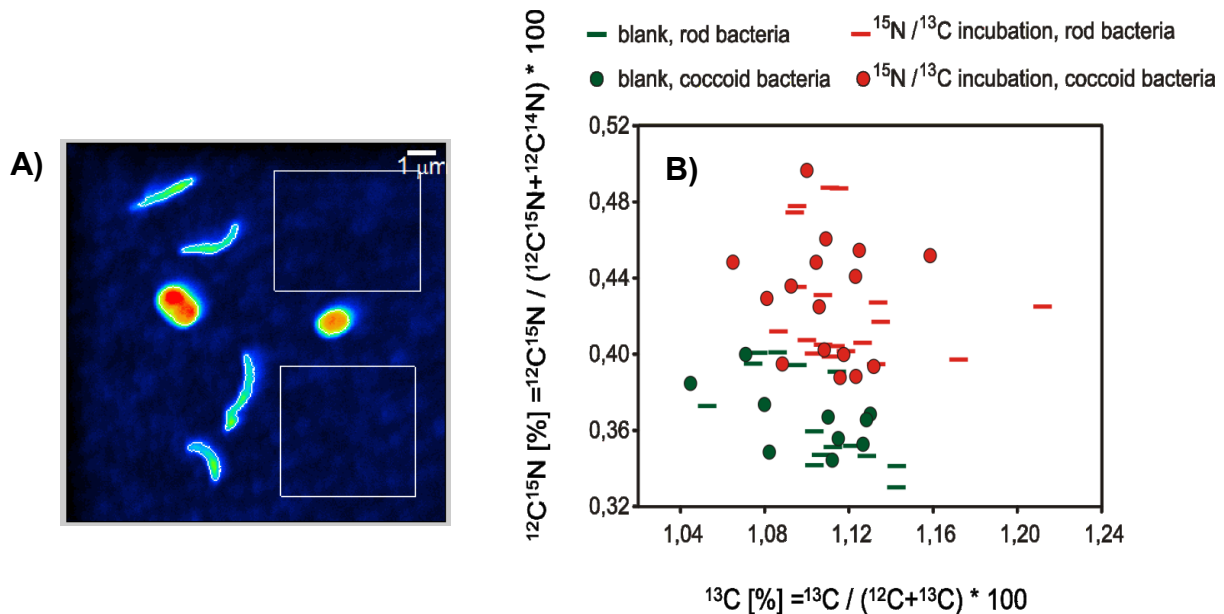


Figure 5.8. NanoSIMS analysis. **A)** $^{12}\text{C}^{14}\text{N}$ image used as the basis for definition of the region of interest (ROI). White rectangles represent areas for measuring of background values. **B)** Coccoid and rod bacteria are illustrated according to their shapes. Green colored symbols denote the measured bacteria of the unlabeled blank sample, red symbols the bacteria of the ^{13}C CH_4 and ^{15}N NO_2 incubations.

5.5.10 Biomarker

The detected biomarker composition (Tab. 5.3) represents a highly diverse mixture of different microorganisms. The occurrence of aerobic methanotrophic bacteria could be shown

by the detection of the 16:1 fatty acids and by the abundance of 4 α -methyl-C₂₇-steroid-3 β -ol, which are both representative for type I methanotrophs. The methanotrophy-specific fatty acids were present in a relatively low abundance (16:1 FA: 1.5 – 3.7 %) compared to other unspecific fatty acids, which cannot be precisely assigned to a specific group of organisms. Furthermore, the stable carbon isotopic ratio of the compounds specific for methanotrophic bacteria revealed the lowest measured $\delta^{13}\text{C}$ values of -74.1 ‰ (16:1 FA1) and -81.3 ‰ (4 α -methyl-C₂₇-steroid-3 β -ol).

Table 5.3. Biomarker composition and stable carbon isotope signatures. Biomarkers specific for type I methanotrophic bacteria are marked in bold letters. FA = fatty acid; *i* = iso branched (ω 2 methylated); *ai* = anteiso (ω 3 methylated); *tentatively identified.

Biomarker	Relative abundance [%]	$\delta^{13}\text{C}$ value [‰] (mean; n=2)
14:0 FA	1.5	-44.0
<i>i</i> 15:0 FA	0.4	-31.0
<i>ai</i> 15:0 FA	0.5	-29.4
15:0 FA	3.8	-28.6
<i>i</i> 16:0 FA	1.2	-30.7
16:1 FA1	3.7	-74.1
16:1 FA2	1.5	-69.6
16:1 FA3	1.7	-31.1
16:0 FA	19.2	-30.8
17:1 FA	2.3	-28.9
18:1 9cis*	28.3	-25.5
18:1 FA2	1.8	-34.5
18:0 FA	11.3	-29.3
19:0 FA	7.7	-25.5
20:0 FA	10.3	-25.8
22:0 FA	5.1	-25.1
4α-methyl-C₂₇-steroid-3β-ol	n.d.	-81.3

5.6 Discussion

5.6.1 Development of microbial biomass

The increase of the cell number by two orders of magnitude within the first four weeks of enrichment implies a rapid accumulation of cell mass (Fig. 5.5, I). The following decrease of the cell number after four weeks together with the formation of particles can be explained by cell aggregation. This means that the major proportion of cells was located in the precipitating aggregates leading to an apparent loss of single cells in the enrichment culture. The minor variations in the following time period (Fig. 5.5, II and III) and the renewed increase of the cell number at the end of the enrichment experiment (Fig. 5.5, IV) showed an obvious correlation to the sampling events. This relation became particularly evident at week 40 (Fig. 5.5, IV), where almost two-thirds of the culture liquid was removed due to the sampling for Stable Isotope Probing and NanoSIMS analysis. The removing of a considerable amount of cell mass and the subsequent filling with nutrient solution caused a strong dilution of the culture liquid. Therefore, the sampling led firstly to a decrease of the cell number by withdrawal of cell mass and subsequently to an increase of the cell number during the filling period (1 liter per week), which was followed by a renewed pronounced formation of particles.

Furthermore, the formation of particles was accompanied by an increase of the microbial activity (Fig. 5.5, period II: increasing methane oxidation and denitrification). The trigger of the cell aggregation cannot be clarified in this study. However, the aggregation of cells can be explained by active accumulation of single cells (quorum sensing) or by passive collision and agglutination (cell adhesion) (Benoit et al., 2000; Waters and Bassler, 2005). Especially the quorum sensing allows bacteria to communicate with their surrounding environment using hormone-like molecules, leading to the formation of multicellular organisms. The aggregation of cells enables a beneficial process in a large cell number, which would be not executable by an individual single organism (Waters and Bassler, 2005). Besides the formation of particles, the supply of nutrient solution may positively impact the microbial activity due to the concentration reduction of toxic metabolism products during the filling period.

5.6.2 Methane oxidation coupled to denitrification

During the enrichment experiment, the low content of oxygen (0.5 μM dissolved oxygen) was not actively adjusted, but continuously maintained by the input of oxygen through gas tubings with a low permeability to oxygen. The measured oxygen concentration in the culture vessel was lower than the observed concentration at the sampling depth within the Gotland Deep redox zone where the inoculum for the bioreactor was taken (2.7 μM O_2). It is known that oxygen suppresses the enzyme (nitrate/nitrite reductase) responsible for denitrification. However, R  nner and S  rensson (1985) have proven an upper tolerance limit of 9 μM O_2 for the denitrification under oxygen-limited conditions within the Baltic Sea water column. Moreover, Modin et al. (2007) and references therein provided clear evidences for the methane-dependent denitrification in the presence of oxygen. These studies demonstrated that the concentration of oxygen should be high enough to enable the oxidation of methane, but at the same time on a level which is not inhibiting denitrification.

Compared to previous studies investigating the coupling of denitrification and methane oxidation using enrichment cultures from oxic fresh water habitats, the present study provides first indication for a methane-dependent denitrification in the marine realm. The concentration profiles of nitrite/nitrate showed a correlation with the turnover of methane during the first twenty weeks of enrichment (Fig. 5.5, I and II). The obvious decrease of nitrite and nitrate from week 12 to week 18 (Fig. 5.5, II) was accompanied by increasing methane oxidation rates between week 7 and 13. Conversely, increasing nitrite and nitrate concentrations after week 18 (Fig. 5.5, III) were accompanied by an apparent decrease of the methane oxidation rates implying a coupling between methane consumption and denitrification under suboxic conditions. However, the pronounced reduction of nitrite and nitrate was not in accordance with the measured denitrification rates, because these rates are too low to achieve the observed concentration decrease of nitrite and nitrate during the time period (Fig. 5.5, II). An explanation could be the contamination with oxygen during ^{15}N -labeling experiments leading to an underestimation of the measured denitrification rates due to suppressing of the nitrite/nitrate reductase activity (Dalsgaard et al., 2013). Furthermore, a large proportion of nitrogen could be incorporated into the microbial biomass of heterotrophic denitrifiers during assimilation of nitrite and nitrate (Jetten et al., 1997). The following concentration increase as well as the exceeded nitrite and nitrate concentrations between week 30 and 40 (Fig. 5.5, III

and IV) might be explained by the production of nitrite and nitrate, because some species of denitrifiers (e.g. *Thiosphaera pantotropha*) are also known to act as heterotrophic nitrifiers (Jetten et al., 1997).

In contrast to Rönner and Sörensson (1985) and Jensen et al. (2009), previous studies in the Baltic Sea water column showed that denitrification was not detectable under suboxic conditions, but occurred slightly below within the anoxic water layer (Dalsgaard et al., 2013; Hietanen et al., 2012). The removal of nitrogen within the anoxic water layer of the Baltic Sea is suggested to be regulated by autotrophic denitrification which is driven by the oxidation of reduced sulfur compounds (Brettar et al., 2006; Brettar and Rheinheimer, 1991; Hietanen et al., 2012). Therefore, the coupled process between methane oxidation and heterotrophic denitrification which is assumed to be relevant in the present study plays most likely a subordinate role for the nitrogen cycle under the prevailing environmental conditions within the Baltic Sea redox zone. However, the enrichment experiment showed first implications of a methane-dependent denitrification by microorganisms obtained from a pelagic marine environment.

5.6.3 Phylogenetic and activity analysis

The detection of the *pmoA* gene together with sequence analysis clearly indicate the involvement of type I methanotrophic bacteria which are phylogenetically affiliated to an uncultured *Methylococcus* sp.. This finding could be verified by biomarker analysis which also confirmed the occurrence of type I methanotrophic bacteria by the detection of specific fatty acids (16:1) and 4-Me sterol (4 α -methyl-C₂₇-steroid-3 β -ol). The latter was previously found to be especially prominent in *Methylococcus capsulatus* (Bird et al., 1971; Elvert and Niemann, 2008). The relatively low $\delta^{13}\text{C}$ values of these biomarkers are in agreement with the high isotopic fractionation of type I methanotrophic bacteria (Jahnke et al., 1999). However, the temporal development of the microbial community (SSCP analysis) showed no direct evidence for the involvement of methanotrophic bacteria. Besides uncultured organisms the occurrence of bacteria belonging to the *Hyphomonas* sp. could be proven using SSCP analysis. These bacteria are known as denitrifiers, which use $> \text{C}_1$ compounds as a carbon source (Moore et al., 1984), indicating potentially coexisting denitrifiers which are dependent

on hydrocarbon species other than the supplied methane substrate. Whether these required organic compounds were produced by methanotrophic bacteria or rather originate from decomposed cell material cannot be clarified in this study.

In accordance with the biomarker analysis a diverse mixture of different organisms was detected by analyzing the incubation assays for stable isotope probing (Fig. 5.7). The aim of using enhanced nitrite and nitrate concentrations as well as providing methane as the sole carbon source during the enrichment experiment was to enrich selectively denitrifying and methanotrophic bacteria. Especially nitrite is known to inhibit bacterial processes. However, the nitrite concentration (1 mM) of the nutrient solution was much lower than the toxicity limit of many other bacterial species (e.g. methanogenic bacteria: ~ 3 M, Philips et al. (2002)) explaining the high bacterial diversity in the enrichment culture. Besides a variety of unlabeled organisms, two groups of ^{13}C -enriched bacteria were observable, including type I methanotrophs. Among the unlabeled bacteria, clone sequences of these organisms were closely affiliated to a heterotrophic denitrifying bacterium belonging to *Denitromonas* sp. (family Rhodocyclaceae), which was already described as a dominant bacterium in denitrifying sludge reactors (Etchebehere et al., 2003; Lew et al., 2012). Interestingly, this bacterium was associated with the formation of particles in the liquid media, whereas aggregation in pure *Denitromonas* cultures could not be observed. Therefore, Lew et al. (2012) supposed a symbiotic interaction between different organisms leading to the formation of particles. The formation of particles was also observed in the present study shortly before the time when denitrification and increasing methane oxidation rates were detected, supporting the assumption of an involved syntrophic microbial community. However, the isotopic signal from the ^{13}C -enriched methanotrophic bacteria was not adequately transferred into the biomass of coexisting denitrifiers, according to the described mechanism of the methane-dependent denitrification under oxic conditions. Instead of that, bacteria affiliated to the order *Desulfuromonadales* were identified as the second group of ^{13}C -enriched microorganisms. Probably, differences in the metabolism (i.e. utilization of soluble organic compounds as energy and/or carbon source) of coexisting microorganisms may explain differing ^{13}C incorporation rates. Also, temporal delays in the propagation of the ^{13}C signal from the methanotrophic to the denitrifying organism during incubation have to be considered as well.

The incorporation of ^{13}C into the microbial biomass was also observed at the cellular level using NanoSIMS analysis (Fig. 5.8). Only 9 % of all measured bacteria in the labeled sample showed a clear ^{13}C enrichment, which is in agreement with the relatively low abundance of the detected fatty acids specific for type I methanotrophs. The ratio of ^{13}C -labeled cells suggest a strong accumulation of methanotrophic cells in the culture vessel compared to the abundance of methanotrophs under environmental conditions, e.g. Black Sea, where only 2.5 % of DAPI-stained cells in the oxic water column accounts for methanotrophic bacteria (Durisch-Kaiser et al., 2005). Also other bioreactor experiments inoculated with environmental samples investigating the methane-dependent denitrification showed a large number of non-methanotrophic bacteria in the enrichment culture (Eisentraeger et al., 2001; Modin et al., 2007). Furthermore, our NanoSIMS analysis illustrates that the majority of the measured bacteria were enriched in ^{15}N , including ^{13}C labeled bacteria. Most of these ^{15}N -enriched bacteria can be probably assigned to denitrifying bacteria. The simultaneous enrichment of ^{13}C and ^{15}N was most likely caused by methanotrophic bacteria during assimilation of nitrogen, which represents an essential compound in the metabolism of methanotrophic bacteria (Hanson and Hanson, 1996; Madigan and Martinko, 2009). Therefore, the uptake of nitrogen by methanotrophic bacteria in the present study could be covered by ^{15}N -labeled nitrogen released from denitrifying bacteria. Especially some of the type I methanotrophs (e.g. *Methylococcus* sp.) are able to fix molecular nitrogen (Ward et al., 2004). Another possibility is the direct uptake of the labeled inorganic nitrogen (i.e. $^{15}\text{N NO}_2^-$, $^{15}\text{N NO}_3^-$) by methanotrophic bacteria. The observed isotopic enrichment pattern obtained via NanoSIMS was in agreement with the conducted phylogenetic analysis (stable isotope probing), representing an involved denitrifying methanotrophic community.

5.7 Conclusion

The present study provides the first indication of the occurrence of a methane-dependent denitrification within the pelagic redox zone of the central Baltic Sea. The bioreactor experiment showed a correlation between the consumption of methane and degradation of nitrate/nitrite thus implying a direct linkage between both processes. The molecular biological analysis that was identified involved type I methanotrophic and denitrifying bacteria indicating the possible role of methanotrophs which may support heterotrophic denitrifiers by

the release of organic compounds and accordingly representing a particular contribution for the nitrogen removal under suboxic conditions in marine environments. The bioreactor experiment showed the potential possibility of a methane-dependent denitrification under the prevailing environmental conditions within the Baltic Sea redox zone. However, it can be assumed that the nitrogen removal within the Baltic Sea redox zone is not being dominated by this process due to the main regulation by chemolithoautotrophic denitrification, which is considered as the relevant process for the nitrogen removal in the Baltic Sea. The selective chemical settings in the bioreactor led rather to an enhancement of the observed coupling process. The direct dependency of methanotrophy and denitrification from each other needs to be examined using specific inhibitors for methane oxidation and denitrification. Furthermore, for a better mechanistic understanding of the interaction between methanotrophs and denitrifiers, the microorganisms involved in this process should be firstly labeled by fluorescence in situ hybridization (FISH) and further investigated by NanoSIMS analysis to gain a clear assignment between the activity and identity of involved microorganisms.

General conclusions and future perspectives

In the present thesis, the pelagic microbial methane oxidation within the redox zones of the Gotland Deep and Landsort Deep (central Baltic Sea) was investigated to reveal their dependence on different oceanographic conditions such as the vertical transport rate of methane towards the redox zones as well as differing situations of disturbance within the redox zone. To identify influencing factors and their impacts on the seasonal and spatial distribution of methane and to track changes in the associated microbial methane consumption, a sampling campaign of, in total, 11 cruises from August 2011 to August 2013 was carried out along a transect from the eastern to the western Gotland Basin, central Baltic Sea. Another goal of this thesis was the investigation of the methane-dependent denitrification in a marine environment.

In the redox zones of the Gotland Deep and Landsort Deep microbial methane consumption was identified by the distribution patterns of the concentration of methane, ^{13}C CH_4 and elevated methane oxidation rates. In the redox zones at both sampling sites only one phylotype of aerobic type I methanotrophic bacteria was identified, implying that the different oceanographic conditions at both deeps do not influence the diversity of the methanotrophic community. In contrast, the microbial turnover of methane in the redox zones reveals considerable differences with lower methane oxidation rates in the Gotland Deep than in the Landsort Deep. The turnover of methane within the redox zone is controlled by the intensity of lateral intrusions and the vertical transport rate of methane from the deep anoxic water into the redox zone. Furthermore, the obtained results confirm that the microbial methane consumption within redox gradients represent an efficient methane sink preventing the escape of methane from the deep anoxic zone into the atmosphere.

The two year sampling campaign showed that seasonal and episodic temporal hydrographic events impact the water column methane distribution and the associated methanotrophic response within the pelagic redox zone. In the eastern Gotland Basin, deep water methane concentrations are regulated by seasonally occurring mixing events, whereas those in the western Gotland Basin are mainly regulated by infrequent episodic lateral weak intrusions. The methane oxidizing community at the redox zone reacts effectively to changes in methane supply by adapting the population size of methanotrophs and/or the rate of methane oxidation,

which is determined by the transport from the deep anoxic methane pool. Furthermore, methane production under oxic conditions was identified below the thermocline by elevated concentrations of methane and its stable isotope pattern, and appears to persist all summer and within the entire central Baltic Sea.

The investigation of the methane-dependent denitrification using the accumulation of involved microorganisms provides first indications of a dependency between aerobic methane oxidation and nitrogen conversion in a marine environment. The correlation of both processes was mirrored by a simultaneous increase or decrease of methane oxidation and denitrification. The detection of type I methanotrophic bacteria and coexisting heterotrophic denitrifiers in the enrichment culture inoculated with a water sample from the Gotland Deep redox zone demonstrates the potential impact of aerobic methanotrophy on the nitrogen removal in pelagic marine environments.

During the drafting of this present thesis further questions have arisen and will form the basis of future work. Firstly, open questions regarding the involvement of other electron acceptors besides oxygen, particularly the clear evidence of sulfate-depending anaerobic oxidation of methane (AOM) in the deep anoxic waters need to be clarified in further studies using suitable radio labeling techniques. This would be also linked to the question about the regulation mechanisms of AOM processes in anoxic, sulfate bearing waters as present in the deep basins of the central Baltic Sea. The present work could show that hydrographic events impact the water column methane distribution and the associated microbial response within the pelagic redox zone. However, for a detailed methane budget of the central Baltic Sea additional studies are needed to determine for example the methane source strength from the sediment, the microbial methane consumption in the anaerobic water layer, and methane production in the oxic water column. Moreover, there needs to be an examination of whether the microbial response on variable methane fluxes is caused by changes in the microbial population size or if this is related more to the adaptation of the cell activity. Based on the enrichment experiment further studies such as the labeling of involved microorganisms by fluorescence in situ hybridization (FISH) combined with NanoSIMS measurements would be helpful to gain a more precise assignment between involved microorganisms and activity measurements. In addition, the interaction between methanotrophic and denitrifying bacteria could be investigated by the use of specific inhibitors for methane oxidation and denitrification. Besides additional analytical studies the optimization of the enrichment

conditions such as shortening of the enrichment duration and the decrease of the time interval for the mineral medium supply could reduce the accumulation of dead cell material and toxic metabolism products. Furthermore, a more selective enrichment of process-involved microorganisms could be achieved by an increase of the nitrate and nitrite concentrations. These optimizations are promising measures in order to improve the mechanistic understanding of the coupling between aerobic methane oxidation and denitrification. The conducted enrichment experiment provides first indications that aerobic methane oxidation has a favorable impact on the denitrification under suboxic conditions in marine environments. This impact plays most likely a subordinate role for the Baltic Sea, because chemolithoautotrophic denitrification is suggested as a dominating process for the nitrogen reduction in the Baltic Sea. However, in the open oceans, where denitrification under suboxic conditions is thought also to be regulated by heterotrophic denitrification, the influence of aerobic methane oxidation on the nitrogen cycle appears to play an important role in these aquatic systems.

References

- Altschul, S.F., Gish, W., Miller, W., Myers, E.W., Lipman, D.J., 1990. Basic local alignment search tool. *J. Mol. Biol.* 215, 403-410.
- Amaral, J.A., Archambault, C., Richards, S.R., Knowles, R., 1995. Denitrification associated with Groups I and II methanotrophs in a gradient enrichment system. *FEMS Microbiology Ecology* 18, 289-298.
- Axell, L.B., 1998. On the variability of Baltic Sea deepwater mixing. *J. Geophys. Res.-Oceans* 103, 21667-21682.
- Balch, W.E., Fox, G., Magrum, L., Woese, C., Wolfe, R., 1979. Methanogens: reevaluation of a unique biological group. *Microbiological reviews* 43, 260.
- Bange, H.W., Bartell, U.H., Rapsomanikis, S., Andreae, M.O., 1994. Methane in the Baltic and North Seas and a reassessment of the marine emission of methane. *Global Biogeochem. Cy.* 8, 465-480.
- Bange, H.W., Bergmann, K., Hansen, H.P., Kock, A., Koppe, R., Malien, F., Ostrau, C., 2010. Dissolved methane during hypoxic events at the Boknis Eck time series station (Eckernförde Bay, SW Baltic Sea). *Biogeosciences* 7, 1279-1284.
- Bange, H.W., Dahlke, S., Ramesh, R., Meyer-Reil, L.A., Rapsomanikis, S., Andreae, M.O., 1998. Seasonal Study of Methane and Nitrous Oxide in the Coastal Waters of the Southern Baltic Sea. *Estuarine, Coastal and Shelf Science* 47, 807-817.
- Beal, E.J., House, C.H., Orphan, V.J., 2009. Manganese- and Iron-Dependent Marine Methane Oxidation. *Science* 325, 184-187.
- Benoit, M., Gabriel, D., Gerisch, G., Gaub, H.E., 2000. Discrete interactions in cell adhesion measured by single-molecule force spectroscopy. *Nature cell biology* 2, 313-317.
- Berg, C., Beckmann, S., Jost, G., Labrenz, M., Jürgens, K., 2013. Acetate-utilizing bacteria at an oxic-anoxic interface in the Baltic Sea. *FEMS microbiology ecology* 85, 251-261.
- Berndmeyer, C., Thiel, V., Blumenberg, M., 2014. Test of microwave, ultrasound and Bligh & Dyer extraction for quantitative extraction of bacteriohopanepolyols (BHPs) from marine sediments. *Organic Geochemistry* 68, 90-94.
- Berndmeyer, C., Thiel, V., Schmale, O., Blumenberg, M., 2013. Biomarkers for aerobic methanotrophy in the water column of the stratified Gotland Deep (Baltic Sea). *Org. Geochem.* 55, 103-111.
- Berndt, M.E., Allen, D.E., Seyfried, W.E., 1996. Reduction of CO₂ during serpentinization of olivine at 300 °C and 500 bar. *Geology* 24, 351-354.

- Best, A.I., Richardson, M.D., Boudreau, B.P., Judd, A.G., Leifer, I., Lyons, A.P., Martens, C.S., Orange, D.L., Wheeler, S.J., 2006. Shallow seabed methane gas could pose coastal hazard. *EOS* 87, 213-215.
- Biderre-Petit, C., Jézéquel, D., Dugat-Bony, E., Lopes, F., Kuever, J., Borrel, G., Viollier, E., Fonty, G., Peyret, P., 2011. Identification of microbial communities involved in the methane cycle of a freshwater meromictic lake. *FEMS Microbiol. Ecol.* 77, 533-545.
- Bird, C.W., Lynch, J.M., Pirt, F.J., Reid, W.W., Brooks, C.J.W., Middleditch, B.S., 1971. Steroids and Squalene in *Methylococcus capsulatus* grown on Methane. *Nature* 230, 473-474.
- Blumenberg, M., Berndmeyer, C., Moros, M., Muschalla, M., Schmale, O., Thiel, V., 2013. Bacteriohopanepolyols record stratification, nitrogen fixation and other biogeochemical perturbations in Holocene sediments of the central Baltic Sea. *Biogeosciences* 10, 2725-2735.
- Blumenberg, M., Hoppert, M., Krüger, M., Dreier, A., Thiel, V., 2012. Novel findings on hopanoid occurrences among sulfate reducing bacteria: Is there a direct link to nitrogen fixation? *Organic Geochemistry* 49, 1-5.
- Blumenberg, M., Krüger, M., Nauhaus, K., Talbot, H.M., Oppermann, B.I., Seifert, R., Pape, T., Michaelis, W., 2006. Biosynthesis of hopanoids by sulfate-reducing bacteria (genus *Desulfovibrio*). *Environmental Microbiology* 8, 1220-1227.
- Blumenberg, M., Seifert, R., Michaelis, W., 2007. Aerobic methanotrophy in the oxic-anoxic transition zone of the Black Sea water column. *Org. Geochem.*
- Boetius, A., Ravensschlag, K., Schubert, C.J., Rickert, D., Widdel, F., Gieseke, A., Amann, R., Joergensen, B.B., Witte, U., Pfannkuche, O., 2000. A marine microbial consortium apparently mediating anaerobic oxidation of methane. *Nature* 407, 623-626.
- Bourne, D.G., McDonald, I.R., Murrell, J.C., 2001. Comparison of *pmoA* PCR Primer Sets as Tools for Investigating Methanotroph Diversity in Three Danish Soils. *Appl. Environ. Microbiol.* 67, 3802-3809.
- Brettar, I., Labrenz, M., Flavier, S., Bötel, J., Kuosa, H., Christen, R., Höfle, M.G., 2006. Identification of a *Thiomicrospira denitrificans*-Like Epsilonproteobacterium as a Catalyst for Autotrophic Denitrification in the Central Baltic Sea. *Applied and Environmental Microbiology* 72, 1364-1372.
- Brettar, I., Rheinheimer, G., 1991. Denitrification in the Central Baltic: evidence for H₂S-oxidation as motor of denitrification at the oxic-anoxic interface. *Mar. Ecol. Prog. Ser.* 77, 157-169.
- Brettar, I., Rheinheimer, G., 1992. Influence of carbon availability on denitrification in the central Baltic Sea. *Limnol. Oceanogr.* 37, 1146-1163.
- Brooks, J.M., Reid, D.F., Bernard, B.B., 1981. Methane in the upper water column of the northwestern Gulf of Mexico. *Journal of Geophysical Research: Oceans* 86, 11029-11040.

- Bruland, K., 1983. Trace Elements in Sea Water, in: Riley, J.P., and Chester, R. (Ed.), Chemical Oceanography. Academic Press, London, pp. 147-220.
- Bruns, A., Cypionka, H., Overmann, J., 2002. Cyclic AMP and Acyl Homoserine Lactones Increase the Cultivation Efficiency of Heterotrophic Bacteria from the Central Baltic Sea. *Applied and Environmental Microbiology* 68, 3978-3987.
- Cicerone, R.J., Oremland, R.S., 1988. Biogeochemical aspects of atmospheric methane. *Global Biogeochemical Cycles* 2, 299-327.
- Coleman, D.D., Risatti, J.B., Schoell, M., 1981. Fractionation of carbon and hydrogen isotopes by methane-oxidizing bacteria. *Geochim. Cosmochim. Ac.* 45, 1033-1037.
- Costa, C., Dijkema, C., Friedrich, M., García-Encina, P., Fernández-Polanco, F., Stams, A.J.M., 2000. Denitrification with methane as electron donor in oxygen-limited bioreactors. *Appl Microbiol Biotechnol* 53, 754-762.
- Costello, A.M., Lidstrom, M.E., 1999. Molecular characterization of functional and phylogenetic genes from natural populations of methanotrophs in lake sediments. *Appl. Environ. Microbiol.* 65, 5066-5074.
- Crespo-Medina, M., Meile, C.D., Hunter, K.S., Diercks, A.R., Asper, V.L., Orphan, V.J., Tavormina, P.L., Nigro, L.M., Battles, J.J., Chanton, J.P., Shiller, A.M., Joung, D.J., Amon, R.M.W., Bracco, A., Montoya, J.P., Villareal, T.A., Wood, A.M., Joye, S.B., 2014. The rise and fall of methanotrophy following a deepwater oil-well blowout. *Nature Geosci* 7, 423-427.
- Dalsgaard, T., De Brabandere, L., Hall, P.O., 2013. Denitrification in the water column of the central Baltic Sea. *Geochimica et Cosmochimica Acta* 106, 247-260.
- Damm, E., Helmke, E., Thoms, S., Schauer, U., Nöthig, E., Bakker, K., Kiene, R.P., 2010. Methane production in aerobic oligotrophic surface water in the central Arctic Ocean. *Biogeosciences* 7, 1099-1108.
- De Angelis, M.A., Lee, C., 1994. Methane production during zooplankton grazing on marine phytoplankton. *Limnology and Oceanography* 39, 1298-1308.
- Dellwig, O., Leipe, T., März, C., Glockzin, M., Pollehne, F., Schnetger, B., Yakushev, E.V., Böttcher, M.E., Brumsack, H.-J., 2010. A new particulate Mn-Fe-P-shuttle at the redoxcline of anoxic basins. *Geochim. Cosmochim. Ac.* 74, 7100-7115.
- Dellwig, O., Schnetger, B., Brumsack, H.-J., Grossart, H.-P., Umlauf, L., 2012. Dissolved reactive manganese at pelagic redoxclines (part II): Hydrodynamic conditions for accumulation. *J. Marine Syst.* 90, 31-41.
- Dlugokencky, E.J., Nisbet, E.G., Fisher, R., Lowry, D., 2011. Global atmospheric methane: budget, changes and dangers. *Philosophical Transactions of the Royal Society A: Mathematical, Physical and Engineering Sciences* 369, 2058-2072.

- Durisch-Kaiser, E., Klauser, L., Wehrli, B., Schubert, C., 2005. Evidence of intense archaeal and bacterial methanotrophic activity in the Black Sea water column. *Appl. Environ. Microbiol.* 71, 8099-8106.
- Dzyuban, A.N., Krylova, I.N., Kuznetsova, I.A., 1999. Properties of Bacteria Distribution and Gas Regime within the water Column of the Baltic Sea in winter. *Oceanology* 39, 348-351.
- Eisentraeger, A., Klag, P., Vansbotter, B., Heymann, E., Dott, W., 2001. Denitrification of groundwater with methane as sole hydrogen donor. *Water Research* 35, 2261-2267.
- Elvert, M., Niemann, H., 2008. Occurrence of unusual steroids and hopanoids derived from aerobic methanotrophs at an active marine mud volcano. *Organic Geochemistry* 39, 167-177.
- Etchebehere, C., Cabezas, A., Dabert, P., Muxi, L., 2003. Evolution of the bacterial community during granules formation in denitrifying reactors followed by molecular, culture-independent techniques. *Water Science & Technology* 48, 75-79.
- Ettwig, K.F., Butler, M.K., Le Paslier, D., Pelletier, E., Mangenot, S., Kuypers, M.M.M., Schreiber, F., Dutilh, B.E., Zedelius, J., de Beer, D., Gloerich, J., Wessels, H.J.C.T., van Alen, T., Luesken, F., Wu, M.L., van de Pas-Schoonen, K.T., Op den Camp, H.J.M., Janssen-Megens, E.M., Francoijs, K.-J., Stunnenberg, H., Weissenbach, J., Jetten, M.S.M., Strous, M., 2010. Nitrite-driven anaerobic methane oxidation by oxygenic bacteria. *Nature* 464, 543-548.
- Feistel, R., Nausch, G., Mohrholz, V., Lysiak-Pastuszek, E., Seifert, T., Matthaus, W., Kruger, S., Hansen, I.S., 2003. Warm waters of summer 2002 in the deep Baltic Proper. *Oceanologia* 45.
- Fonselius, S., 1981. Oxygen and hydrogen sulphide conditions in the Baltic Sea. *Marine Pollution Bulletin* 12, 187-194.
- Gast, V., Gocke, K., 1988. Vertical distribution of number, biomass and size-class spectrum of bacteria in relation to oxic/anoxic conditions in the central Baltic Sea. *Marine ecology progress series*. Oldendorf 45, 179-186.
- Glaubitx, S., Lueders, T., Abraham, W.-R., Jost, G., Jürgens, K., Labrenz, M., 2009. ¹³C-isotope analyses reveal that chemolithoautotrophic Gamma- and Epsilonproteobacteria feed a microbial food web in a pelagic redoxcline of the central Baltic Sea. *Environ Microbiol.* 11, 326-337.
- Grasshoff, K., Ehrhardt, M., Kremling, K., 1999. *Methods of seawater analysis*, 3 ed. Verlag Chemie, Gulf Publishing Houston.
- Grossart, H.-P., Frindte, K., Dziallas, C., Eckert, W., Tang, K.W., 2011. Microbial methane production in oxygenated water column of an oligotrophic lake. *Proceedings of the National Academy of Sciences* 108, 19657-19661.
- Gülzow, W., Gräwe, U., Kedzior, S., Schmale, O., Rehder, G., 2014. Seasonal variation of methane in the water column of Arkona and Bornholm Basin, western Baltic Sea. *Journal of Marine Systems* 139, 332-347.

- Gülzow, W., Rehder, G., Schneider v. Deimling, J., Seifert, T., Tóth, Z., 2013. One year of continuous measurements constraining methane emissions from the Baltic Sea to the atmosphere using a ship of opportunity. *Biogeosciences* 10, 81-99.
- Gustafsson, B.G., Stigebrandt, A., 2007. Dynamics of nutrients and oxygen/hydrogen sulfide in the Baltic Sea deep water. *Journal of Geophysical Research: Biogeosciences* (2005–2012) 112.
- Hanson, R.S., Hanson, T.E., 1996. Methanotrophic bacteria. *Microbiological Reviews* June 1996, 439-471.
- Heyer, J., 1990. Der Kreislauf des Methans. *Mikrobiologie, Ökologie, Nutzung. Internationale Revue der gesamten Hydrobiologie und Hydrographie*, 95-99.
- Heyer, J., Berger, U., 2000. Methane Emission from the Coastal Area in the Southern Baltic Sea. *Estuarine, Coastal and Shelf Science* 51, 13-30.
- Hietanen, S., Jäntti, H., Buizert, C., Jurgens, K., Labrenz, M., Voss, M., Kuparinen, J., 2012. Hypoxia and nitrogen processing in the Baltic Sea water column. *Limnology and Oceanography* 57, 325.
- Hoehler, T., Alperin, M.J., Albert, D.B., Martens, C., 1994. Field and laboratory studies of methane oxidation in an anoxic marine sediment: evidence for a methanogen-sulfate reducer consortium. *Global Biogeochemistry Cycles* 8, 451-463.
- Holmes, A.J., Costello, A., Lidstrom, M.E., Murrell, J.C., 1995. Evidence that particulate methane monooxygenase and ammonia monooxygenase may be evolutionarily related. *FEMS Microbiol. Lett.* 132, 203-208.
- Holtappels, M., Lavik, G., Jensen, M.M., Kuypers, M.M., 2011. ¹⁵N-labeling experiments to dissect the contributions of heterotrophic denitrification and anammox to nitrogen removal in the OMZ waters of the ocean. *Methods in enzymology* 486, 223-251.
- Holtermann, P.L., Burchard, H., Gräwe, U., Klingbeil, K., Umlauf, L., 2014. Deep-water dynamics and boundary mixing in a nontidal stratified basin: A modeling study of the Baltic Sea. *Journal of Geophysical Research: Oceans*, n/a-n/a.
- Holtermann, P.L., Umlauf, L., 2012. The Baltic Sea Tracer Release Experiment: 2. Mixing processes. *J. Geophys. Res.* 117, C01022.
- Holtermann, P.L., Umlauf, L., Tanhua, T., Schmale, O., Rehder, G., Waniek, J.J., 2012. The Baltic Sea Tracer Release Experiment: 1. Mixing rates. *J. Geophys. Res.* 117, C01021.
- Islas-Lima, S., Thalasso, F., Gómez-Hernandez, J., 2004. Evidence of anoxic methane oxidation coupled to denitrification. *Water Research* 38, 13-16.
- Iversen, N., Blackburn, T.H., 1981. Seasonal Rates of Methane Oxidation in Anoxic Marine Sediments. *Applied and Environmental Microbiology* 41, 1295-1300.

- Iversen, N., Jørgensen, B.B., 1985. Anaerobic methane oxidation rates at the sulfate-methane transition in marine sediments from Kattegat and Skagerrak (Denmark). *Limnology and Oceanography* 30, 944-955.
- Jahnke, L.L., Summons, R.E., Hope, J.M., Des Marais, D.J., 1999. Carbon isotopic fractionation in lipids from methanotrophic bacteria II: The effects of physiology and environmental parameters on the biosynthesis and isotopic signatures of biomarkers. *Geochimica et Cosmochimica Acta* 63, 79-93.
- Jakobs, G., Rehder, G., Jost, G., Kießlich, K., Labrenz, M., Schmale, O., 2013. Comparative studies of pelagic microbial methane oxidation within the redox zones of the Gotland Deep and Landsort Deep (central Baltic Sea). *Biogeosciences* 10, 7863-7875.
- Jensen, M.M., Petersen, J., Dalsgaard, T., Thamdrup, B., 2009. Pathways, rates, and regulation of N₂ production in the chemocline of an anoxic basin, Mariager Fjord, Denmark. *Marine Chemistry* 113, 102-113.
- Jetten, M.M., Logemann, S., Muyzer, G., Robertson, L., de Vries, S., van Loosdrecht, M.M., Kuenen, J.G., 1997. Novel principles in the microbial conversion of nitrogen compounds. *Antonie Van Leeuwenhoek* 71, 75-93.
- Jørgensen, B.B., Fossing, H., 2011. Methane emission in the Baltic Sea: Gas storage and effects of climate change and eutrophication. BALTIC Gas final report, <http://www.bonusportal.org/>.
- Jost, G., Zubkov, M.V., Yakushev, E.V., Labrenz, M., Jürgens, K., 2008. High abundance and dark CO₂ fixation of chemolithoautotrophic prokaryotes in anoxic waters of the Baltic Sea. *Limnol. Oceanogr.* 53, 14-22.
- Kamyshny, A., Jr., Yakushev, E.V., Jost, G., Podymov, O.I., 2013. Role of Sulfide Oxidation Intermediates in the Redox Balance of the Oxidic–Anoxic Interface of the Gotland Deep, Baltic Sea, in: Yakushev, E.V. (Ed.), *Chemical Structure of Pelagic Redox Interfaces*. Springer Berlin Heidelberg, pp. 95-119.
- Karl, D.M., Beversdorf, L., Bjorkman, K.M., Church, M.J., Martinez, A., Delong, E.F., 2008. Aerobic production of methane in the sea. *Nature Geosci* 1, 473-478.
- Karl, D.M., Tilbrook, B.D., 1994. Production and transport of methane in oceanic particulate organic matter. *Nature* 368, 732-734.
- Keir, R., Schmale, O., Seifert, R., Sültenfuß, J., 2009. Isotope fractionation and mixing in methane plumes from the Logatchev hydrothermal field. *Geochem. Geophys. Geosy.* 10, Q05005.
- Keir, R.S., Schmale, O., Walter, M., Sültenfuß, J., Seifert, R., Rhein, M., 2008. Flux and dispersion of gases from the "Drachenschlund" hydrothermal vent at 8°18' S, 13°30' W on the Mid-Atlantic Ridge. *Earth Planet Sc. Lett.* 270, 338-348.
- Kessler, J.D., Valentine, D.L., Redmond, M.C., Du, M., Chan, E.W., Mendes, S.D., Quiroz, E.W., Villanueva, C.J., Shusta, S.S., Werra, L.M., Yvon-Lewis, S.A., Weber, T.C., 2011. A

- Persistent Oxygen Anomaly Reveals the Fate of Spilled Methane in the Deep Gulf of Mexico. *Science* 331, 312-315.
- Knittel, K., Boetius, A., 2009. Anaerobic Oxidation of Methane: Progress with an Unknown Process. *Annu. Rev. Microbiol.* 63, 311-334.
- Knittel, K., Losekann, T., Boetius, A., Kort, R., Amann, R., 2005. Diversity and Distribution of Methanotrophic Archaea at Cold Seeps. *Appl. Environ. Microbiol.* 71, 467-479.
- Knowles, R., 2005. Denitrifiers associated with methanotrophs and their potential impact on the nitrogen cycle. *Ecological Engineering* 24, 441-446.
- Kolb, S., Knief, C., Stubner, S., Conrad, R., 2003. Quantitative Detection of Methanotrophs in Soil by Novel *pmoA*-Targeted Real-Time PCR Assays. *App. Environ. Microb.* 69, 2423-2429.
- Labrenz, M., Jost, G., Pohl, C., Beckmann, S., Martens-Habenna, W., Jürgens, K., 2005. Impact of Different In Vitro Electron Donor/Acceptor Conditions on Potential Chemolithoautotrophic Communities from Marine Pelagic Redoxclines. *Appl. Environ. Microbio.* 71, 6664-6672.
- Labrenz, M., Sintes, E., Toetzke, F., Zumsteg, A., Herndl, G.J., Seidler, M., Jürgens, K., 2010. Relevance of a crenarchaeotal subcluster related to *Candidatus Nitrosopumilus maritimus* to ammonia oxidation in the suboxic zone of the central Baltic Sea. *ISME J.* 4, 1496-1508.
- Laier, T., Jensen, J., 2007. Shallow gas depth-contour map of the Skagerrak-western Baltic Sea region. *Geo-Marine Letters* 27, 127-141.
- Lass, H.U., Matthäus, W., 2008. General oceanography of the Baltic Sea, in: Feistel, R., Nausch, G., Wasmund, N. (Eds.), *State and evolution of the Baltic Sea, 1952-2005*. John Wiley & Sons, Inc., New Jersey, pp. 5-44.
- Lass, H.U., Prandke, H., Liljebladh, B., 2003. Dissipation in the Baltic proper during winter stratification. *J. Geophys. Res.* 108, 3187.
- Lew, B., Stief, P., Beliaevski, M., Ashkenazi, A., Svitlica, O., Khan, A., Tarre, S., de Beer, D., Green, M., 2012. Characterization of denitrifying granular sludge with and without the addition of external carbon source. *Bioresource Technology* 124, 413-420.
- Madigan, M.T., Martinko, J.M., 2009. *Brock Mikrobiologie*, 11 ed. Pearson Deutschland GmbH.
- Matthäus, W., Nehring, D., Feistel, R., Nausch, G., Mohrholz, V., Lass, H.U., 2008. The inflow of high saline water into the Baltic Sea, in: Feistel, R., Nausch, G., Wasmund, N. (Eds.), *State and evolution of the Baltic Sea, 1952-2005*. John Wiley & Sons, Inc., New Jersey, pp. 265-310.
- Mau, S., Blees, J., Helmke, E., Niemann, H., Damm, E., 2013. Vertical distribution of methane oxidation and methanotrophic response to elevated methane concentrations in stratified waters of the Arctic fjord Storfjorden (Svalbard, Norway). *Biogeosciences* 10, 6267-6278.

- Mau, S., Rehder, G., Sahling, H., Schleicher, T., Linke, P., 2012. Seepage of methane at Jaco Scar, a slide caused by seamount subduction offshore Costa Rica. *Int J Earth Sci (Geol Rundsch)*, 1-15.
- McDonald, I.R., Bodrossy, L., Chen, Y., Murrell, J.C., 2008. Molecular Ecology Techniques for the Study of Aerobic Methanotrophs. *Appl. Environ. Microbiol.* 74, 1305-1315.
- Meier, M.H.E., 2007. Modeling the pathways and ages of inflowing salt- and freshwater in the Baltic Sea. *Estuarine, Coastal and Shelf Science* 74, 610-627.
- Michaelis, W., Gerhard, B., Jenisch, A., Ladage, S., Richnow, H.H., Seifert, R., Stoffers, P., 1990. Methane and ^3He anomalies related to submarine intraplate volcanic activities. *Mitteilungen aus dem Geologisch-Paläontologischen Institut der Universität Hamburg* 69, 117-127.
- Milucka, J., Ferdelman, T.G., Polerecky, L., Franzke, D., Wegener, G., Schmid, M., Lieberwirth, I., Wagner, M., Widdel, F., Kuypers, M.M.M., 2012. Zero-valent sulphur is a key intermediate in marine methane oxidation. *Nature* 491, 541-546.
- Modin, O., Fukushi, K., Yamamoto, K., 2007. Denitrification with methane as external carbon source. *Water Res.* 41, 2726-2738.
- Moore, R.L., Weiner, R.M., Gebers, R., 1984. Notes: Genus *Hyphomonas* Pongratz 1957 nom. rev. emend., *Hyphomonas polymorpha* Pongratz 1957 nom. rev. emend., and *Hyphomonas neptunium* (Leifson 1964) comb. nov. emend. (*Hyphomicrobium neptunium*). *International journal of systematic bacteriology* 34, 71-73.
- Musat, N., Halm, H., Winterholler, B., Hoppe, P., Peduzzi, S., Hillion, F., Horreard, F., Amann, R., Jørgensen, B.B., Kuypers, M.M.M., 2008. A single-cell view on the ecophysiology of anaerobic phototrophic bacteria. *Proceedings of the National Academy of Sciences* 105, 17861-17866.
- Nausch, G., Feistel, R., Umlauf, L., Mohrholz, V., Nagel, K., Siegel, H., 2012. Hydrographisch-hydrochemische Zustandseinschätzung der Ostsee 2011. *Meereswiss. Ber., Warnemünde* 86.
- Nausch, G., Feistel, R., Umlauf, L., Mohrholz, V., Nagel, K., Siegel, H., 2013. Hydrographisch-hydrochemische Zustandseinschätzung der Ostsee 2012. *Meereswiss. Ber., Warnemünde* 91.
- Nausch, G., Nehring, D., Nagel, K., 2008. Nutrient concentrations, trends and their relation to eutrophication, in: Feistel, R., Nausch, G., Wasmund, N. (Eds.), *State and evolution of the Baltic Sea, 1952-2005*. John Wiley & Sons, Inc., New Jersey, pp. 337-366.
- Nichols, P.D., Glen A, S., Antworth, C.P., Hanson, R.S., White, D.C., 1985. Phospholipid and lipopolysaccharide normal and hydroxy fatty acids as potential signatures for methane-oxidizing bacteria. *FEMS Microbiology Letters* 31, 327-335.
- Norði, K.á., Thamdrup, B., 2014. Nitrate-dependent anaerobic methane oxidation in a freshwater sediment. *Geochimica et Cosmochimica Acta* 132, 141-150.

- Parkes, R.J., Cragg, B.A., Banning, N., Brock, F., Webster, G., Fry, J.C., Hornibrook, E., Pancost, R.D., Kelly, S., Knab, N., Jørgensen, B.B., Rinna, J., Weightman, A.J., 2007. Biogeochemistry and biodiversity of methane cycling in subsurface marine sediments (Skagerrak, Denmark). *Environmental Microbiology* 9, 1146-1161.
- Philips, S., Laanbroek, H., Verstraete, W., 2002. Origin, causes and effects of increased nitrite concentrations in aquatic environments. *Re/Views in Environmental Science and Bio/Technology* 1, 115-141.
- Piker, L., Schmaljohann, R., Imhoff, J.F., 1998. Dissimilatory sulfate reduction and methane production in Gotland Deep sediments (Baltic Sea) during a transition period from oxic to anoxic bottom water (1993-1996). *Aquatic Microbial Ecology* 14, 183-193.
- Polerecky, L., Adam, B., Milucka, J., Musat, N., Vagner, T., Kuypers, M.M.M., 2012. Look@NanoSIMS – a tool for the analysis of nanoSIMS data in environmental microbiology. *Environmental Microbiology* 14, 1009-1023.
- Porter, K.G., 1980. The use of DAPI for identifying and counting aquatic microflora. *Limnol. Oceanogr.* 25, 943-948.
- Prokhorenko, Y.A., Krasheninnikov, B.N., Agafonov, E.A., Basharin, V.A., 1994. Experimental studies of the deep turbid layer in the Black Sea. *Phys. Oceanogr.* 5, 133-139.
- Rabalais, N.N., Diaz, R.J., Turner, R.E., Gilbert, D., Zhang, J., 2010. Dynamics and distribution of natural and human-caused hypoxia. *Biogeosciences* 7, 585-619.
- Raghoebarsing, A.A., Pol, A., van de Pas-Schoonen, K.T., Smolders, A.J.P., Ettwig, K.F., Rijpstra, W.I.C., Schouten, S., Damste, J.S.S., Op den Camp, H.J.M., Jetten, M.S.M., Strous, M., 2006. A microbial consortium couples anaerobic methane oxidation to denitrification. *Nature* 440, 918-921.
- Rasigraf, O., Kool, D.M., Jetten, M.S.M., Sinninghe Damsté, J.S., Ettwig, K.F., 2014. Autotrophic Carbon Dioxide Fixation via the Calvin-Benson-Bassham Cycle by the Denitrifying Methanotroph “Candidatus Methyloirabilis oxyfera”. *Applied and Environmental Microbiology* 80, 2451-2460.
- Reeburgh, W.S., 2007. Ocean methane biogeochemistry. *Chem. Rev.* 107, 486-513.
- Reeburgh, W.S., Ward, B.B., Whalen, S.C., Sandbeck, K.A., Kilpatrick, K.A., Kerkhof, L.J., 1991. Black Sea methane geochemistry. *Deep-Sea Res.* 38, 1189-1210.
- Reissmann, J.H., Burchard, H., Feistel, R., Hagen, E., Lass, H.U., Mohrholz, V., Nausch, G., Umlauf, L., Wiczorek, G., 2009. Vertical mixing in the Baltic Sea and consequences for eutrophication - A review. *Progr. Oceanogr.* 82, 47-80.
- Rhee, G.-Y., Fuhs, G.W., 1978. Wastewater denitrification with one-carbon compounds as energy source. *Journal (Water Pollution Control Federation)*, 2111-2119.

- Röling, W.F.M., 2007. Do microbial numbers count? Quantifying the regulation of biogeochemical fluxes by population size and cellular activity. *FEMS Microbiology Ecology* 62, 202-210.
- Rönner, U., Sörensson, F., 1985. Denitrification rates in the low-oxygen waters of the stratified Baltic proper. *Applied and environmental microbiology* 50, 801-806.
- Schmale, O., Blumenberg, M., Kießlich, K., Jakobs, G., Berndmeyer, C., Labrenz, M., Thiel, V., Rehder, G., 2012. Aerobic methanotrophy within the pelagic redox-zone of the Gotland Deep (central Baltic Sea). *Biogeosciences* 9, 4969-4977.
- Schmale, O., Haeckel, M., McGinnis, D.F., 2011. Response of the Black Sea methane budget to massive short-term submarine inputs of methane. *Biogeosciences* 8, 911-918.
- Schmale, O., Schneider von Deimling, J., Gülzow, W., Nausch, G., Waniek, J.J., Rehder, G., 2010. Distribution of methane in the water column of the Baltic Sea. *Geophys. Res. Lett.* 37, L12604.
- Schmaljohann, R., 1996. Methane dynamics in the sediment and water column of Kiel Harbour (Baltic Sea). *Marine Ecology Progress Series* 131, 263-273.
- Schubert, C.J., Coolen, M.J.L., Neretin, L.N., Schippers, A., Abbas, B., Durisch-Kaiser, E., Wehrli, B., Hopmans, E.C., Sinninghe Damsté, J.S., Wakeham, S., Kuypers, M.M.M., 2006a. Aerobic and anaerobic methanotrophs in the Black Sea water column. *Environ. Microbiol.* 8, 1844-1856.
- Schubert, C.J., Durisch-Kaiser, E., Holzner, C.P., Klauser, L., Wehrli, B., Schmale, O., Greinert, J., McGinnis, D., De Batist, M., Kipfer, R., 2006b. Methanotrophic microbial communities associated with bubble plumes above gas seeps in the Black Sea. *Geochem. Geophys. Geosy.* 7, doi: 10.1029/2005GC001049.
- Schubert, C.J., Durisch-Kaiser, E., Klauser, L., Vazquez, F., Wehrli, B., Holzner, C.P., Kipfer, R., Schmale, O., Greinert, J., Kuypers, M.M.M., 2006c. Recent studies on sources and sinks of methane in the Black Sea, in: Neretin, L.N. (Ed.), *Past and present water column anoxia*, IV. *Earth and Environmental Sciences* ed. Springer, Netherlands, pp. 419-441.
- Schwieger, F., Tebbe, C.C., 1998. A New Approach To Utilize PCR–Single-Strand-Conformation Polymorphism for 16S rRNA Gene-Based Microbial Community Analysis. *Applied and Environmental Microbiology* 64, 4870-4876.
- Scranton, M.I., 1988. Temporal variations in the methane content of the Cariaco Trench. *Deep-Sea Res.* 35, 1511-1523.
- Shakhova, N., Semiletov, I., Salyuk, A., Yusupov, V., Kosmach, D., Gustafsson, Ö., 2010. Extensive Methane Venting to the Atmosphere from Sediments of the East Siberian Arctic Shelf. *Science* 327, 1246-1250.

- Sivan, O., Adler, M., Pearson, A., Gelman, F., Bar-Or, I., John, S.G., Eckert, W., 2011. Geochemical evidence for iron-mediated anaerobic oxidation of methane. *Limnology and Oceanography* 56, 1536-1544.
- Sørensen, K.B., Finster, K., Ramsing, N.B., 2001. Thermodynamic and kinetic requirements in anaerobic methane oxidizing consortia exclude hydrogen, acetate, and methanol as possible electron shuttles. *Microb Ecol* 42, 1-10.
- Talbot, H.M., Summons, R.E., Jahnke, L.L., Cockell, C.S., Rohmer, M., Farrimond, P., 2008. Cyanobacterial bacteriohopanepolyol signatures from cultures and natural environmental settings. *Org. Geochem.* 39, 232-263.
- Talbot, M., Watson, D.F., Murrell, J.C., Carter, J.F., Farrimond, P., 2001. Analysis of intact bacteriohopanepolyols from methanotrophic bacteria by reversed-phase high-performance liquid chromatography-atmospheric pressure chemical ionisation mass spectrometry. *Journal of Chromatography A* 921, 175-185.
- Tang, K.W., Glud, R.N., Glud, A., Rysgaard, S., Nielsene, T.G., 2011. Copepod guts as biogeochemical hotspots in the sea: Evidence from microelectrode profiling of *Calanus* spp. *Limnol. Oceanogr* 56, 666-672.
- Thalasso, F., Vallecillo, A., García-Encina, P., Fdz-Polanco, F., 1997. The use of methane as a sole carbon source for wastewater denitrification. *Water Research* 31, 55-60.
- Thomas, S., 2011. Vergleich und Optimierung analytischer Methoden zur Bestimmung des Methangehalts in Seewasser. Diplomarbeit Universität Rostock.
- Tragana, E.D., Swinnerton, J.W., Cheek, C.H., 1979. Methane supersaturation and ATP-zooplankton blooms in near-surface waters of the Western Mediterranean and the subtropical North Atlantic Ocean. *Deep Sea Research Part A. Oceanographic Research Papers* 26, 1237-1245.
- Treude, T., Boetius, A., Knittel, K., Wallmann, K., Barker Joergensen, B., 2003. Anaerobic oxidation of methane above gas hydrates at Hydrate Ridge, NE Pacific Ocean. *Mar. Ecol.-Prog. Ser.* 264, 1-14.
- Treude, T., Krüger, M., Boetius, A., Jørgensen, B.B., 2005. Environmental control on anaerobic oxidation of methane in the gassy sediments of Eckernförde Bay (German Baltic). *Limnol. Oceanogr.*, 1771-1786.
- Tyson, R.V., Pearson, T.H., 1991. Modern and ancient continental shelf anoxia: an overview. Geological Society, London, Special Publications 58, 1-24.
- Valentine, D.L., 2011. Emerging topics in marine methane biogeochemistry. *Annual review of marine science* 3, 147-171.
- Valentine, D.L., Blanton, D.C., Reeburgh, W.S., Kastner, M., 2001. Water column methane oxidation adjacent to an area of active hydrate dissociation, El River Basin. *Geochim. Cosmochim. Ac.* 65, 2633-2640.

- Valentine, D.L., Kessler, J.D., Redmond, M.C., Mendes, S.D., Heintz, M.B., Farwell, C., Hu, L., Kinnaman, F.S., Yvon-Lewis, S., Du, M., Chan, E.W., Tigreros, F.G., Villanueva, C.J., 2010. Propane Respiration Jump-Starts Microbial Response to a Deep Oil Spill. *Science* 330, 208-211.
- Valentine, D.L., Reeburgh, W.S., 2000. New perspectives on anaerobic methane oxidation. *Environ. Microbiol.* 2, 477-484.
- von Klein, D., Arab, H., Völker, H., Thomm, M., 2002. *Methanosarcina baltica*, sp. nov., a novel methanogen isolated from the Gotland Deep of the Baltic Sea. *Extremophiles* 6, 103-110.
- Waki, M., Suzuki, K., Osada, T., Tanaka, Y., 2005. Methane-dependent denitrification by a semi-partitioned reactor supplied separately with methane and oxygen. *Bioresource Technology* 96, 921-927.
- Waki, M., Suzuki, K., Osada, T., Tanaka, Y., Ike, M., Fujita, M., 2004. Microbiological activities contributing to nitrogen removal with methane: effects of methyl fluoride and tungstate. *Bioresource Technology* 94, 339-343.
- Ward, N., Larsen, Ø., Sakwa, J., Bruseth, L., Khouri, H., Durkin, A.S., Dimitrov, G., Jiang, L., Scanlan, D., Kang, K.H., 2004. Genomic insights into methanotrophy: the complete genome sequence of *Methylococcus capsulatus* (Bath). *PLoS biology* 2, e303.
- Waters, C.M., Bassler, B.L., 2005. Quorum sensing: cell-to-cell communication in bacteria. *Annu. Rev. Cell Dev. Biol.* 21, 319-346.
- Weinbauer, M.G., Fritz, I., Wenderoth, D.F., Höfle, M.G., 2002. Simultaneous extraction from bacterioplankton of total RNA and DNA suitable for quantitative structure and functional analyses. *Appl. Environ. Microbiol.* 68, 1082-1084.
- Weiss, R.F., 1970. The solubility of nitrogen, oxygen and argon in water and seawater. *Deep-Sea Research* 17, 721-735.
- White, D.C., Ringelberg, D.B., 1998. Signature lipid biomarker analysis. In: R. S. Burlage, R. Atlas, D. Stahl, G. Geesey and G. Saylor (Ed.), *Techniques in Microbial Ecology*. Oxford University Press: New York.
- Whiticar, M.J., 1999. Carbon and hydrogen isotope systematics of bacterial formation and oxidation of methane. *Chem. Geol.* 161, 291-314.
- Widdel, F., Bak, F., 1992. Gram-Negative Mesophilic Sulfate-Reducing Bacteria, in: Balows, A., Trüper, H., Dworkin, M., Harder, W., Schleifer, K.-H. (Eds.), *The Prokaryotes*. Springer New York, pp. 3352-3378.
- Widdel, F., Kohring, G.-W., Mayer, F., 1983. Studies on dissimilatory sulfate-reducing bacteria that decompose fatty acids. *Arch. Microbiol.* 134, 286-294.

- Wiesenburg, D.A., Norman L. Guinasso, J., 1979. Equilibrium solubilities of methane, carbon monoxide, and hydrogen in water and sea water. *Journal of Chemical and Engineering Data* 24, 356-360.
- Wuebbles, D.J., Hayhoe, K., 2002. Atmospheric methane and global change. *Earth-Sci. Rev.* 57, 177-210.
- Yakushev, E.V., Pollehne, F., Jost, G., Kuznetsov, I., Schneider, B., Umlauf, L., 2007. Analysis of the water column oxic/anoxic interface in the Black and Baltic seas with a numerical model. *Marine Chemistry* 107, 388-410.

List of Figures

1.1	Pathway of aerobic methane oxidation.....	3
1.2	Proposed pathway of anaerobic methane oxidation in the presence of nitrite.....	6
1.3	Large-scale circulation of the Baltic Sea.....	8
2.1	Schematic view of the combustion line.....	15
2.2	Calculation of the integrated methane oxidation rate.....	17
2.3	Principle procedure of Stable Isotope Probing.....	24
3.1	Flow diagram of the methods used in conjunction with the field studies.....	28
3.2	Sampling sites in the central Baltic Sea.....	29
3.3	Gotland Deep. Physical parameters, gas chemistry, methane oxidation rates.....	31
3.4	Landsort Deep. Physical parameters, gas chemistry, methane oxidation rates.....	33
3.5	Turnover rate constants of the Gotland Deep and Landsort Deep.....	36
3.6	$\delta^{13}\text{C}$ CH_4 versus $1/\text{CH}_4$ of the Gotland Deep and Landsort Deep.....	38
3.7	Temperature-salinity diagrams.....	42
4.1	Sampling sites in the eastern and western Gotland Basin.....	46
4.2	Salinity distribution.....	48
4.3	Contour plots of oxygen and hydrogen sulfide.....	50
4.4	Gotland Deep. Physical parameters and methane chemistry.....	51
4.5	Contour plots of the vertical methane distribution.....	52
4.6	Vertical distribution of aminotetrol and aminopentol.....	53
4.7	Gotland Deep. Methane anomaly in the upper water column.....	54
4.8	Landsort Deep. Physical parameters and methane chemistry.....	55
4.9	Landsort Deep. Methane anomaly in the upper water column.....	56
4.10	Calculated vertical turbulent diffusivities.....	59
4.11	Temporal development of the methane and salinity distribution.....	60
5.1	Flow diagram of the analytical approach of the enrichment experiment.....	68
5.2	Gotland Deep. Gas chemistry, methane oxidation and nitrite/nitrate conc.....	69
5.3	Bioreactor set up.....	70
5.4	Microscopy examination of DAPI stained cells.....	73
5.5	Result overview.....	74
5.6	SSCP analysis.....	76
5.7	Stable Isotope Probing.....	77
5.8	NanoSIMS analysis.....	78

List of Tables

3.1	Comparative studies of pelagic microbial methane oxidation: result summary	34
4.1	Seasonal and spatial methane dynamics: analyzed parameter	47
4.2	Methane oxidation rates, turnover rate constants, and methane turnover times	56
5.1	Bioreactor enrichment experiment: composition of the nutrient solution	71
5.2	SSCP sequence analysis	76
5.3	Biomarker composition and stable carbon isotope signatures	79

List of Abbreviations

AMO	ammonium monooxygenase
ANME	anaerobic methanotrophic archaea
AOM	anaerobic oxidation of methane
APE	atom percent enrichment
BHP	bacteriohopanepolyol
CTD	conductivity temperature depth
DAPI	4',6-diamidino-2-phenylindole
DGGE	denaturing gradient gel electrophoresis
DNA	deoxyribonucleic acid
EGB	eastern Gotland Basin
FA	fatty acid
FD	Farö Deep
GC-C-IRMS	gas chromatography combustion isotope ratio mass spectrometry
GD	Gotland Deep
IOW	Leibniz Institute for Baltic Sea Research Warnemünde
LD	Landsort Deep
MCR	methyl coenzyme M reductase
<i>mcrA</i>	methyl coenzyme M reductase alpha-subunit
MMO	methane monooxygenase
MOB	aerobic methanotrophic bacteria
mRNA	messenger ribonucleic acid
NanoSIMS	nanometer-scale secondary ion mass spectrometer
PCR	polymerase chain reaction
pMMO	particulate methane monooxygenase
<i>pmoA</i>	particulate methane monooxygenase alpha-subunit
RNA	ribonucleic acid
ROI	region of interest
rRNA	ribosomal ribonucleic acid
RuMP	ribulose monophosphate
sMMO	soluble methane monooxygenase

SMTZ	sulfate methane transition zone
SRB	sulfate-reducing bacteria
SSCP	single strand conformation polymorphism
VPDB	Vienna Pee Dee Belemnite
WGB	western Gotland Basin

Contributions to the manuscripts

Jakobs, G., Rehder, G., Jost, G., Kießlich, K., Labrenz, M., Schmale, O., (2013). **Comparative studies of pelagic microbial methane oxidation within the redox zones of the Gotland Deep and Landsort Deep (central Baltic Sea)**. *Biogeosciences* 10, 7863-7875.

Assistance of experimental and field work planning and design: O. Schmale and G. Rehder. Specific contributions: Experiments, data analysis and manuscript writing by G. Jakobs. Assistance with the interpretation of data: O. Schmale, M. Labrenz, and G. Rehder. Technical assistance and manuscript writing by O. Schmale and G. Rehder. Molecular biological work was carried by K. Kießlich. Assistance during the establishment of the labeling experiments: G. Jost, O. Schmale and G. Rehder. Revision of the manuscript: O. Schmale, G. Jost, G. Kießlich, M. Labrenz, and G. Rehder. Principal investigator of the project: O. Schmale.

Jakobs, G., Holtermann, P., Berndmeyer, C., Rehder, G., Blumenberg, M., Jost, G., Nausch, G., Schmale, O., (2014). **Seasonal and spatial methane dynamics in the water column of the central Baltic Sea (Gotland Sea)**. *Continental Shelf Research* (in press).

Assistance of experimental and field work planning and design: O. Schmale and G. Rehder. Specific contributions: Experiments, data analysis and manuscript writing by G. Jakobs. Assistance with the interpretation of data by O. Schmale, C. Berndmeyer, G. Nausch and G. Rehder. Technical assistance by O. Schmale. Biomarker analyses were carried out by C. Berndmeyer and M. Blumenberg. Oxygen and hydrogen sulfide data were provided by G. Nausch. Physical oceanographic description of the water column: P. Holtermann. Revision of the manuscript: P. Holtermann, C. Berndmeyer, G. Rehder, G. Jost, G. Nausch, and O. Schmale. Principal investigator of the project: O. Schmale.

Jakobs, G., Schmale, O., Kießlich, K., Vogts, A., Blumenberg, M., Rehder, G., Nausch, G., Labrenz, M., **Bioreactor studies to investigate the methane-dependent denitrification under suboxic conditions within the redox zone of the central Baltic Sea**. in preparation.

Assistance of experimental and field work planning and design: O. Schmale and G. Rehder. Specific contributions: Experiments, data analysis and manuscript writing by G. Jakobs.

Assistance during data interpretation by O. Schmale, G. Rehder, and M. Labrenz. Technical assistance by O. Schmale and M. Labrenz. Biomarker analyses were carried out by M. Blumenberg. Molecular biological work was carried by K. Kießlich. Nitrite and nitrate data were provided by G. Nausch. NanoSIMS measurements by A. Vogts. Revision of the manuscript: O. Schmale, K. Kießlich, A. Vogts, M. Blumenberg, G. Rehder, and M. Labrenz. Principal investigator of the project: O. Schmale.

Danksagung

Zuerst möchte ich Herrn Prof. Dr. Gregor Rehder danken, der mir die Gelegenheit gab, die vorliegende Arbeit am Leibniz Institut für Ostseeforschung Warnemünde anzufertigen. In diesem Zusammenhang möchte ich mich für das entgegengebrachte Vertrauen und die fachliche Unterstützung bedanken.

Ein besonderer Dank gebührt Dr. Oliver Schmale, der mich uneingeschränkt und über das „normale“ Betreuungsverhältnis hinaus unterstützt hat. Ich möchte mich bei Ihm für den sachkundigen Beistand als auch für die unermüdliche Geduld bedanken, die mir den Einstieg in die Meeresforschung außerordentlich erleichtert hat. Sein Engagement hat maßgeblich zum Gelingen dieser Arbeit geführt.

Außerdem möchte ich mich bei unseren Projektpartnern Prof. Dr. Thiel und Dr. Martin Blumenberg bedanken, die durch zahlreiche Diskussionen, Manuskript-Durchsichten und Hilfestellungen dazu beigetragen haben, meine Arbeit in die richtige Bahn zu lenken. An dieser Stelle möchte ich meiner Mit-Doktorandin Christine Berndmeyer einen herzlichen Dank aussprechen, mit der ich schöne Stunden auf See verbringen durfte, lange fachliche Diskussionen am Telefon führte und mit der ich mich stets auch auf persönlicher Ebene austauschte.

Darüber hinaus möchte ich mich bei Katrin Kießlich und PD Dr. habil. Matthias Labrenz bedanken, die die molekularbiologischen Untersuchungen durchgeführt haben und mir jeder Zeit mit fachlichem Rat zur Seite standen. Im Besonderen bedanke ich mich bei Stine Kedzior und Michael Glockzin, die mich aufopferungsvoll in allen labortechnischen und gasanalytischen Fragestellungen unterstützt haben. Weiterhin bedanke ich mich bei Dr. Joachim Kuss für die zahlreichen fachlichen Ratschläge sowie für den persönlichen Austausch, der eine angenehme Arbeitsatmosphäre schuf.

Weiterhin bedanke ich mich bei allen Mitarbeitern des Leibniz Instituts für Ostseeforschung Warnemünde, die zum Gelingen dieser Arbeit beigetragen haben.

Abschließend möchte ich mich bei meiner Familie und allen Freunden bedanken, die stets ein offenes Ohr hatten und mich motivierend durch meine Promotion begleiteten.

Eidesstattliche Erklärung

Ich versichere hiermit an Eides statt, dass ich die vorliegende Arbeit selbstständig angefertigt und ohne fremde Hilfe verfasst habe. Dazu habe ich keine außer den von mir angegebenen Hilfsmitteln und Quellen verwendet und die den benutzten Werken inhaltlich und wörtlich entnommenen Stellen habe ich als solche kenntlich gemacht.

Gunnar Jakobs

Rostock, den 26.09.2014